Hydrogen bonding formation and physicochemical properties of chemically modified cellulose

HYDROGEN BONDING FORMATION AND PHYSICOCHEMICAL PROPERTIES OF CHEMICALLY MODIFIED CELLULOSE

化学修飾したセルロースの水素結合形成と物理化学的特性

関口裕香

静岡大学
大学院電子科学研究科
電子材料科学専攻

平成14年2月

Contents

ABSTRACT

Properly modified cellulose derivatives have chemical stability and biodegradability as does the natural cellulose, and increasing attention has been paid to the cellulose derivatives as substitutes for the synthetic polymers, because they have potential to be endowed with new physicochemical properties by modification with various functional groups. Recently developed method to prepare regioselectively substituted cellulose derivatives is expected to be applied to produce the ecological materials for the next generation. However, facile methods to characterize cellulose derivatives are lacking, and the relationship between the physical properties and the formation of hydrogen bonds of the derivatives is not clarified. This probably is the main reason why only a few kinds of cellulose derivatives have commercial values.

This thesis is focused on three aims. The first aim is to establish a facile method to determine the distribution of the substituents in regioselectively substituted *O*-methylcellulose (2,3MC-n: n = 1-3). The second concerns with the effect of the formation of hydrogen bonds on gelation of 2,3MC-n and commercially available *O*-methylcellulose (R-MC) in two-components solvent systems. The third is the preparation of two kinds of cotton fabrics by randomly and low degree substitution of functional groups which have potential to widen application of cellulose derivatives.

Chapter 2 is devoted to the establishment of a new convenient method to determine the distribution of methyl groups in 2,3MC-n on anhydroglucose unit using solution ^{1}H-NMR analysis. The determination was based on the assignment of the signals of each proton, which directly attached to the glucopyranose ring carbon for 2,3MC-n samples observed in D_2O. The results of the new method were in agreement with those based on the gas-chromatographic analysis. This method can also be applied to the measurements of the distribution of methyl groups for R-MC.

Chapter 3 describes the effect of the formation of hydrogen bonds and the distribution of methyl groups on gelation using 2,3MC-n and R-MC. 2,3MC-n and R-MC behaved differently in forming gel and the DSC thermograms on heating. The formation of hydrogen bonds with each water molecule in the sample solution has been revealed by the curve fitting of OH stretching region of water molecules in the near IR

spectra, which were composed of water species S0, S1, and S2. The presence of intermolecular hydrogen bonds between samples and water molecule was observed. The gelation of *O*-methylcellulose was attributed to the hydrophobic interactions and also to the hydrogen bonds which depended on the amount of hydroxyl groups at C(6) position.

Chapter 4 describes the effect of dimethyl sulfoxide (Me_2SO)/water composition on gelation behavior of 2,3MC-n and R-MC investigated by NIR. All the 2,3MC-n series and R-MC samples were observed that the gelation occurred at room temperature in Me_2SO/water (70/30 (wt/wt%)) system, while all the samples remained as a sol in Me_2SO. On the other hand, some of them showed a gelation upon heating in water. These gelation behaviors can be correlated to the change in the areas of S0, S1 and S2 of OH band in the solutions. When Me_2SO/water composition was between 90/10 and 80/20, Me_2SO interacts poorly with Me_2SO or water, this suggests the presence of intermolecular hydrogen bonds between the samples and water. The strong interaction between Me_2SO and water molecules causes the reduction of the interaction of the sample with either Me_2SO or water when Me_2SO/water composition was between 70/30 and 50/50.

In Chapter 5, the preparation of three kinds of water-repellent cotton fabrics, A, B, and C, is described. Sample A was prepared by alkylation through acetylation without mercerization, Sample B, by direct alkylation after mercerization, and Sample C, by alkylation by means of allylation and bromination. Water repellency of the treated samples was similar to that of cotton fabric treated with Scotch-Gard®, however water repellency of the samples did not fade out through twenty launderings in contrast to that treated with Scotch-Gard®. Durability of water-repellency after repeated launderings depended on the fabric construction. These samples retained a fabric hand, water-vapor permeability, and biodegradability similar to those of untreated cellulose fabric.

Chapter 6 is described successful preparation of durable flame retardant cotton fabric by partial orthophosphorylation and pyrophosphorylation, followed by metal-complexation. Metal content, the residue after thermal degradation, and flame retardancy depended on total phosphorus content. Pyrophosphorylated cotton fabric treated with Ni^{2+} had an LOI (limited oxygen index) value of 28, which was comparable to that obtained by the resin finishes of cotton fabric with an organophosphorus compound. Flame retardment, tensile strength and elongation of the treated fabrics did

not decrease after launderings. The pyrophosphorylated sample had a tensile strength, elongation, fabric hand and biodegradability similar to those of untreated fabrics.

In Chapter 7, conclusions of this study are briefly summarized. Future directions for the study are also indicated.

The results presented in this thesis will open new application in the field of cellulose science and industry, as well as in the other fields of polysaccharide sciences.

Chapter 1

General Introduction

1.1 Present Situation and Subject of Cellulose and Its Derivatives

People have been utilizing and consuming organic and inorganic natural resources since ancient times. In the 20th century, they produced, consumed and disposed the synthetic materials made from fossil fuel to pursuit of convenient life. This posed various problems, such as the energy shortage due to drying of fossil fuel, the global warming by the increase of carbon dioxide, and the global pollution caused by non-biodegradable materials. The subject in the 21st century is the conversion of an energy-wasting society to so-called 3R society[1], that promotes reduction, reutilization, and recycling of materials. Increasing attention has been focused on the circulatable natural resources such as cellulose, chitin and chitosan. These resources will not disappear permanently if people use them appropriately, and the utilization of these resources will not invite the environmental pollution.

Cellulose is the biomass resource that is produced about two hundred billion tons[2] of total amount on the earth every year. Figure 1-1 shows the schematic diagram and amount of production of cellulose materuals produced from wood and cotton in Japan[2]. The cellulose fibers, which are widely used to the clothes, paper, pulp and industrial materials are produced about two hundred million tons per year. While rayon, cupra, and acetate, which are known as the representative industrial fibers, are produced two hundred seventy thousand tons. However the total amount of production of these regenerated celluloses is decreasing year by year. Regrettably the manufacturing lines of viscose rayon were forced to close last year. Nonetheless, researches of the cellulose continue enthusiastically, because the cellulose is equipped with excellent chemical and physical properties which are not replaced with artificial products. Recently, "tencel" and "lyocell" spun from cellulose solution in *N*-methylmorpholine *N*-oxide were developed as new cellulose textiles. Therefore the cellulose is spotlighted by its reproducibility, recyclability, and biodegradability, also perfect "green polymer"[3] even for earth in this century.

The cellulose derivatives, which are modified cellulose, are less commercialized in

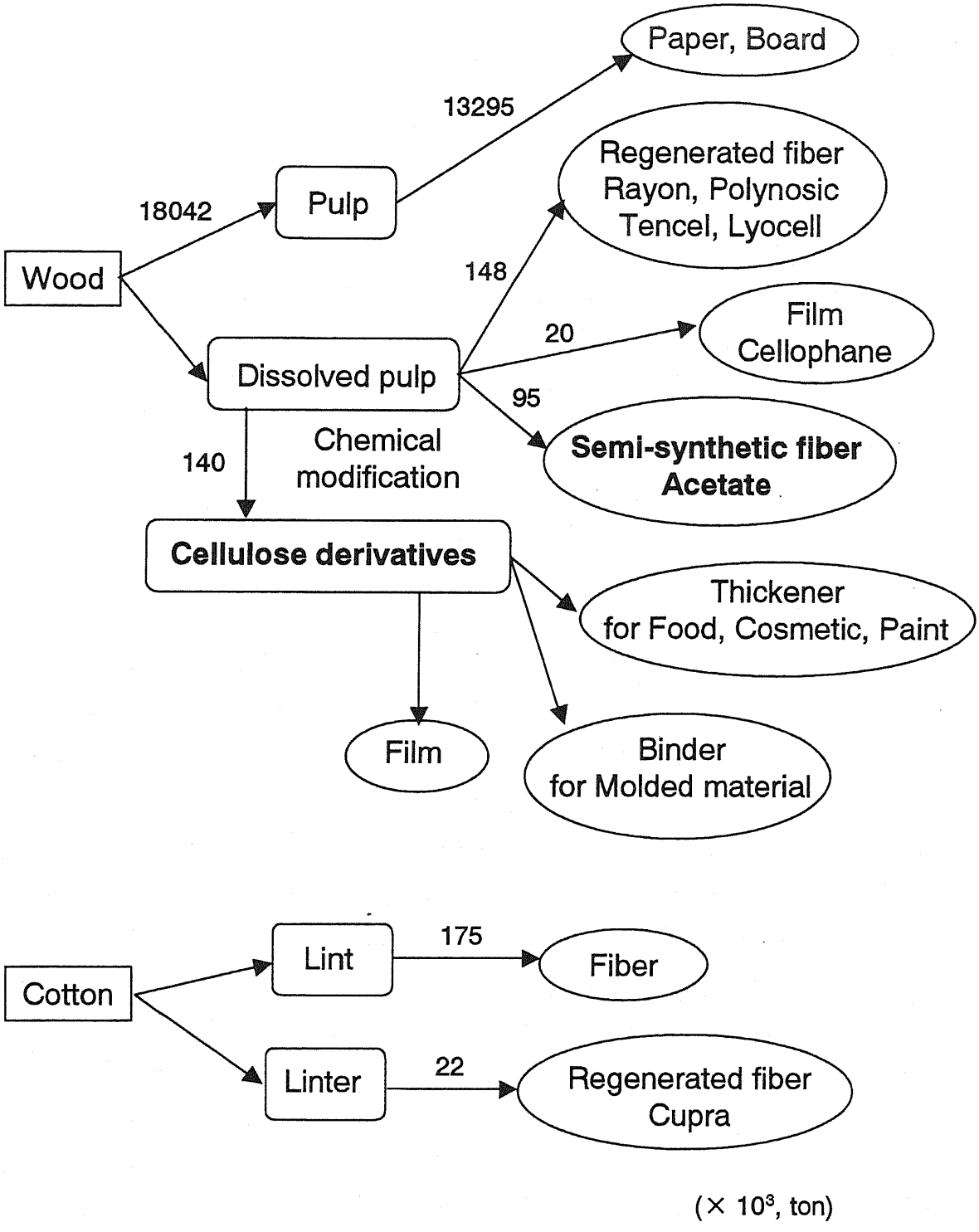

Figure 1-1. Amount of production of cellulose materials produced from wood an d cotton per year in Japan.

the industry, although the derivatives have been studied extensively. In order for the materials to take place of the synthetic polymers in the future, it is important to study and realize the following points. (i) Chemical modifications not relying on the purity of material cellulose. (ii) Establishment of the optimal reaction conditions to obtain required derivative by adjusting the reaction temperature, the reaction time, and the amount of the reagent. (iii) Establishment of a system where the reagents and solvents are recovered. (iv) Simple isolation and purification of the cellulose derivatives. (v) Control of the distribution of substituents within the anhydroglucose units as well as along the molecular chains of cellulose. (vi) Stable and biodegradable control on the cellulose derivatives. If these points are solved, the cellulose derivatives will be widely used instead of the synthetic polymers.

1.2 Cellulose Derivatives

To produce the cellulose derivatives that are considered the above mentioned points, it is necessary to understand the chemical structure of cellulose and the factors that influence the physicochemical properties of the derivatives.

1.2.1 Cellulose Structure and Its Chemical Reactivity

Cellulose is a polymer of an extended structure composed of β-1,4 glucosidic linkages between anhydroglucose repeating units. Each unit has three hydroxyl (OH) groups with different polarities, that is the secondary OHs at C(2) and C(3), and the primary OH at C(6) position. As the cellulose has the properties of polyhydric alcohol, it can be modified such as esterification, etherification, halogenation, acetalation, and oxidation. In these reactions the three OH groups have different reactivities in the cellulose molecule.

Cellulose crystal has networks of hydrogen-bonding system, which have been extensively studied by IR spectroscopy[4,5]; cellulose has intermolecular hydrogen bonds which are between C(6)-OH and the OH groups of another molecular chain, and has two different intramolecular hydrogen bonds which are between C(3)-OH and ether oxygen of the adjacent ring (In this text, the adjacent ring means the one located on the reducing side of the chain), and between C(6)-OH and C(2)-OH of the adjacent ring (Figure 1-2[6]). These hydrogen bonds among three OH groups reduce the reactivity of

OH groups in cellulose. To raise the reactivity, either the power of the hydrogen bond is weakened or the hydrogen bond is broken. As a reagent needs to be approached the OH groups. The methods to raise the reactivity of the OH groups are at present such as swelling in water, catalyst application, and destruction of the crystallinity of the molecule[7]. Another method is the preparation of the cellulose intermediates which connected reactively functional groups (for example, alkali-cellulose and cellulose acetate[8]).

1.2.2 Factors Influencing the Physicochemical Properties of Cellulose Derivatives

There are various kinds of methods to prepare cellulose derivatives, and many kinds of functional groups exist. The properties of the derivatives strongly depend on the kind of functional group, as well as on the degree of substitution, distribution of the substituents, and the distribution of molecular weights.

Degree of substitution (DS) is an average value of the number of substituted OH groups within the anhydroglucose units. The maximum value of DS is 3. This value influences the solubility and the swelling of the cellulose derivatives. Generally, partially substituted *O*-methylcellulose dissolves in water, because the hydrogen bonds are disrupted by the substitution of the methyl groups. The solubility[9,10] to the water of commercial *O*-methylcellulose with DS = 1.4-2.0 is higher than that of *O*-methylcellulose with DS = 0.1-1.1 and with DS = 2.4-2.8. This indicates that *O*-methylcellulose bearing 50-70 % methyl groups is easy to dissolve in water.

Distribution of substituents has two different meanings, that is, the distribution within the anhydroglucose units, and the distribution along the molecular chain. Randomly substituted derivatives within the anhydroglucose units are produced by heterogeneous reactions, whereas, regioselectively substituted derivatives within the anhydroglucose units can be produced by homogeneous reactions. The chemical structures of these derivatives are shown in Figure 1-3 (B) and (C)[6]. The solubility of the cellulose derivatives depends on the distribution of substituents within the anhydroglucose units. The solubility to water of 2,3-di-*O*-methylcellulose with DS = 2.0 is lower than that of randomly substituted *O*-methylcellulose with DS = 1.4-2.0. While the solubility to water of 6-*O*-methylcellulose with DS = 1.0 is lower than that of

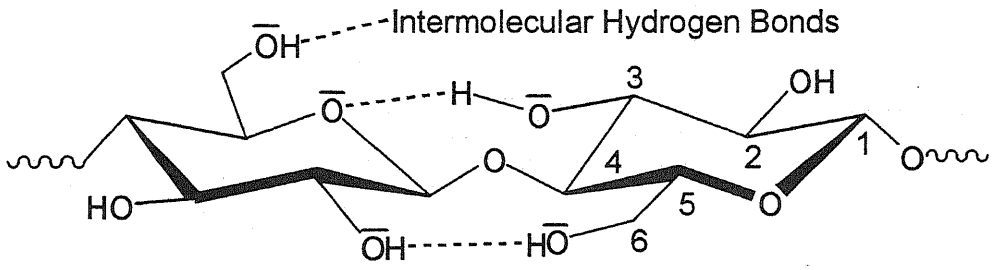

Figure 1-2. Schematic representation of possible hydrogen bonds in cellobiose units of cellulose.

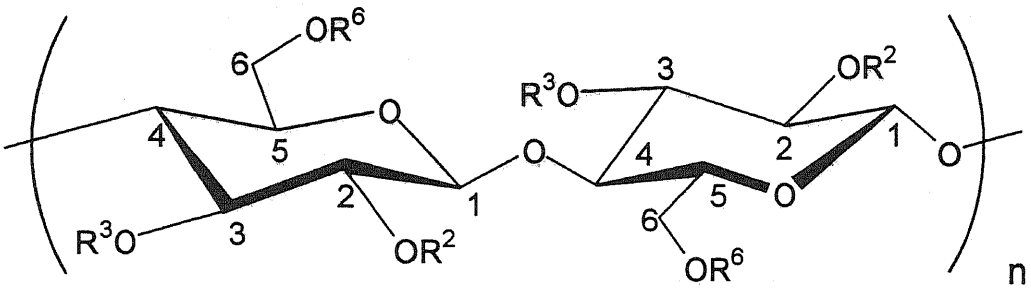

	R^2	R^3	R^6
(A) Cellulose	H	H	H
(B) 2,3-di-*O*-	R	R	H
(C) 6-*O*-	H	H	R
(D) randomly	R or H	R or H	R or H

R: functional group

Figure 1-3. The chemical structures of cellulose and its derivatives.

randomly substituted *O*-methylcellulose with DS = 0.1-1.1. It has been reported that the solubility of cellulose acetate[11,12] and carboxymethylcellulose (CMC)[13] are dependent on the effects of the distribution of substituents.

In the case of heterogeneous reactions, the distribution of substituents along the molecular chains is dependent on the size and the distribution of the crystal regions. The molecular chains in crystal regions are difficult to be modified, because the crystal regions are formed with intra- and intermolecular hydrogen bonds. Mann *et al.*[14] and Sikkema *et al.*[15] synthesized the block-like CMC by using the differences in the chemical reactivities of OH groups in crystal regions and amorphous regions. The distribution of substituents along the molecular chains influences the viscosity of the solution of the molecule.

The increase in the degree of polymerization (DP) or molecular weight of the cellulose derivatives will result in the improved physical properties of the cellulose. However the derivatives will be difficult to mold, because the viscosity of the derivative's solution become high with increasing of DP. The DP of the derivatives needs to be controlled by choice of DP of the starting materials and the optimization of the conditions, where cellulose is reacted, to meet market demand.

1.3 Aim of This Thesis

Based on above-mentioned structure of the cellulose and the derivatives thereof, this paper is focused on three aims to research core points for wider applications of the cellulose derivatives.

1.3.1 Characterization of Regioselectively Substituted Cellulose Derivatives

In the research of the cellulose derivatives, new functional cellulose derivatives are divided into two groups. The one is produced by the covalent binding of enzymes[16], medicines[17], and functional groups having ion exchange and oxidation-reduction to cellulose molecule to endow it new functions. The other is the derivatives modified by controlled introduction of functional groups to introduce new physicochemical properties, that is, the cellulose derivatives in which OH groups are regioselectively substituted under homogeneous conditions as mentioned in 1.1 (v) of this chapter. The structure of the derivatives is that the OH groups at C(2), C(3) and C(6) positions in

cellulose are regioselectively substituted within anhydroglucose units as well as along the molecular chain. Five methods to produce these cellulose derivatives are known. (1) The polymer-analogous reaction of cellulose[18]. (2) The enzymatically catalyzed regioselective modification[19,20]. (3) The enzyme catalyzed polymerization of glucose derivatives to give macromolecules with a preset structure[21]. (4) The stepwise construction of sequential cellulose-based macromolecules from glucose derivatives. (5) The cationic ring-opening polymerization of orthoesters form of glucose derivatives[22].

The methods to determine the kind of the functional group, average degree of substitution, and distribution of molecular weights has been developed in the characterization of regioselectively substituted cellulose derivatives. The method to measure the distribution of substituents has not been established yet. The methods to measure the distribution of substituents within anhydroglucose units have been developed by liquid-chromatography[23-27] and ^{13}C-NMR spectroscopy[11,12,28,29], but these methods take long time with a lot of sample amount. The purpose of this thesis is to establish a method to measure the distribution of substituents in regioselectively substituted *O*-methylcellulose using ^{1}H-NMR spectroscopy with a shorter measurements time and small amount of samples.

1.3.2 Effects of Hydrogen Bonding Formation on the Sol-Gel Transition in Regioselectively Substituted Cellulose Derivatives

The distribution of substituents of regioselectively substituted cellulose derivatives[30-32] influences not only the properties of the derivative, but also intra- and intermolecular hydrogen bonds as described by Kondo *et al.*[6,33-35]. For example, 2,3-di-*O*-methylcellulose (Figure 1-3 (B)) has intermolecular hydrogen bonds, which are between C(6)-OH and the OH groups of another molecular chain, and intramolecular hydrogen bonds which are between C(6)-OH and C(2)-OCH_3 of the adjacent ring. 6-*O*-methylcellulose (Figure 1-3 (C)) has two different intramolecular hydrogen bonds, which are between C(3)-OH and ether oxygen of the adjacent ring or between C(6)-OCH_3 and C2-OH on the adjacent ring. It was also demonstrated that the formation of intra- and intermolecular hydrogen bonds of the derivatives influences the physicochemical properties, such as the solubility[10], crystallizability[10], liquid crystallizability[36], gelation characteristics[37,38], and degradability[39,40]. It was suggested

that the distribution of substituents controls the formation of intra- and intermolecular hydrogen bonds and in turn influences the physical properties. Therefore, the regioselectively substituted cellulose derivatives which have known distribution of substituents and the definite intra- and intermolecular hydrogen bonds are a model compound to elucidate the various physicochemical properties.

Some studies have been performed to indicate that the distribution of substituents of *O*-methylcellulose influences the solubility. However it is not known how the distribution of substituents plays a role on the gelation behavior of *O*-methylcellulose[41-44]. The almost all studies of the gelation behavior of *O*-methylcellulose have so far been conducted with randomly substituted and commercially available *O*-methylcellulose (Figure 1-3 (D))[45-48] preparations. It is, therefore, difficult to analyze the influence of the distribution of methyl groups on the gelation behavior. This thesis is also attempted to elucidate the hydrogen bonding formation on the gelation of regioselectively substituted *O*-methylcellulose. This *O*-methylcellulose has already afforded us the information of the distribution of substituents along the molecular chain and the formation of intra- and intermolecular hydrogen bonds.

1.3.3 Chemical Modification of Cotton Fabrics for Some Application

In addition to the research conducted under basic and theoretical viewpoints to understand the properties and reactivity of cellulose and the derivatives thereof, some practical applications to endow the cellulose with properties that are useful in the present society as discussed in 1.1 (i)-(iv) of this chapter. The most of cotton is composed of native crystalline cellulose (cellulose I). However, chemical modification of cellulose fiber is feasible only on the OH groups in the amorphous region. In order to retain the properties as cellulose fiber, such as tensile strength and chemical stability, the crystal regions should not be destroyed. In addition, it is desirable to retain fabric hand if cotton is used as fabrics. Therefore, it was attempted to modify cellulose only in the amorphous regions to obtain sufficiently improved properties in spite of low degrees of substitution under heterogeneous conditions.

Cotton fiber is strong and hard, and its DP of the cellulose is as high as 3,000. Also cotton has high water and moisture absorbability, and chemical resistance. However cotton is easy to be wrinkled, shrank, wet and burned. Thereupon, many chemical

reformings and finishings of the cotton have been practiced from the old days, for example, not only crease resistant finish, shrink resistant finish, and improvement of dyeing absorbability, but also special processing such as water-repellent finish[49-57], flame retardant finish[58-64], and deodorant antibacterial finish[65]. These special finishes are accomplished by applying various kinds of additives composed of resins[49-54,58-64], organohalogens[49,50,53,55-57,59,60] and heavy metals[51]. The bonding strengths between OH groups in cellulose and these additives are weak, and these finishes were apt to lose effect after several cycles of usages and washings.

In this thesis, two kinds of improved cotton fabrics, water-repellant, and flame-retardant, are presented as examples of randomly substitution of cellulose molecule. Water repellent cotton was prepared by replacing very little portion of OH groups of cellulose with alkyl groups longer than C_{12}, whereas flame retardant cotton, by rather dense esterification of OH groups with phosphoric and pyrophosphoric acids, without losing, in both cases, such important characteristics as a fabric hand, tensile strength, and biodegradability of cellulose fabrics.

1.4 Outlines of This Thesis

This thesis consists of three parts as shown in Figure 1-4; First part (Chapter 2) deals with the determination of the distribution of substituents in regioselectively substituted cellulose derivatives. Second part (Chapters 3,4) concerns with the effect of the formation of hydrogen bonds on the gelation of regioselectively substituted cellulose derivatives in two components solvent systems. Third part (Chapters 5,6) deals with two kinds of cotton fabrics by randomly and low degree substitution of functional groups.

Chapter 2 is devoted to a new convenient method to determine the distribution of the methyl groups in regioselectively substituted *O*-methylcelluloses within the anhydroglucose units using solution NMR spectroscopy. The proton signals in ^{1}H-NMR spectra of *O*-methylcellulose are assigned by two-dimensional ^{1}H-^{13}C-NMR spectroscopy. The DS of the methyl groups at each position in *O*-methylcellulose is calculated from the intensity of proton signals directly attached to the ring carbon atoms and proton signals of the methyl groups, and the results are compared with the DS determined by gas chromatography.

In Chapter 3, attempts are presented of the investigation about the hydrogen bond

networks formed in aqueous solutions of the regioselectively substituted *O*-methylcellulose using near infrared (NIR) spectroscopy, differential scanning calorimetry (DSC) and small angle X-ray scanning (SAXS). The formation of hydrogen bonds in sample solution is determined by the curve fitting of OH bands in NIR spectra. This method may show the presence of intermolecular hydrogen bonds between the sample and water. At the same time the gelation behaviors of regioselectively substituted *O*-methylcellulose are compared with that of randomly substituted one.

In Chapter 4, the results are presented to characterize the formation of hydrogen bonds in the regioselectively substituted *O*-methylcellulose and the randomly substituted *O*-methylcellulose in the dimethyl sulfoxide (Me_2SO)/water mixtures using the NIR spectroscopy. In this solvent system, Me_2SO interacts strongly with water resulting in the change of mode of hydrogen bonding networks among the sample and water. These behaviors, which are independent of the solvent composition, can be demonstrated by the method in Chapter 3.

Chapter 5 deals with durably water-repellent cotton fabrics prepared by low-degree substitution of long chain alkyl groups. The fabrics are produced by three kinds of alkylation techniques. Water repellence of the treated fabrics, which lasted even after repeated launderings, was evaluated by contact-angle measurements and spray tests. A fabric hand, water-vapor permeability, and biodegradability of the treated fabrics are compared with those of untreated cellulose fabrics.

Chapter 6 deals with the method for preparing durably flame retardant cotton fabrics, and mercerized cotton fabrics with orthophosphoric and pyrophosphoric acids followed by metal-complexation. The flame retardation of treated fabrics is demonstrated by the measurement of the limited oxygen index. The effects of various metal ions complexed with the orthophospho or pyrophospho groups on cellulose are compared for flame retardation of treated fabrics. A fabric hand, tensile strength, elongation, and biodegradability of the treated fabrics are also compared with those of untreated cellulose fabrics.

In Chapter 7, conclusions of this study are briefly summarized. Future directions for the study are also indicated.

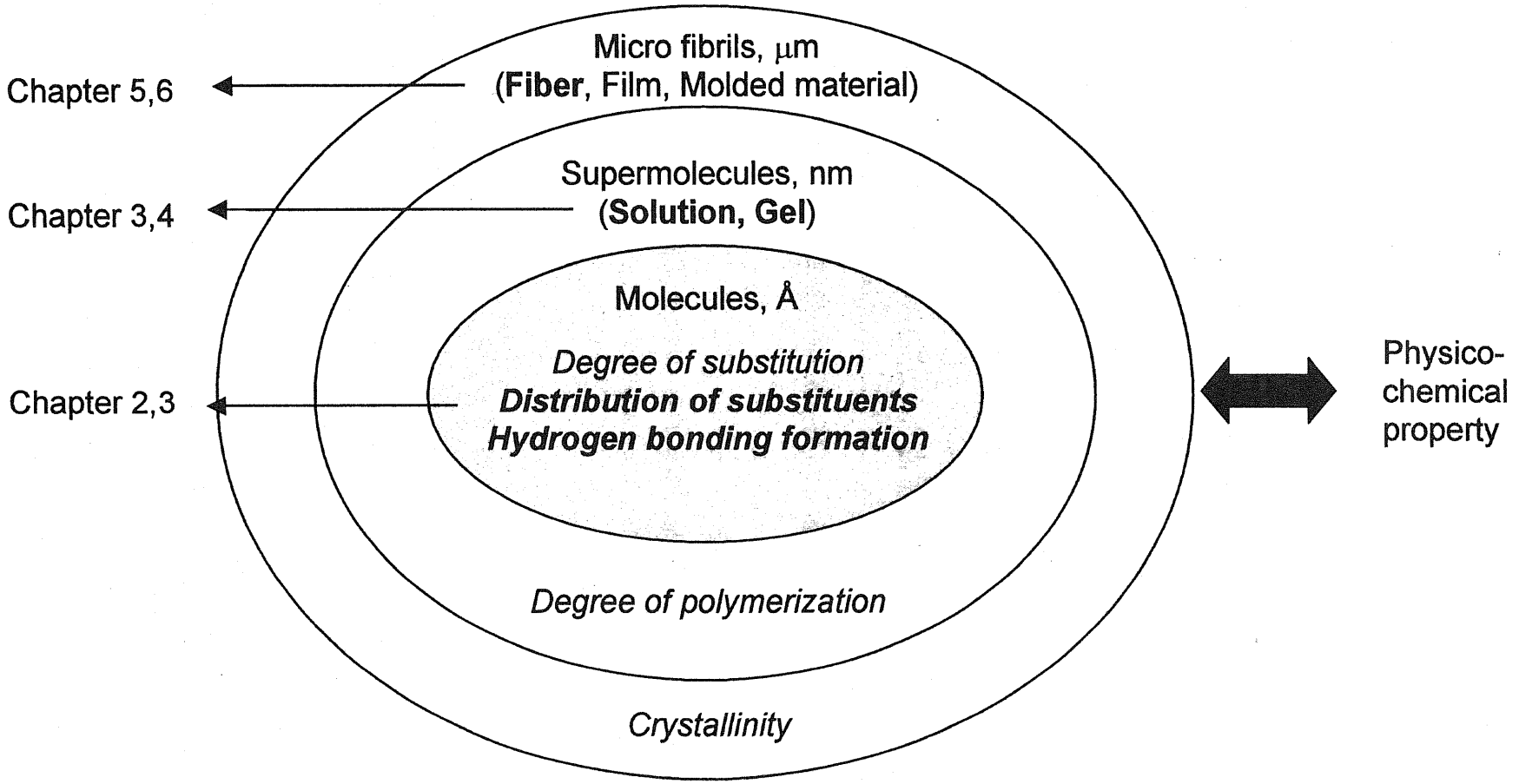

Figure 1-4. Schematic constituent of three part in this thesis.

References

1. I. Itaru, *Sen'i-gakkaishi*, **57**, 197 (2001) in Japanese.
2. F. Horii, *Sen'i-gakkaishi*, **57**, 143 (2001) in Japanese.
3. ACS, *Chemical & Engineering News*, July 16, 27 (2001).
4. C. Y. Liang, R. H. Marchessault, *J. Polym. Sci.*, **37**, 269 (1959).
5. R. H. Marchessault, C. Y. Liang, *J. Polym. Sci.*, **38**, 71 (1960).
6. T. Kondo, *J. Polym. Sci. B: Polym. Phys.*, **32**, 1229 (1994).
7. A. Isogai, R. H. Atalla, *J. Polym. Sci. A: Polym. Phys.*, **29**, 113 (1991).
8. T. Kondo, A. Isogai, A, Ishizu, J. Nakano, *J. Appl. Polym. Sci.*, **34**, 55 (1987).
9. H.Q. Liu, L. N. Zhang, A. Takaragi, T. Miyamoto, *Cellulose*, **4**, 321 (1997).
10. T. Kondo, *J. Polym. Sci. B: Polym. Phys.*, **35**, 717 (1995).
11. T. Miyamoto, Y. Sato, T. Shibata, H. Inagaki, M. Tanahashi, *J. Polym. Sci. A: Polym. Chem.*, **22**, 2363 (1984).
12. T. Miyamoto, Y. Sato, T. Shibata, H. Inagaki, M. Tanahashi, *J. Polym. Sci. A: Polym. Chem.*, **23**, 1373 (1985).
13. A. Taguchi, T. Omiya, K. Shimizu, *Japan Pat.* S60(1985) –35361, 42241,37121.
14. G. Mann, J. Kunze, F. Loth, H, Fink, *Polymer*, **39**, 3155 (1998).
15. D. J. Sikkema, *Macromolecules*, **22**, 364 (1989).
16. S. Dumitriu, M. Popa, C. Dumitriu, *J. Macromol. Sci.*, **24**, 1135,1987
17. F. Lapicque, E. Dellacherie, *J. Appl. Polym. Sci.*, **32**, 2851 (1986)
18. D. O. Klemm, in *"Cellulose Derivatives -Modification, Characterization, and Nanostructures-"* T. J. Heinze, W. G. Glasser, eds., ACS Symp. Ser. **688** (1998) Chapter 2, pp. 19-37.
19. M. Theriosod, A. M. Klibanov, *J. Am. Chem. Soc.*, **108**, 5683 (1986).
20. J. Riva, Chopineau, A. P. G. Kieboom, A. M. Klibanov, *J. Am. Chem. Soc.*, **110**, 584 (1988).
21. S. Kobayashi, S. Shoda, H. Uyama, *Adv. Polym. Sci.*, **121**, 1 (1995).
22. F. Nakatsubo, H. Kamitakahara, M. Hori, *J. Am. Chem. Soc.*, **118**, 1677 (1996).
23. H. G. Johns, in *"Methods in Carbohydrate Chemistry"* vol. VI, R. C. Whistler, J. N. Bemiler, eds., Academic Press, New York (1972) p. 25.
24. I. Croon, B. Lindberg, *Svensk Papperstidn.*, **61**, 919 (1958).
25. I. Croon, B. Lindberg, *Svensk Papperstidn.*, **60**, 843 (1957).

26. P. Mischnick, O. Wilke, *Carbohydr. Res.*, **275**, 309 (1995).
27. P. Mischnick, M. Lange, M. Gohdes, A. Stein, K. Petzold, *Carbohydr. Res.*, **277**, 179 (1995).
28. Y. Tezuka, K. Imai, M. Oshima, T. Chiba, *Macromolecules*, **20**, 2413 (1987).
29. Y. Tezuka, K. Imai, M. Oshima, T. Chiba, *Macromol. Chem.*, **191**, 681 (1990).
30. T. Kondo, D. G. Gray, *Carbohydr. Res.*, **220**, 173 (1991).
31. T. Kondo, *Carbohydr. Res.*, **238**, 231 (1993).
32. T. Kondo, D. G. Gray, *J. Appl. Polym. Sci.*, **45**, 417 (1992).
33. T. Kondo, *Cellulose*, **4**, 281 (1997).
34. T. Kondo, C, Sawatari, *Polymer*, **37**, 393 (1996)
35. T. Kondo, in "*Polysaccharides -Structural Diversity and Functional Versatility-*" S. Dumitriu, ed., Mercel Dekker, New York, Basel, Hong Kong (1998) Chapter 4, pp. 131-172.
36. T. Kondo, T. Miyamoto, *Polymer*, **39**, 1123 (1998).
37. H. Itagaki, I. Takahashi, M. Natsume, T. Kondo, *Polym. Bull.*, **32**, 77 (1994).
38. H. Itagaki, M. Tokai, T. Kondo, *Polymer*, **38**, 4201 (1997).
39. T. Kondo, M. Nojiri, *Chem. Lett.*, 1003 (1994).
40. M. Nojiri, T. Kondo, *Macromolecules*, **29**, 2392 (1996).
41. S. Takaragi, T. Fujimoto, T. Miyamoto, H. Inagaki, *J. Polym. Sci. A: Polym. Chem.*, **25**, 987 (1987).
42. M. Vigouret, M. Rinaoudo, J. Desbrières, *J. Chem. Phys.*, **93**, 858 (1996).
43. M. Hirren, J. Desbrières, M. Rinaoudo, *Carbohydr. Polym.*, **31**, 243 (1997).
44. M. Hirren, C. Chevillard, J. Desbrières, M. A. V. Axelose, M. Rinaoudo, *Polymer*, **39**, 6251 (1998).
45. T. Kato, M. Yokoyama, A. Takahashi, *Colloid Polym. Sci.*, **256**, 15 (1978).
46. K. Suzuki, Y. Taniguchi, T. Enomoto, *Bull. Chem. Soc. Jpn.*, **45**, 336 (1978).
47. N. Sarkar, *J. Appl. Polym. Sci.*, **24**, 1073 (1979).
48. N. Sarkar, *Carbohydr. Polym.*, **26**, 195 (1995).
49. J. P. Moreau, G. L. Drake Jr., *Am. Dyest Rep.*, **58**, 21 (1969).
50. J. P. Moreau, S. E. Ellezey Jr., G. L. Drake Jr., *Am. Dyest Rep.*, **56**, 117 (1967).
51. W. B. Blumenthal, *Ind. Eng. Chem.*, **42**, 640 (1950).
52. J. B. Bullock, C. M. Welch, *Textile Res. J.*, **35**, 459 (1965).

53. Y. Sato, T. Wakida, S. Tokino, S. Niu, M, Ueda, *Textile Res. J.*, **64**, 316 (1994).
54. H. A. Schuyten, J. W. Weaver, J. G. Frick Jr., J. D. Reid, *Textile Res. J.*, **22**, 424 (1952).
55. W. J. Connick Jr., S. E. Ellezey Jr., *Am. Dyest Rep.*, **57**, 71 (1968).
56. R. J. Berni, R. R. Benerito, F. J. Phirips, *Textile Res. J.*, **30**, 576 (1960).
57. F. J. Phirips, L. Segai, L. Loeb, *Textile Res. J.*, **27**, 369 (1957).
58. B. M. Baum, *Chemtech*, 311 (1973).
59. J. D. Reid, J. G. Frick Jr., R. L. Arceneaux, *Textile Res. J.*, **26**, 137 (1956).
60. C. Hamalaonen, W. A. Reeves, J. D. Guthrie, *Textile Res. J.*, **26**, 145 (1956).
61. W. A. Reeves, G. L. Drake Jr., L. H. Chance, J. D. Guthrie, *Textile Res. J.*, **27**, 260 (1957).
62. R. B. LeBlanc, *Textile Res. J.*, **59**, 307 (1989).
63. S. Nakanishi, C. Aoki, *J. Home Econ. Jpn.*, **42**, 67 (1991) in Japanese.
64. S. Nakanishi, F. Ohkouchi, *J. Home Econ. Jpn.*, **43**, 121 (1992) in Japanese.
65. C. C. Chu, in *"High-Tech Fibrous Materials –Composites, Biomedical Materials, Protective Clothing, and Geotextile-"* T. L. Vigo, A. F. Turbak, eds., ACS Symp. Ser. **457** (1991) Chapter 12, pp. 167-211.

Chapter 2

A Facile Method of Determination for Distribution of the Substituents in *O*-Methylcelluloses Using ^{1}H-NMR Spectroscopy

2.1 Introduction

Methods to measure the distribution of substituents within the anhydroglucose units of cellulose derivatives have been developed although it has not been found yet definite methods to determine the distribution of substituents along the molecular chain[1].

The first analytical method was based on the gas- or liquid-chromatographic analysis of partially methylated alditol acetates[2-4] derived by acetylation of hydrolyzed and reduced cellulose derivatives. Recently, Mischnick *et al.* reported the improved methods[5,6]. These methods were, however, laborious because cellulose ethers had to be converted to analyzable derivatives after several chemical steps.

The convenient methods to determine the distribution of substituents within the anhydroglucose units by solution ^{13}C-NMR spectroscopy were also introduced by Miyamoto *et al.*[7,8]. They proposed that the distribution of acetyl groups in cellulose acetate was determined by considering that the acetyl carbonyl carbon ^{13}C-NMR signals of acetylated samples were split into a triplet corresponding to C(2), C(3) and C(6) positions on the anhydroglucose units. Recently, Tezuka *et al.*[9,10] reported a method to determine the methyl group distribution of *O*-methylcelluloses using ^{13}C-NMR spectroscopy after acetylation of the unsubstituted hydroxyl (OH) groups in the *O*-methylcelluloses. But these methods take longer time with a lot of sample. Therefore, a facile method to determine precisely the distribution pattern has been eagerly desired.

If it was possible to easily determine the distribution of the methyl substituents on *O*-methylcellulose using ^{1}H-NMR, it would make the measurement time shorter with small amounts of the sample. In this chapter, the author will propose a new convenient method to determine the distribution of the methyl substituents within the anhydroglucose units in regioselectively *O*-methylcellulose using solution ^{1}H-NMR

spectroscopy. It should be noted that in the present method, the author has focused on the proton signals directly attached to the ring carbon, not as for the hydroxyl proton.

2.2 Experimental

2.2.1 Materials

A series of *O*-methylcellulose samples (2,3MC-n: n = 1-3, Figure 2-1(A)) which were regioselectively substituted only at C(2) and C(3) positions were prepared by multiple methylation of 6-*O*-triphenylmethylcellulose (6-*O*-trithylcellulose, 6TC) as a starting material basically followed by the method reported previously[11], as shown in Figure 2-2. In the present study, the second and the third methylation steps were repeated exactly in the same manner of the first methylation step. The numbering of the sample corresponded to repeating number of the methylation step; for example 2,3MC-1 indicates the sample single-methylated of 6TC. R-MC (Figure 2-1(B)) was indicated as commercially available and randomly methylated *O*-methylcellulose having blocky trimethyl glucose ethers or non-methylated glucose sequences (Shin-Etsu Chemical Co.).

The above samples were dissolved in water, and centrifuged to remove insoluble impurities. The supernatant was isolated and dried at 50 °C.

2.2.2 Measurements

The two-dimensional-NMR spectra were obtained using a JEOL Alpha 500 spectrometer (500 MHz for ^{1}H and 125.65 MHz for ^{13}C). The pulse program of the phase-sensitive ^{1}H-^{13}C HSQC (heteronuclear single quantum coherence) using bilinear rotation decoupling pulse was employed from the JEOL software library. The internal standard, sodium 3-(trimethylsilyl)propionate-2,2,3,3-d_4 (δH: 0 ppm) and the central signal of dimethyl sulfoxide-d_6 ($(CD_3)_2SO$) (δC: 39.5 ppm) were used as reference for ^{1}H-^{13}C NMR spectra, respectively. ^{1}H-NMR was measured with a JEOL-GX 400 FT-NMR spectrometer (400 MHz) at 15 °C in three solvent systems: D_2O, $(CD_3)_2SO$ and the mixture of $(CD_3)_2SO$ and D_2O. The mixed solvent system was composed of $(CD_3)_2SO$ containing 1% (v/v) D_2O ($(CD_3)_2SO/D_2O$). The chemical shift in $(CD_3)_2SO$ and $(CD_3)_2SO/D_2O$ was obtained relative to that of tetramethylsilane (δH: 0 ppm), while in D_2O, the chemical shift was calculated relative to that of HDO (δH: 4.8 ppm). The

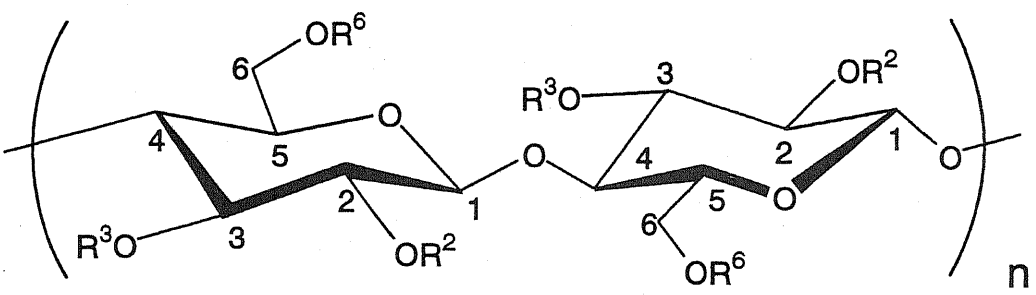

	R^2	R^3	R^6
(A) Partially 2,3-*O*-methylcellulose (2,3MC-n)	CH_3 or H	CH_3 or H	H
(B) Commercial *O*-methylcellulose (R-MC)	CH_3 or H	CH_3 or H	CH_3 or H

Figure 2-1. The chemical structures of the *O*-methylcellulose samples in this study.

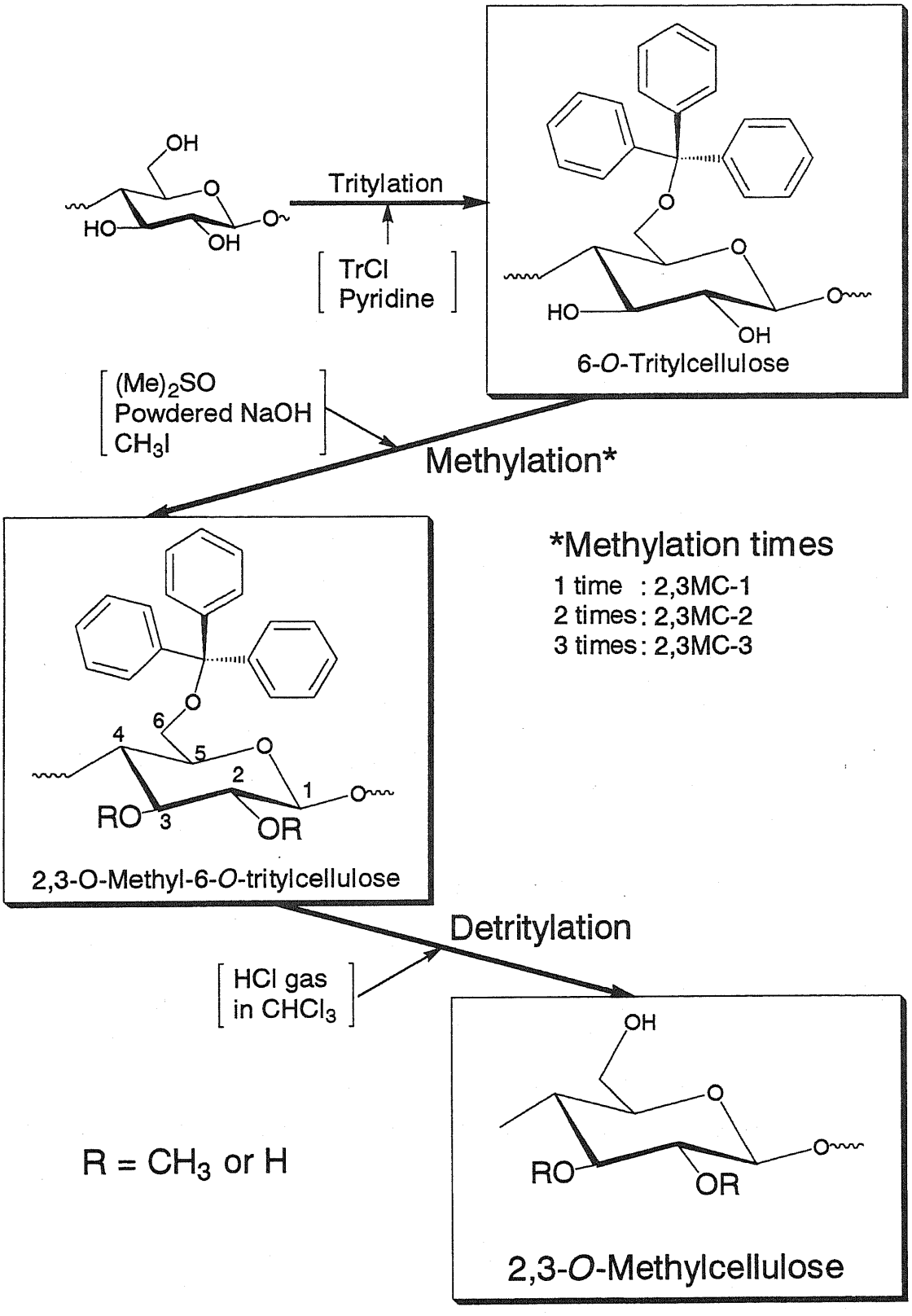

Figure 2-2. Procedure for the preparation of 2,3-*O*-methylcellulose.

spectra were recorded after 400 scans for commercial *O*-methylcellulose and 40 scans for 2,3MC-n samples, respectively.

The gas-chromatographic analysis for the determination of the distribution of the substituents in the samples was reported in the previous paper[11,12].

2.3 Results and Discussion

In ^{1}H-NMR spectra for cellulose and its derivatives, the individual signal in the polymers is supposed to be broader than the monomer (anhydroglucose unit), because the segment of the polymer molecular chain is less flexible. Nevertheless, the proton signals which overlap with each other in the ^{1}H-NMR spectra could be identified as separated as a signal using the two-dimensional ^{1}H-^{13}C-NMR spectroscopy[13]. Figure 2-3 shows the two-dimensional ^{1}H-^{13}C-NMR spectrum of 2,3MC-1 in $(CD_3)_2SO$ containing a slight amount of D_2O[14]. The signal number indicates the number of the carbon position on the anhydroglucose unit in the figure; for example the carbon signal at C(1) position is labeled as C-1. The carbon signals of methyl groups at C(2) and C(3) position are labeled as C-7 and C-8, respectively. The possible assignments of the carbon signals were already proposed[15]. The proton signals can be assigned using correlation between the proton signals and those of ^{13}C on two-dimensional ^{1}H-^{13}C-NMR spectra. The signal of C-1 bearing two oxygen atoms differs from those of C-2, C-3 and C-5. The signal of C-6 locates in the higher magnetic field because C-6 is in a primary alcohol group.

The solvent may also influence resolution of the proton signals attached directly to ring carbons. Therefore three-different solvent systems for ^{1}H-NMR measurements were compared as shown in Figure 2-4. The signal number indicates the number of the carbon position on the anhydroglucose unit in the figure; for example the proton signal at C(1) position is labeled as H-1. The proton signals of the unsubstituted OH groups at C(2), C(3) and C(6) position of the carbon are labeled as 2-, 3- and 6-OH, respectively. The proton signals of methyl groups at C(2), C(3) and C(6) position are labeled as 2-, 3- and 6-Me, respectively. The signals due to 2-Me and 3-Me were not well distinguished with each other in these spectra. While H-1 overlapped with that of 6-OH in $(CD_3)_2SO$ (Figure 2-4 (C)), it became a single signal in D_2O or $(CD_3)_2SO/D_2O$. This is due to deuteration of three OH groups (2-, 3- and 6-OH) into OD. In $(CD_3)_2SO/D_2O$ and

$(CD_3)_2SO$ (Figure 2-4 (B) and (C)), the signals (3.3-3.4 ppm) due to moisture in the sample overlapped with the signal of 2-Me and 3-Me observed at 3.4-3.5 ppm. In D_2O, the proton signal directly attached to C-2 to which methoxyl groups were attached (labeled as H-2(2-OMe)) appeared as a doublet, and was separated from that attached to C-2 to which did not have methoxyl groups attached (labeled as H-2(2-OH)). In $(CD_3)_2SO$ and $(CD_3)_2SO/D_2O$, the H-2(2-OH) overlapped with those of H-3 and H-5, and then only H-2(2-OMe) appeared as a triplet signal (Figure 2-4 (B) and (C)).

According to Nojiri and Kondo[14], the signal of H-2(2-OMe) may shift depending upon conformational changes of the polymer; the conformation may depend on whether 3-OH in either the same or the adjacent anhydroglucose unit is methylated or not. This can account for the separation of H-2(2-OMe) into triplet in $(CD_3)_2SO$ and $(CD_3)_2SO/D_2O$ solvents. In D_2O, H-2(2-OMe) splits into a doublet, probably because the methylation of OH groups at C(3) position on the adjacent anhydroglucose unit is less influential than in $(CD_3)_2SO$ or $(CD_3)_2SO/D_2O$ solvents. Therefore it would be possible to determine the degree of substitution (DS) at C(2) position on the basis of the signal intensity at H-2(2-OMe) in D_2O. Furthermore the DS at C(3) position was calculated by subtracting the DS at C(2) position from the total DS of at C(2) and C(3) position.

The ^{1}H-NMR spectra for samples of 2,3MC-n series in D_2O at 15 °C are shown in Figure 2-5. As the series of the samples were systematically and regioselectively methylated in increasing the degree of methylation only at C(2) and C(3) positions as listed in Table 2-1, the author could follow the change of ^{1}H-NMR signals on the multiple methylation. The relative intensity for left signal of the doublet (see the arrow in Figure 2-5) for H-2(2-OMe) and the intensity for the signal of 2-Me and 3-Me increased significantly on multiple methylation steps. This indicates that the left signal of the doublet of H-2(2-OMe) is identified as that for H-2 in the anhydroglucose unit where the 3-OH is methylated, and the right signal also identified as that of H-2 with unsubstituted 3-OH on the same unit. As the protons of the methyl groups and the protons directly bound to the carbon chain in these samples are not engaged in hydrogen bonds, the amount of protons are considered to be proportional to the area of proton signals. Therefore the DS of the individual methyl group at each position can be cal ulated by the following equations:

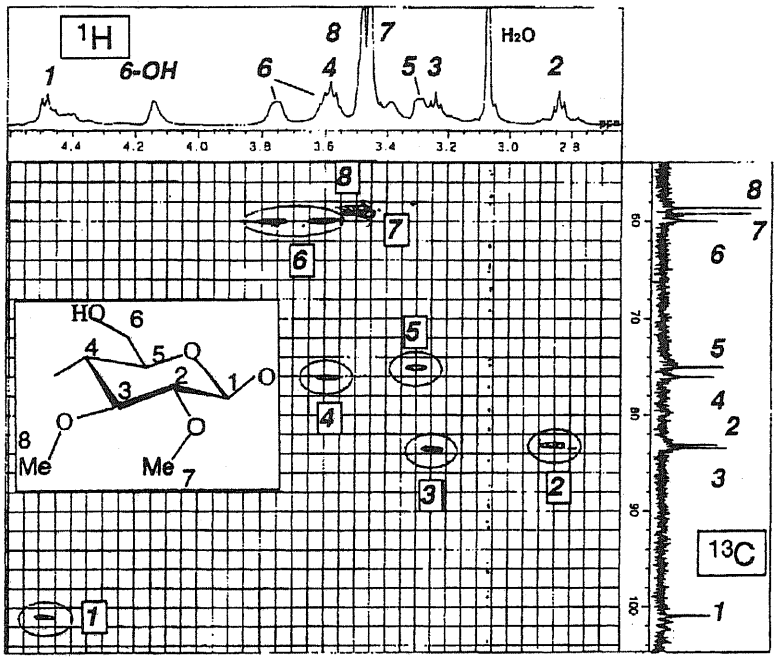

Figure 2-3. ^{1}H-^{13}C-NMR spectrum of 2,3MC-1 in $(CD_3)_2SO$ (containing a slight amount of D_2O).

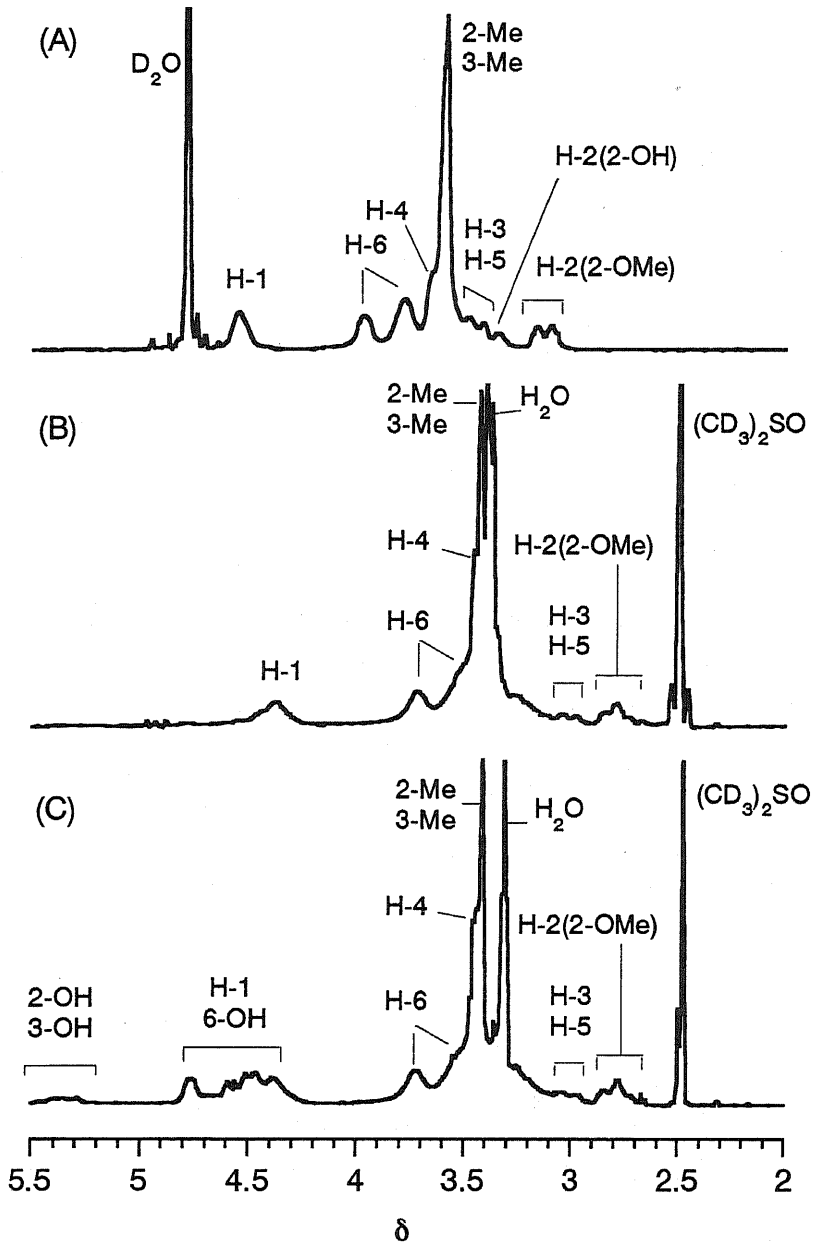

Figure 2-4. ^{1}H-NMR spectra of 2,3MC-1 at 15 °C: (A) in D_2O, (B) in $(CD_3)_2SO$ and D_2O (containing 1% D_2O) and (C) in $(CD_3)_2SO$.

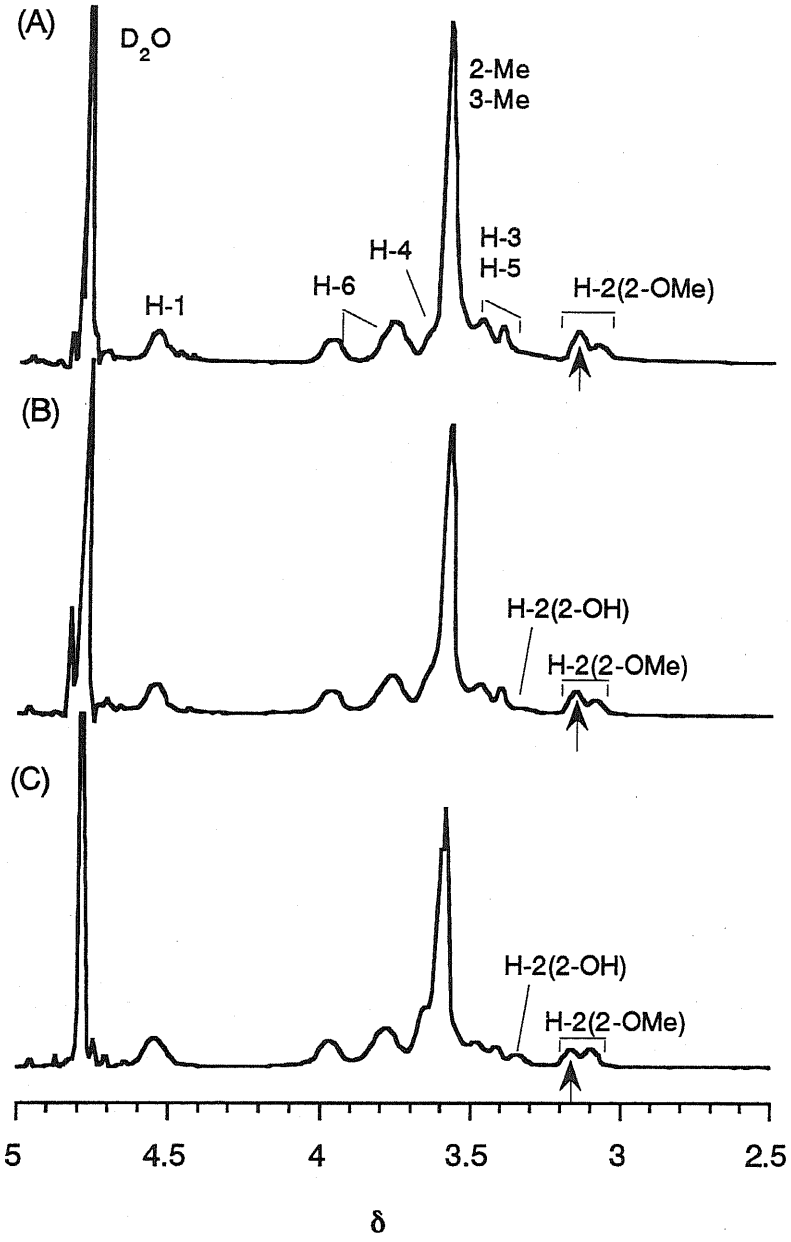

Figure 2-5. ^{1}H-NMR spectra for 2,3MC-n series of in D_2O at 15 °C: (A) 2,3MC-3, (B) 2,3MC-2 and (C) 2,3MC-1.

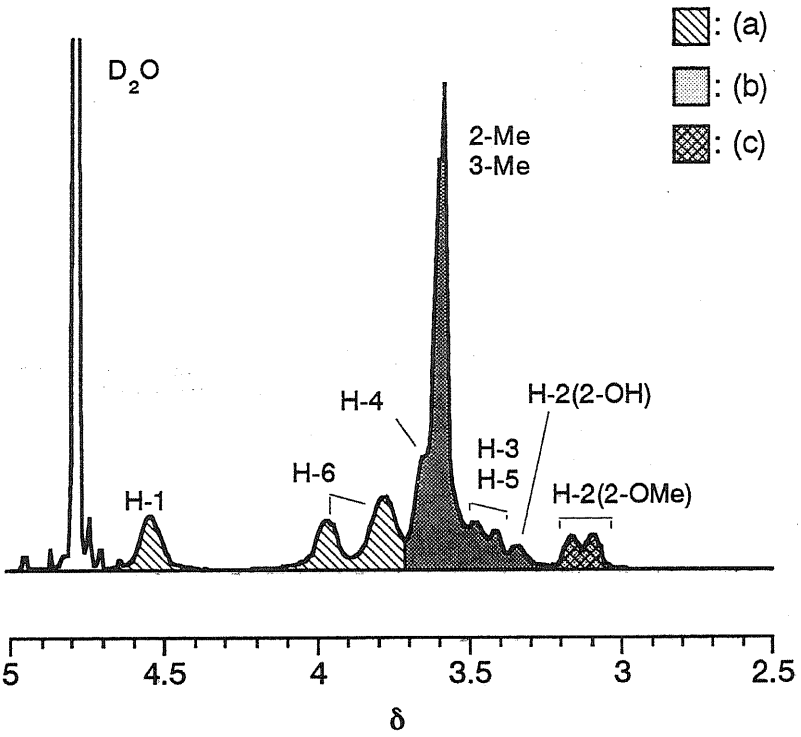

Figure 2-6. Schematic determination for distribution of the substituents from ^{1}H-NMR spectrum of 2,3MC-1: (a) H-1 + H-6, (b) H-4 + 2-Me + 3-Me + H-5 + H-3 + H-2(2-OH) and (c) H-2(2-OMe).

Table 2-1. Substituents distribution of *O*-methylcellulose samples assigned by ^{1}H-NMR method.

Samples	Total DS	DS of methylation at each position		
		R^2	R^3	R^6
2,3MC-1	1.02 (1.33)	0.65 (0.72)	0.38 (0.61)	-
2,3MC-2	1.28 (1.55)	0.77 (0.90)	0.51 (0.65)	-
2,3MC-3	1.85 (1.67)	1.02 (0.99)	0.83 (0.68)	-
R-MC	1.71 (1.60)	0.66 (0.69)	0.30 (0.34)	0.75 (0.68)

DS in the parentheses was the mol fraction of alkylated glucitol determined by gas-chromatographic analysis.

$$[H] = (H\text{-}1 + H\text{-}6) / 3 \quad (1)$$

$$DS_{23} = \{(H\text{-}4 + 2\text{-}Me + 3\text{-}Me + H\text{-}5 + H\text{-}3 + H\text{-}2(2\text{-}OMe) + H\text{-}2(2\text{-}OH)) - (4 \times [H])\} / (3 \times [H]) \quad (2)$$

$$DS_2 = H\text{-}2(2\text{-}OMe) / [H] \quad (3)$$

$$DS_3 = DS_{23} - DS_2 \quad (4)$$

where [H] stands for the intensity of a single proton of each anhydroglucose unit. DS_2 and DS_3 stand for DS at C(2) and C(3) positions, respectively, and DS_{23} is the sum of DS_2 and DS_3. H-2 is the sum of signal areas for H-2(2-OMe) and H-2(2-OH). The first term of the numerator of equation (2) can be determined as the total area of unseparated peaks of H-4, 2-Me, 3-Me, H-5, H-3 and H-2 (shown in Figure 2-6).

Table 2-1 illustrates the DS of the individual methyl group determined by the procedure described above together with the DS determined by gas-chromatography in the parentheses[11]. This table indicates that the total DS increases by the multiple methylation step from 2,3MC-1 to 2,3MC-2 and then to 2,3MC-3. The DS of the methyl groups at C(2) position reaches the saturated value of 1 only at the 2,3MC-3 stage. The signal of substituted methyl groups at C(6) position in commercial R-MC are observed at 3.4 ppm (not shown in these figures). The DS_6 (DS at C(6) position) is calculated as follows.

$$DS_{236} = \{(H\text{-}4 + 2\text{-}Me + 3\text{-}Me + 6\text{-}Me + H\text{-}5 + H\text{-}3 + H\text{-}2) - (4 \times [H])\} / (3 \times [H]) \quad (5)$$

$$DS_6 = \{(6\text{-}Me + H\text{-}5 + H\text{-}3 + H\text{-}2) - (3 \times [H])\} / [H] \quad (6)$$

$$DS_3 = DS_{236} - DS_2 - DS_6 \quad (7)$$

As the DS values determined using ^{1}H-NMR spectroscopy described in this study agrees in the range of experimental errors (9 %) with those determined by the authentic gas-chromatographic analysis.

2.4 Conclusion

The present ^{1}H-NMR spectroscopic method in D_2O can be sufficient as a facile and convenient method to measure the distribution of the methyl groups in 2,3MC samples and R-MC within the anhydroglucose units. The proton signals in ^{1}H-NMR spectra of 2,3MC-1 were assigned by two-dimensional ^{1}H-^{13}C-NMR spectroscopy. The DS of the

methyl groups at each position in 2,3MC samples and R-MC was calculated from the intensity of proton signals directly attached to the ring carbon atoms and proton signals of the methyl groups. The method to determine the DS of individual positions in *O*-methylcelluloses using ^{1}H-NMR thus reported is rapid and reliable and could be employed in cellulose chemistry.

References

1. P. Mischnick, G. Kuhn, *Carbohydr. Res.*, **290**,199 (1996).
2. H. G. Johns, in "*Methods in Carbohydrate Chemistry*" vol. VI, R. C. Whistler, J. N. Bemiler, eds., Academic Press, New York (1972) p. 25.
3. I. Croon, B. Lindberg, *Svensk Papperstidn.*, **61**, 919 (1958).
4. I. Croon, B. Lindberg, *Svensk Papperstidn.*, **60**, 843 (1957).
5. P. Mischnick, O. Wilke, *Carbohydr. Res.*, **275**, 309 (1995).
6. P. Mischnick, M. Lange, M. Gohdes, A. Stein, K. Petzold, *Carbohydr. Res.*, **277**, 179 (1995).
7. T. Miyamoto, Y. Sato, T. Shibata, H. Inagaki, M. Tanahashi, *J. Polym. Sci. A: Polym. Chem.*, **22**, 2363 (1984).
8. T. Miyamoto, Y. Sato, T. Shibata, M. Tanahashi, H. Inagaki, *J. Polym. Sci. A: Polym. Chem.*, **23**, 1373 (1985).
9. Y. Tezuka, K. Imai, M. Oshima, T. Chiba, *Macromolecules*, **20**, 2413 (1987).
10. Y. Tezuka, K. Imai, M. Oshima, T. Chiba, *Macromol. Chem.*, **191**, 681 (1990).
11. T. Kondo, D. G. Gray, *Carbohydr. Res.*, **220**,173 (1991).
12. T. Kondo, D. G. Gray, *J. Appl. Polym. Sci.*, **45**, 417 (1992).
13. R. M. Silverstein, G. C. Bassler, T. C. Morrill, "*Spectrometric Identification of Organic Compounds*" John Wiley & Sons, New York (1991).
14. M. Nojiri, T. Kondo, unpublished data.
15. H. Q. Liu, L. N. Zhang, A. Takaragi, T. Miyamoto, *Cellulose*, **4**, 321(1997).

Chapter 3

A Gelation Mechanism Depending on Hydrogen Bonding Formation in Regioselectively Substituted *O*-Methylcelluloses

3.1 Introduction

The distribution of methyl and other substituents within anhydroglucose units as well as along the molecular chain is considered to be an important factor on physicochemical properties of cellulose derivatives. Chemical modifications of cellulose for the commercial propose are generally conducted under heterogeneous conditions. Such heterogeneous reactions cause variety of introduction of the substituents within anhydroglucose units as well as along the molecular chain in cellulose derivatives, which also causes irregular physicochemical properties for them. When cellulose derivatives are composed of homogeneous chemical structure, their physicochemical properties may be directly predicted[1].

Commercial *O*-methylcellulose is widely used, for example, as a thickener for foods and cosmetics, a coating material for medicines, and a binder for ceramic and cement[2]. Aqueous solution of *O*-methylcellulose is also known to form a gel on heating and then reverts to the solution on cooling. The thermo reversible gelation[3-6] of *O*-methylcellulose solution has been proposed to be caused by hydrophobic interaction or micellar interaction by the phase separation, but is not completely clarified. Recently, Vigouret *et al.*[7] and Hirren *et al.*[8] reported the effect of the distribution of substituents on the gelation of *O*-methylcellulose. In this chapter, the author particularly focuses on the influence of inter- and intramolecular hydrogen bonds. The gelation behavior was investigated using *O*-methylcellulose having a systematically controlled distribution of substituents and DS. An aqueous solution of the commercial sample with heterogeneous distribution of substituents was also compared in terms of the gelation process.

3.2 Experimental

3.2.1 Materials

Two types of *O*-methylcellulose used were as same samples in Chapter 2 having the following character; one was the partially methylated 2,3-*O*-methylcellulose series

(2,3MC-n: n = 1-3), which were regioselectively methylated only at C(2) and C(3) positions including non-methylated hydroxyl (OH) groups at C(6) positions. The other was R-MC which indicated as commercially available and randomly methylated *O*-methylcellulose having blocky sequences trimethyl glucose ethers or non-methylated glucose. The above samples were purified as described in Chapter 2.

3.2.2 Characterization of *O*-Methylcellulose Films

HPLC analysis was performed with a Shimadzu Chromatopac C-R7A equipped with a reflective index detector (Shimadzu RID 6A). Column fillings were polymethacrylate (Shodex OHpac SB-800HQ: 8ϕ × 300 mm). The eluent of the chromatography was 0.1 M $NaNO_3$, and the flow rate was 1 mL/min at 55 °C.

^{1}H-NMR spectra was measured with a JEOL-GX 400 FT-NMR spectrometer (400MHz) at 15 °C, using D_2O as solvent. The spectra were recorded after 400 scans for R-MC and 40 scans for 2,3MC-n samples, respectively. The peak signals were assigned based on the previous chapter.

FT-IR spectra were recorded using a Perkin-Elmer FTIR spectrometer, Spectrum 1000. The wavenumber range was 4000-400 cm^{-1}; the data were collected after 32 scans of 2 cm^{-1} resolution. The film specimens used in this chapter were cast from water. Curve fitting[9] for the peak deconvolution of OH groups frequencies was performed by GRAMS/386 'CurveFit' program. The true shape of the peak of OH absorption bands was at first assumed to be a mixture of composition of Gaussian and Lorentzian. The number of peaks involved in frequencies was determined based on the second derivative IR spectra for the samples, in the range of 3700-3100 cm^{-1}. The calculations were repeated until a best fit was obtained with $R^2 > 0.999$, R: correlation factor.

3.2.3 Measurements of *O*-Methylcellulose Solutions

The dried samples were dissolved in water at room temperature, then kept under the same condition over 24 h to assure a complete dissolution. Gelation behaviors of the aqueous sample solutions were observed in a water bath with a constant temperature. After standing for the desired time, the solution was judged to become a gel in a vial when the specimen could not flow by itself from the horizon.

DSC measurements were performed on 700 mg of the solutions using a Setaram

micro DSC3 in a nitrogen atmosphere. The equal amount of distilled water was used as reference to obtain a flat base line. The heating scans were carried out in the temperature range of 25-90 °C at a rate of 1 or 0.1 °C/min.

FT-NIR spectra with a hot stage (Lincam TH-600PM) were measured as follows; the solution was poured into the PET plate (20ϕ × 0.5 mm) with a bore, and the PET plate was sandwiched between two plates of crystal of CaF_2 (20ϕ × 1 mm). The specimen thus prepared was set in the hot stage. The heating scans were carried out in the temperature range of 30-90 °C at a rate of 1 °C/min. The wavenumber ranged was 7800-400 cm^{-1}; the data were collected after 100 scans of 2 cm^{-1} resolution. Curve fitting for the peak in the range of 7400-6000 cm^{-1} was performed as described above.

SAXS measurements were performed at the beam line #15A of photon Factory of the National Laboratory for High Energy Physics (Tsukuba, Japan). The wavelength used in this study was 1.506 Å. The sample was heated using a heating apparatus (Mettler Instrument FP89), and the temperature was kept at 65 °C for 60 min. The diffraction intensity along the meridial direction was recorded using a dimensional position-sensitive proportional counter (PSPC, Rigaku, Tokyo, Japan).

3.3 Results and Discussion

3.3.1 Characterization of *O*-Methylcellulose Films

Prior to characterization of gel states of the samples, *O*-methylcelluloses were characterized as films. The characteristics of the *O*-methylcellulose samples are summarized in Table 3-1. 2,3MC-n samples have partially methylated OH groups only at C(2) and C(3) positions and all free OH groups at C(6) positions. 2,3MC-1 (1a, 1b and 1c) samples have similar DS with different molecular weights. These were prepared by different duration periods for bubbling with HCl gas to remove the triphenylmethyl groups as a protective group at C(6) position. The author should add that these methylation steps did not result in lowering of the molecular weight of the material; namely no depolymerization occurred. 2,3MC-n samples having DS < 1 or DS = 2 were not used in this study, because these samples were insoluble in water[10].

Figure 3-1 shows IR spectra of 2,3MC-n and R-MC films. These IR spectra were normalized at 1110 cm^{-1} attributed to C-O-C stretching within the anhydroglucose ring. As the DS increased, the larger C-H stretching vibration region (3000-2800 cm^{-1}) in the

IR spectra of these samples became, and the smaller OH stretching region (3700-3000 cm^{-1}) was. The shape of OH stretching band in R-MC was different from those in 2,3MC-n samples. The difference may depend on the hydrogen bonding formation in cellulose derivatives. OH stretching bands in cellulose derivatives are assumed to be the combination of bands including not only the inter- and intramolecular hydrogen bonded OH groups, but also a small amouts of 'free' or non-hydrogen bonded OH groups[9].

By a curve fitting method for the IR spectrum in 2,3MC-1b film, the OH stretching absorption band was deconvoluted into three OH bands with peaks at around 3590 (A), 3465 (B), and 3310 cm^{-1} (C), respectively (shown in Figure 3-2). Two types of inter- and intramolecular hydrogen bonds can be involved in pure cellulose film (Figure 3-3(A)) and the 2,3-di-*O*-methylcellulose film (Figure 3-3(B))[11,12]. In the present cases, as 2,3MC-n samples have partially methylated OH groups only at C(2) and C(3) positions, their cast films may have intramolecular hydrogen bonds engaged in either between C(3)-OH and the adjacent ring oxygen or between C(6)-OH and C(2)-OCH_3. Considering above, the band B in Figure 3-2 may be attributed to the intramolecular hydrogen bonds at C(3) position, as well as to the intramolecular hydrogen bonds between the functional groups at C(2) and C(6) positions[9,11,12]. The band C may be due to the intermolecular hydrogen bonds at C(6) positions[9,11,12]. The band A may be due to remaining free OH groups at C(2) position, which had escaped from the methylation, or free OH groups at C(6) position which were not involved in the intermolecular hydrogen bonds[9]. As the molar absorptivity of the intramolecular hydrogen bonded OH groups in these samples are similar to that of the intermolecular hydrogen bonded OH groups[13]. Therefore the individual DS of the OH groups involved in the three types of hydrogen bonding engagements was calculated from the area of OH band, and listed in Table 3-1. Intramolecular hydrogen bonded OH groups in 2,3MC-1a and 2,3MC-1c were comparatively larger than those in the other 2,3MC-n samples.

3.3.2 Gelation of *O*-Methylcellulose Solutions

Aqueous solutions of 2,3MC-n and R-MC films became opaque on heating, and transformed to gel on further heating. The gelation phenomena were time-dependent and thermally reversible with a hysteresis. Three solutions of 2,3MC-n series as well as R-MC solution formed gel. The phase diagram of these samples was shown in Figure 3-

4. The concentration of R-MC (molecular weight (M_n) = 280,000) to form a gel was between 1 and 5 wt%, whereas that of 2,3MC-nb series (M_n = 16,000-18,000) was between 20 and 25 wt%. This means the gelation of R-MC is attributed to hydrophobic interaction among trimethyl glucose sequences at lower concentration[3]. In 2,3MC-1 series, only 2,3MC-1b, which has the lowest intramolecular hydrogen bond in the film state, formed gel (Table 3-1), whereas neither 2,3MC-1a nor 2,3MC-1c formed gel. Since the intramolecular hydrogen bonds between C(3)-OH and the adjacent ring oxygen were suggested to be maintained in the *O*-methylcellulose solutions[11,12], the cellulose molecular chains of 2,3MC-1a and 2,3MC-1c must be less flexible than those of 2,3MC-1b. Thus, the lower flexibility may inhibit the gelation.

The 2,3MC-1b having the lowest DS of methyl group in 2,3MC-nb series formed gel at significantly lower temperatures than 2,3MC-2b and 2,3MC-3b. This indicates that the gelation mechanism of 2,3MC-nb samples may involve other interactions differing from the hydrophobic interaction.

Figure 3-5(a) illustrates the results of calorimetric experiments for solutions of 2,3MC-nb samples and R-MC. The two endothermic peaks (56 and 65 °C) were observed on heating R-MC. While the peak at 56 °C seemed to correspond to interactions involved with the highly substituted units, the peak at 65 °C may be due to the less substituted units as discussed by Hirrien *et al.*[14] using DSC and rheological measurement. The heating DSC thermograms of the 2,3MC-nb solutions showed monotonic endothermic curves. The endothermic deviation of 2,3MC-1b became to slightly decrease at 60 °C, whereas those of 2,3MC-2b and 2,3MC-3b became to barely decrease at 75 °C. In spite of the slight changes, these phenomena correspond to the gelation phase diagram (Figure 3-4), which shows that 2,3MC-1b formed a gel at lower temperatures when compared with 2,3MC-2b and 2,3MC-3b. As the gelation time of 1 wt% R-MC solution was 16 hours, the DSC curve at a heating rate of 1.0 °C/min is considered to indicate thermal transition due to pre-gelation. In the calorimetric experiments carried out at a heating rate of 0.1 °C/min (Figure 3-5(b)), the gelation was also observed. In R-MC solution, the endothermic curves between fast and slow rate scans were totally different. On the other hand, 2,3MC-1b solutions exhibited the similar endothermic curves in both of the slower and faster heating scans. This result also suggests that the gelation mechanism of 2,3MC-nb samples is different from that of

R-MC. This difference was also shown in the gelation of *O*-methylcelluloses with homogeneous distribution of substituents prepared by other methylation[14,15].

3.3.3 Characterization of *O*-Methylcellulose Solutions Before and After Gelation

FT-NIR spectra of 2,3MC-1b and R-MC solutions were obtained to investigate the hydrogen bonding formation of water which may contribute to the gel formation. Figure 3-6 shows the OH band in the NIR region between 6000 and 7400 cm^{-1} which was assigned to be $\nu_\delta + \nu_{as}$. The ν_δ and ν_{as} indicated the OH bending vibration and the OH anti-symmetric stretching vibration, respectively[16,17]. The OH absorption band was resolved into three component bands using the same manner described in film samples, where the peak tops were located at 7060, 6900, and 6660 cm^{-1}. These bands were assigned to be the free water molecules (S0), water molecules with one OH engaged in hydrogen bonds (S1), and those with two OH engaged in hydrogen bonds (S2), respectively[18,19] (shown in Figure 3-7).

As the molar absorptivetiy of each water molecule which is present in identical vibration is same, the amount of water molecules of the three types of hydrogen bonding engagements is relatively calculated from area of OH band. The changes of S0, S1, and S2 areas for 2,3MC-1b and R-MC solutions as a function of temperature, were listed in Table 3-2. At 30 °C, the areas of S1 for both 2,3MC-1b and R-MC solutions were larger than that for solvent alone (pure water), whereas the areas of S2 for both solutions were smaller than that for solvent alone (pure water). This means that some water molecules interacted with the samples to result in forming S1 at 30 °C.

At 90 °C where the gelation of R-MC and 2,3MC-1b solutions was observed, the area of S0 increased, whereas the area of S2 decreased. Because of the breakage of some hydrogen bonds in the water structure at higher temperature, the resulting water molecules may be altered to be free states (S0)[19]. The areas of S1 for both 2,3MC-1b and R-MC solutions were larger than that for solvent alone (pure water) at 90 °C. This suggests that the intermolecular hydrogen bonds between water and the samples are present at high temperatures.

The area of S1 for 2,3MC-1b solution was slightly larger than that for R-MC at 90 °C. In 2,3MC-n samples, methyl groups at C(2) and C(3) positions are almost unable

Table 3-1. Molecular weight and degree of substitution of methyl and hydroxyl groups in the *O*-methylcellulose samples.

Samples	M_n[a]	DS in film				
		Total-DS(OMe)[b]	Total-DS(OH)[c]	Free-OH[d]	Intra-OH[d]	Inter-OH[d]
R-MC	279,300	1.60	1.40	-	-	-
2,3MC-1a	29,300	1.02	1.98	0.009	1.238	0.733
2,3MC-1b	18,100	1.05	1.95	0.014	1.121	0.815
2,3MC-1c	11,900	0.92	2.08	0.017	1.381	0.682
2,3MC-2b	17,700	1.28	1.72	0.025	0.988	0.707
2,3MC-3b	16,200	1.85	1.15	0.008	0.630	0.512

[a] M_n is molecular weight, and determined by HPLC.
[b] Total-DS(OMe) is the degree of substituted methyl groups, and determined by ^{1}H-NMR measurements.
[c] Total-DS(OH) is the degree of unsubstituted hydroxyl groups, and calculated by subtracting the degree of subsitituents methyl groups of Total-DS(OMe) from 3.
[d] DS of Free-, Intra-, and Inter-OH are calculated by multiplying DS of Total-DS(OH) by the percentage of each area to that of the total area of the OH band.

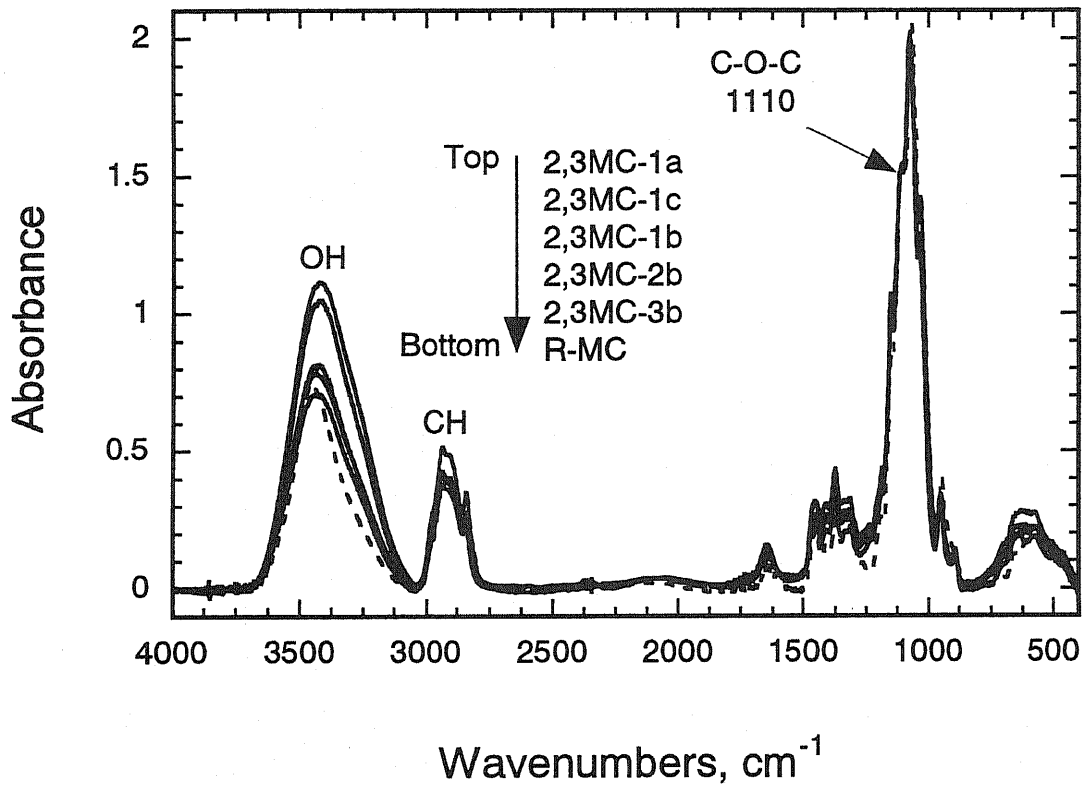

Figure 3-1. IR spectra in the cast film of the *O*-methylcellulose samples.

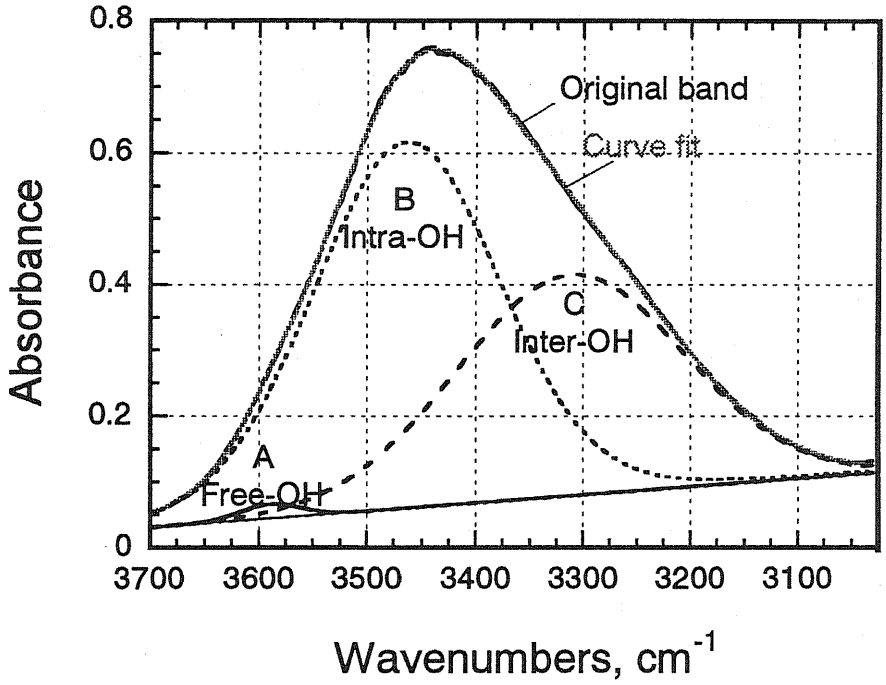

Figure 3-2. Curve fitting and peak assignments for OH band of IR spectrum in the cast film of 2,3MC-1b.

(A) Cellulose

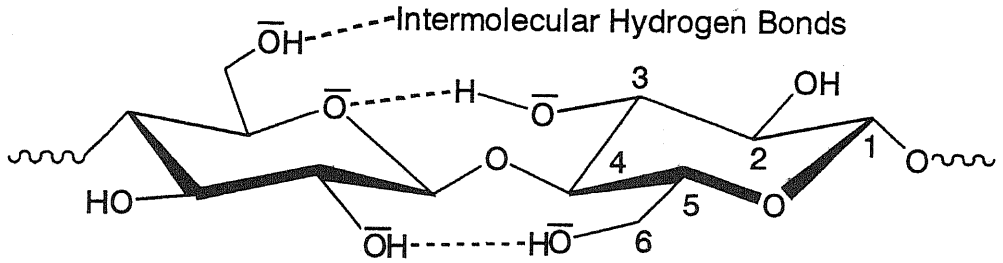

(B) 2,3-di-*O*-methylcellulose

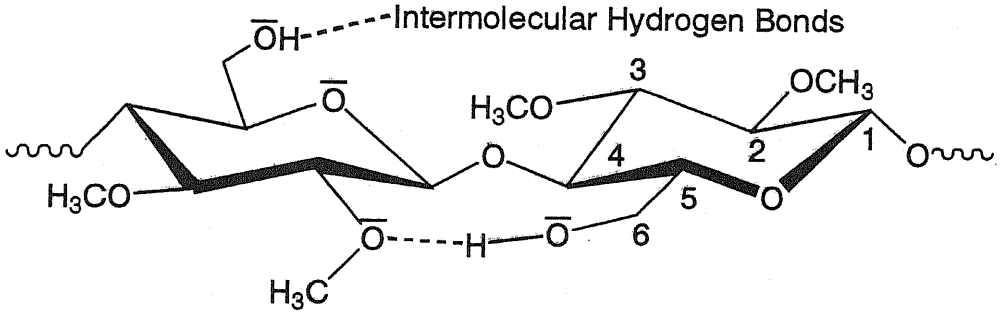

Figure 3-3. Schematic representation of possible hydrogen bonds in cellobiose units of (A) cellulose and (B) 2,3-di-*O*-methylcellulose.

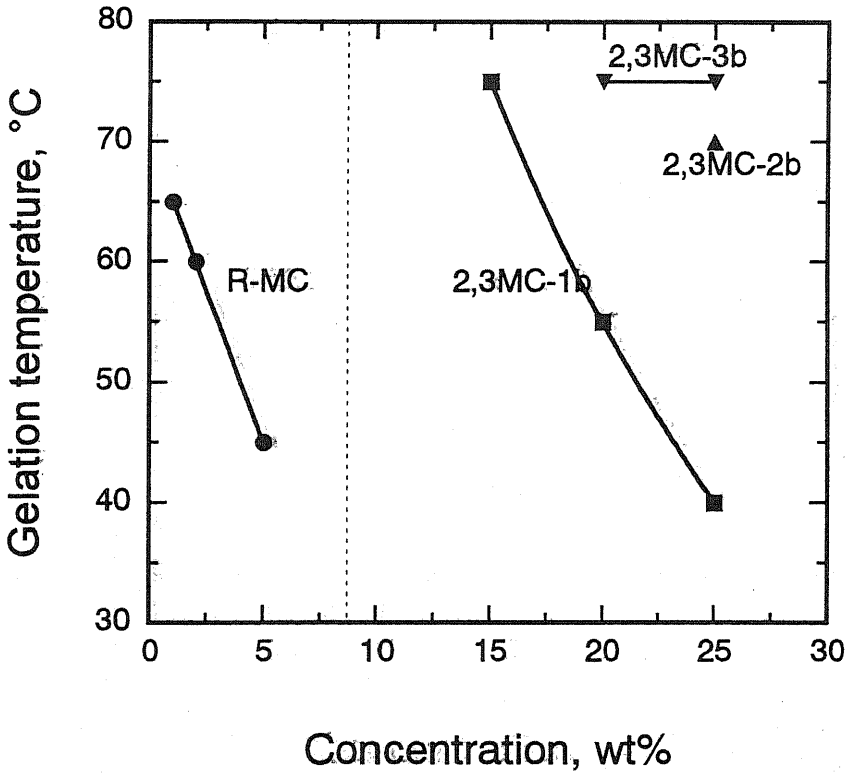

Figure 3-4. Concentration dependence of critical gelation temperature of the *O*-methylcelluloses samples.

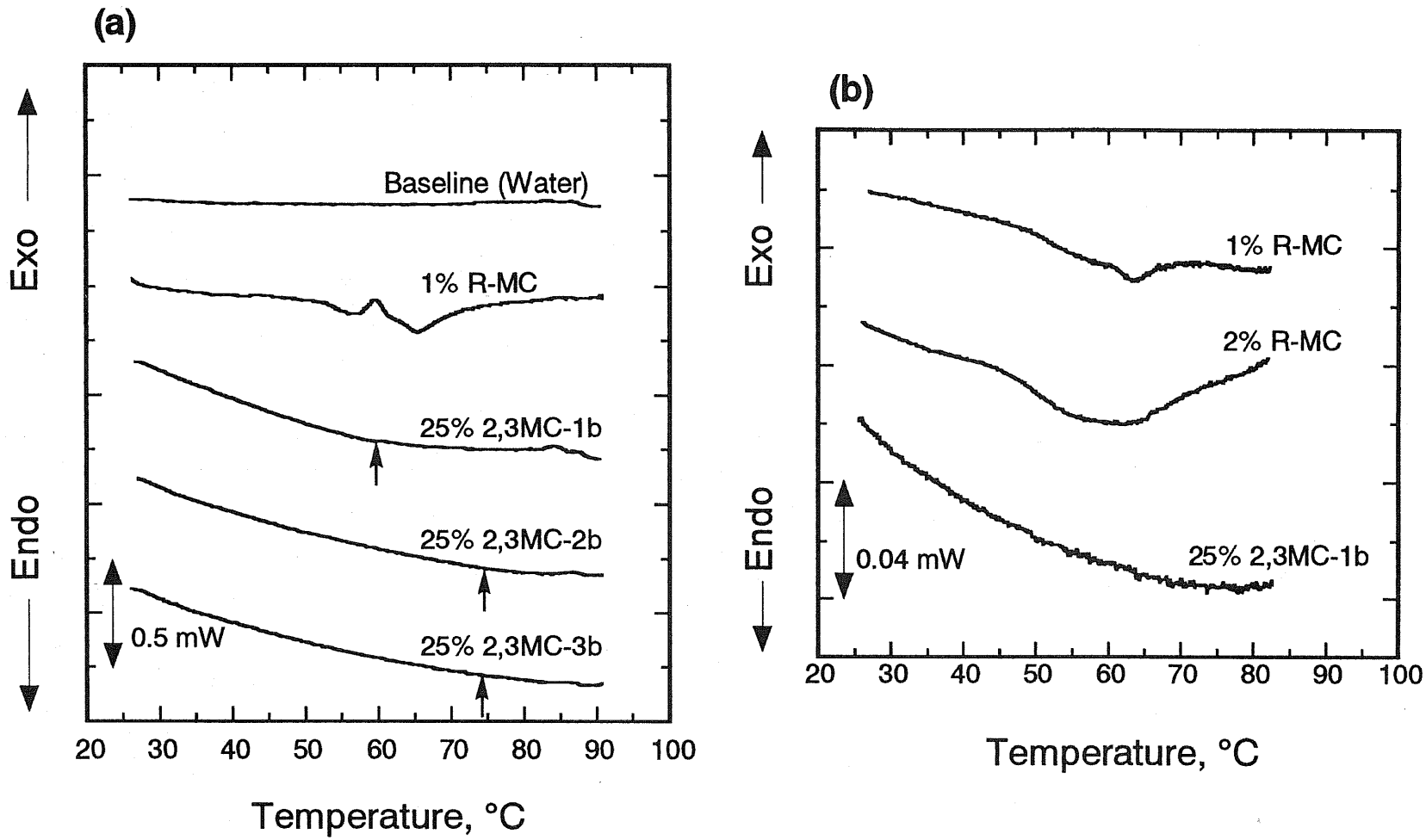

Figure 3-5. Heating DSC thermograms of the *O*-methylcellulose solutions: Heating rates (a) 1.0 °C/min and (b) 0.1 °C/min.

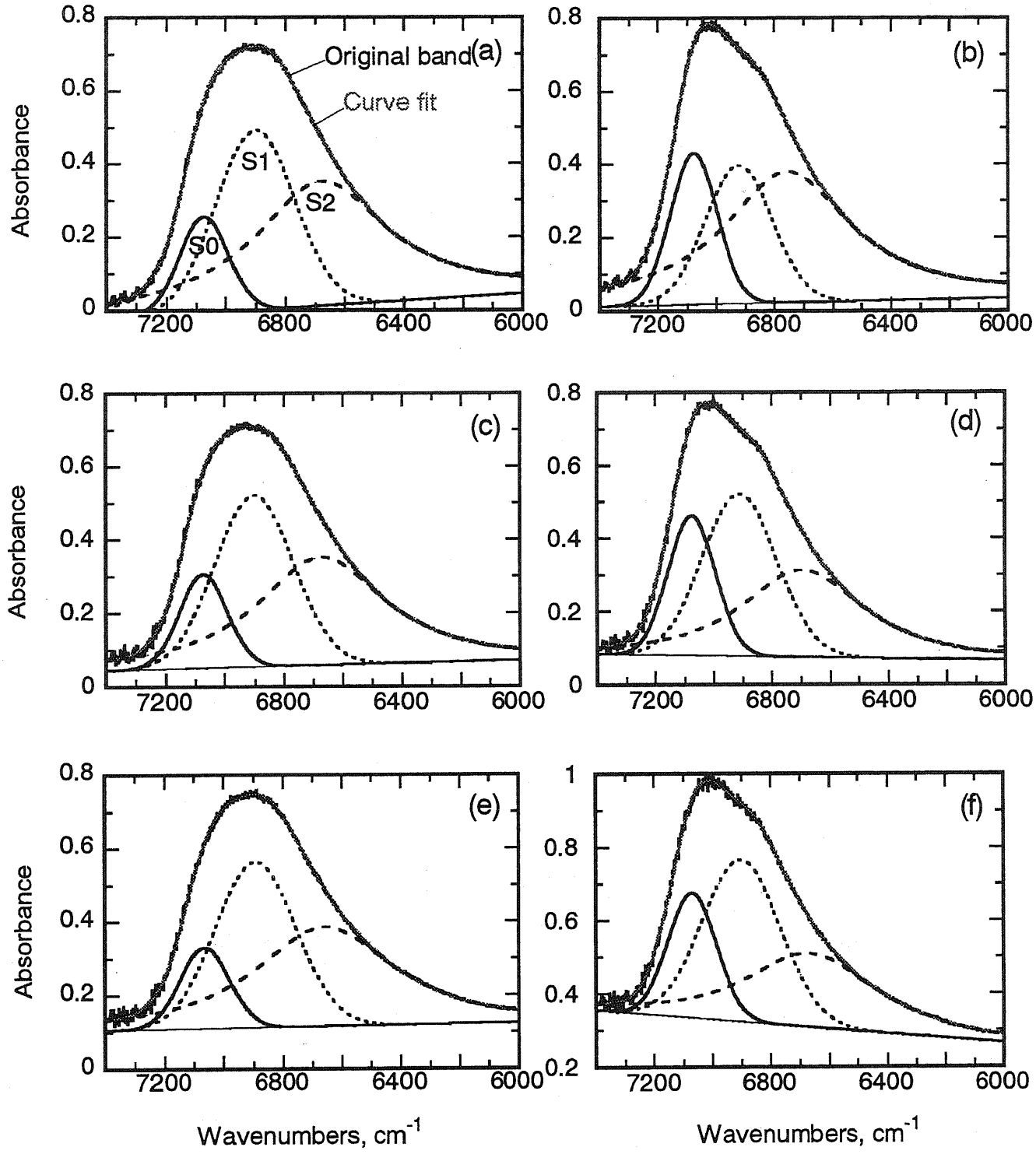

Figure 3-6. Curve fitting and peak assignments for OH band ($\nu_\delta + \nu_{as}$) of water in NIR spectra of (a) water at 30 °C, (b) water at 90 °C, (c) R-MC at 30 °C, (d) R-MC at 90 °C, (e) 2,3MC-1b at 30 °C, and (f) 2,3MC-1b at 90 °C.

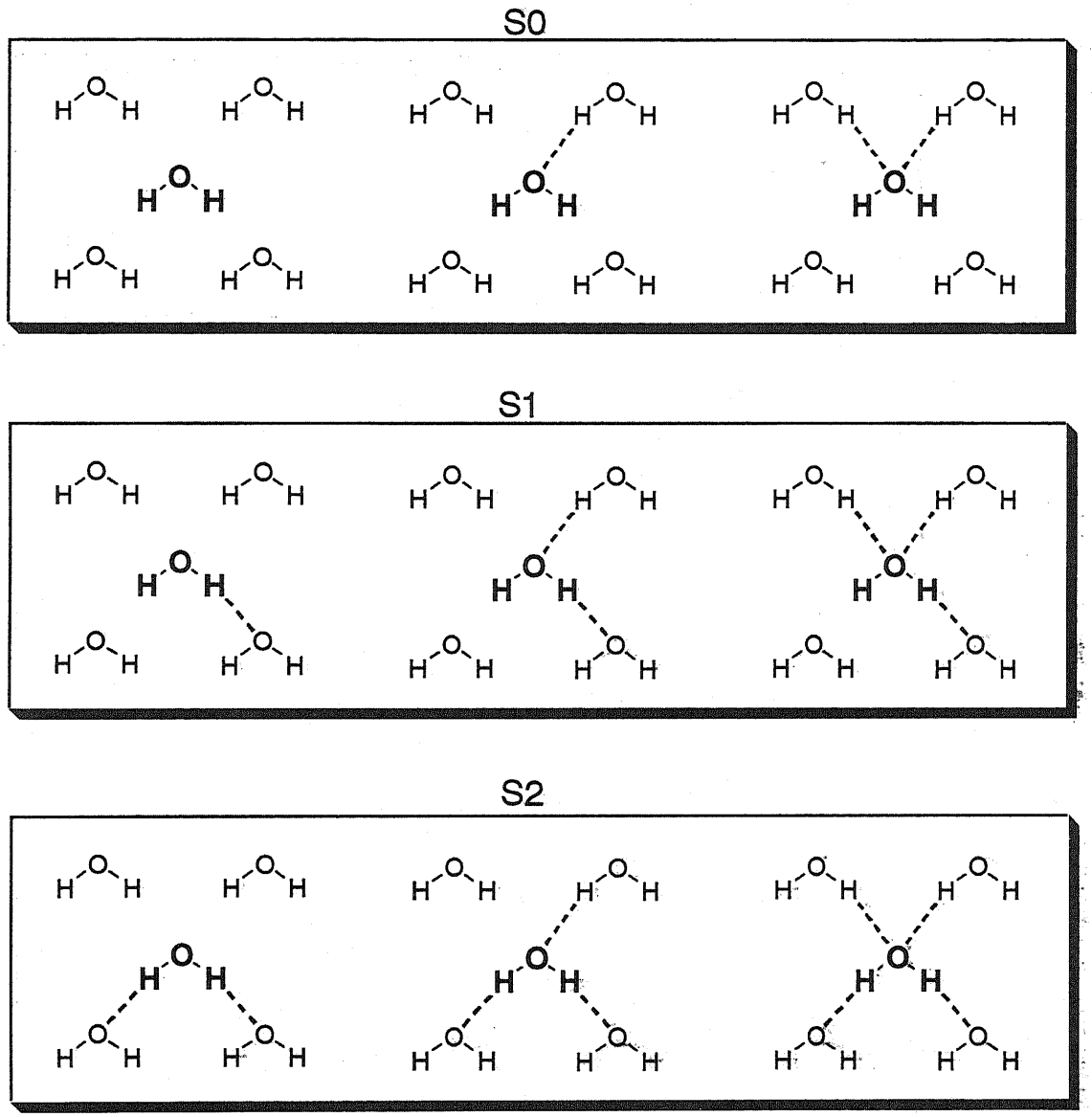

Figure 3-7. Possible structures of water molecules of S0, S1, and S2.

Table 3-2. The changes of S0, S1, and S2 areas in the OH bands of water in NIR spectra of the *O*-methylcellulose solutions on heating.

Temperature	Solvent alone (Water)			R-MC solution (2 wt%)			2,3MC-1b solution (25 wt%)		
	S0[a]	S1[a]	S2[a]	S0[a]	S1[a]	S2[a]	S0[a]	S1[a]	S2[a]
30 °C	12.3	37.2	50.5	13.3	40.0	46.7	12.3	40.9	46.8
90 °C	19.8	26.0	54.2	21.5	39.6	38.9	20.5	43.1	36.4

[a]S0, S1, and S2 indicate the water molecules with non hydrogen bond, one hydrogen bond, and two hydrogen bonds, respectively.

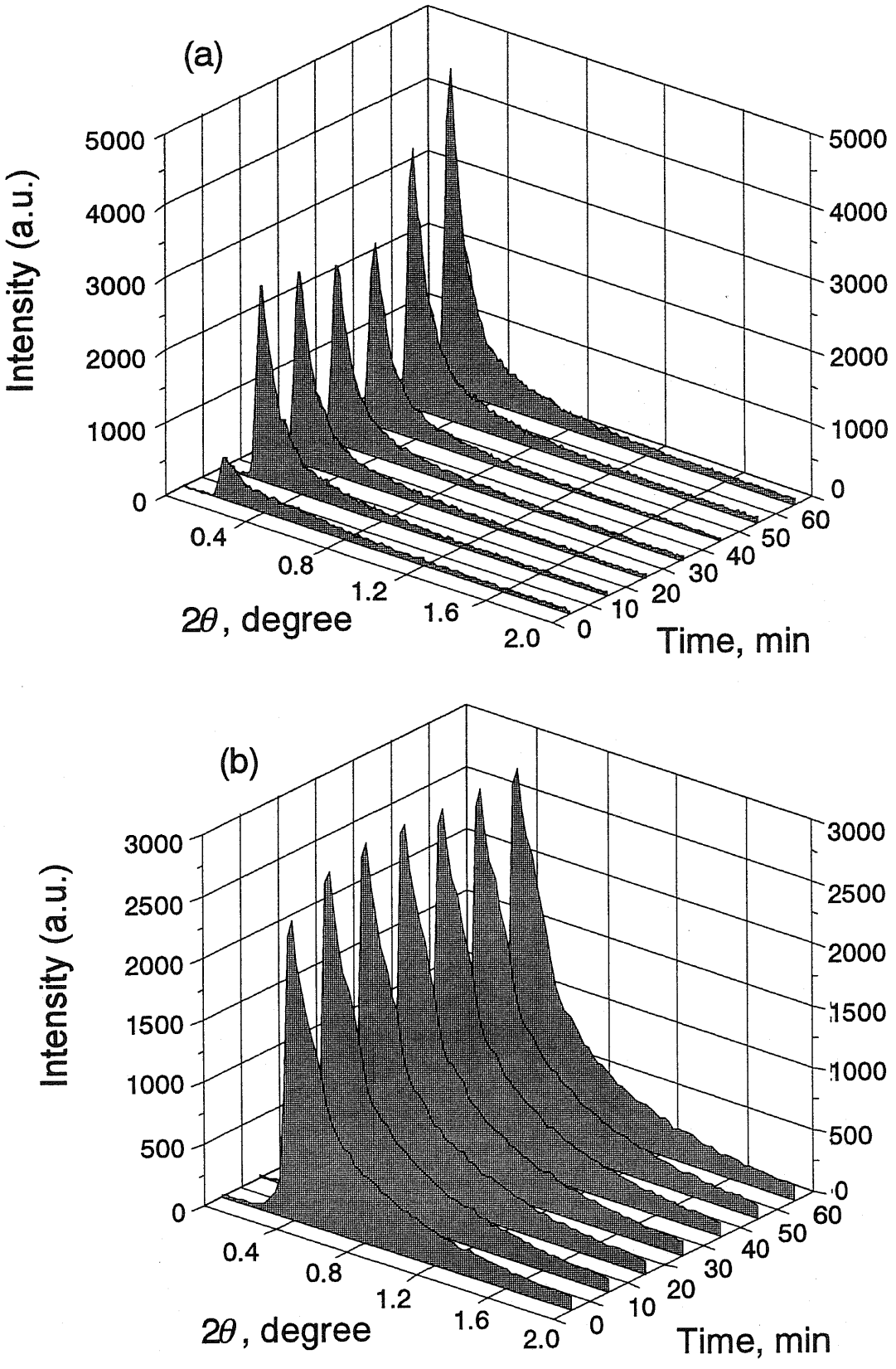

Figure 3-8. SAXS pattern by synchrotron radiation of (a) 2 wt% R-MC and (b) 25 wt% 2,3MC-1b solutions at 65 °C.

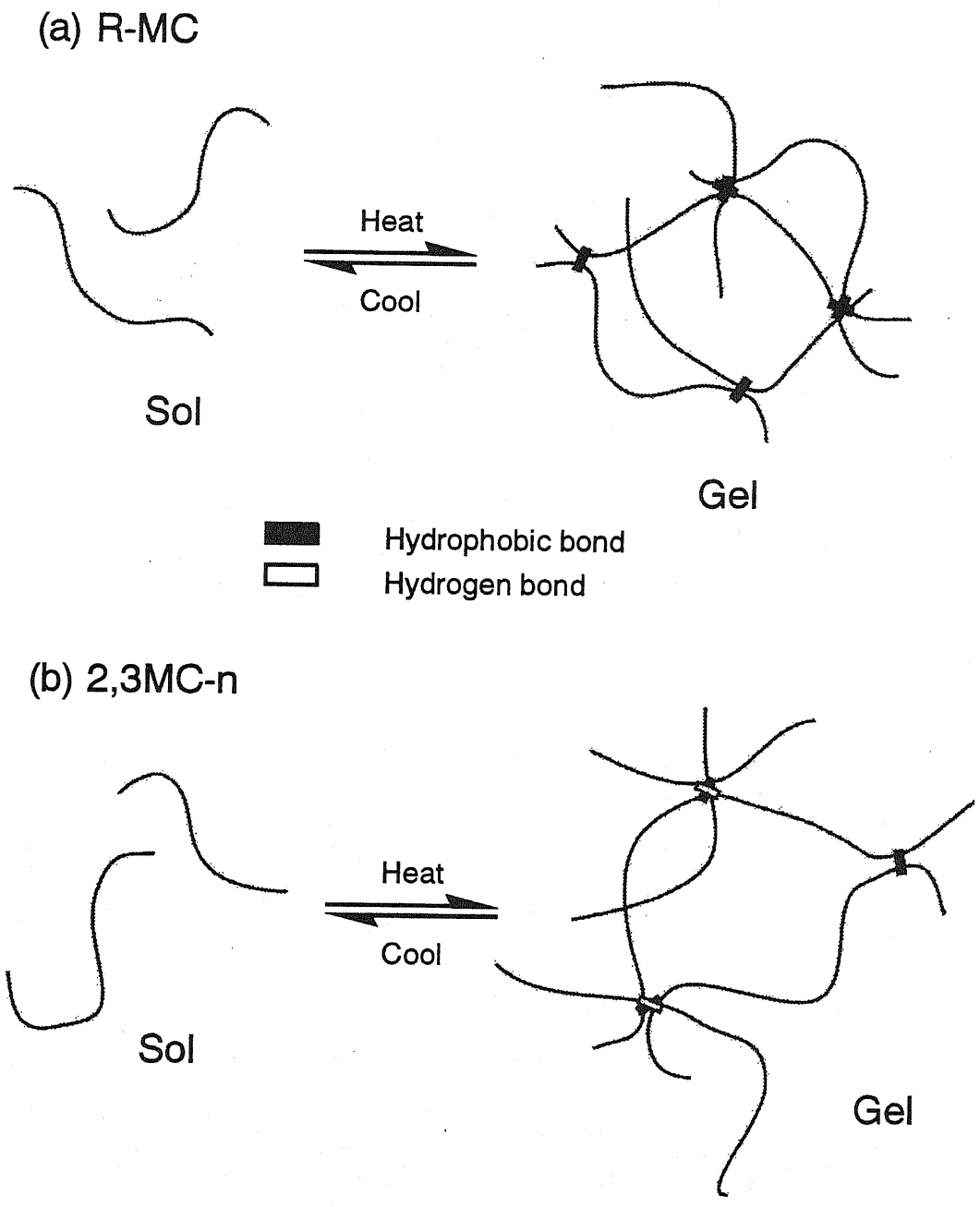

Figure 3-9. The structure of (a) R-MC and (b) 2,3MC-n gels.

to form three-dimensional networks by themselves, but are sterically able to form the intermolecular hydrogen bonds with OH groups at C(6) position to lead to crosslinking networks. Thus in *O*-methylcellulose/water system, the gel formation is caused by the hydrophobic interaction as well as the intermolecular hydrogen bonds. These phenomena were also shown in the gelation of 2,3-di-*O*-benzylcellulose in tetrahydrofuran[20,21]. The main cause for the gelation was the hydrogen bonds with OH groups at C(6) position, whereas the hydrophobic interaction between benzyl groups also kept 2,3-di-*O*-benzylcellulose molecules associated with one other.

The superstructures aggregated states for R-MC and 2,3MC-1b solutions were investigated using SAXS. Figure 3-8 shows the reflections from $2\theta = 0.3$ ($d = 288$ Å) to 1.2° ($d = 72$ Å) in SAXS patterns for R-MC and from $2\theta = 0.4$ ($d = 215$ Å) to 1.6° ($d = 54$ Å) for 2,3MC-1b solutions, respectively. This indicates that the reflection corresponds to the gel structures aggregated in these solutions and yet the gel structures have irregular size. In R-MC, the intensity of the reflection at $2\theta = 0.4$ ($d = 215$Å) increased after 40 min. Because the main cause for the gel formation in R-MC solution is the hydrophobic interaction among trimethyl glucose sequences, the amounts of crosslinking networks may increase (Figure 3-9(a)). In 2,3MC-1b, the intensity of the reflection at $2\theta = 0.7$ ($d = 123$ Å) slightly increased with the measuring time. This means that the crosslinking networks, which were formed by the intermolecular hydrogen bonds with OH groups prior to gelation, are not able to grow sterically (Figure 3-9(b)). Therefore, it indicates that the growing of crosslinking junction may be dependent on the hydrophobic interaction in the gels.

3.4 Conclusion

The gel formation of the 2,3MC-n samples and R-MC in aqueous solution was investigated in this research. The distribution of the unsubstituted OH groups in 2,3MC-n cast films were calculated from the area of OH stretching bands in IR spectra. In 2,3MC-n series, the gelation was dependent on the flexibility of the cellulose molecular chains restrained by the intramolecular hydrogen bonds. 2,3MC-n samples having less intramolecular hydrogen bonds in solutions are prone to form the gel on heating.

Three solutions from 2,3MC-nb series as well as R-MC solution formed gel. The concentration of 2,3MC-nb series to form a gel was between 20 and 25 wt%, whereas

that of R-MC was between 1 and 5 wt%. The DSC thermograms of the 2,3MC-n solutions in the heating scan showed monotonic endothermic curves, whereas that of R-MC showed two endothermic peaks. These results suggest that the gelation mechanism of 2,3MC-nb samples may involve other interactions differing from the hydrophobic interaction as seen in R-MC solutions.

The OH region of water in NIR spectra of the sample solutions was composed of water species involving 0, 1, and 2 hydrogen bonds per molecules (S0, S1, and S2), respectively. The areas of S1 for both 2,3MC-1b were larger than that for solvent alone (pure water), and were slightly larger than that for R-MC at 90 °C. This indicates presence of the intermolecular hydrogen bonds between the sample and water. 2,3MC-1b gel is considered to form the intermolecular hydrogen bonds with OH groups at C(6) position, because methyl groups at C(2) and C(3) positions are almost unable to form three-dimensional networks. The gel formation of 2,3MC-1b solution present here can explain that there is no increasing in the intensity of the reflection at $2\theta = 0.7$ ($d = 123$ Å) in SAXS pattern.

References

1. S. Takaragi, T. Fujimoto, T. Miyamoto, H. Inagaki, *J. Polym. Sci. A: Polym. Chem.*, **25**, 987 (1987).
2. K. Hayakawa, *Cellulose Commun.* **7**, 72 (2000) in Japanese.
3. T. Kato, M. Yokoyama, A. Takahashi, *Colloid Polym. Sci.*, **256**, 15 (1978).
4. K. Suzuki, Y. Taniguchi, T. Enomoto, *Bull. Chem. Soc. Jpn.*, **45**, 336 (1978).
5. N. Sarkar, *J. Appl. Polym. Sci.*, **24**, 1073 (1979).
6. N. Sarkar, *Carbohydr. Polym.*, **26**, 195 (1995).
7. M. Vigouret, M. Rinaoudo, J. Desbrières, *J. Chem. Phys.*, **93**, 858 (1996).
8. M. Hirren, J. Desbrières, M. Rinaoudo, *Carbohydr. Polym.*, **31**, 243 (1997).
9. T. Kondo, *Cellulose*, **4**, 281 (1997).
10. H.Q. Liu, L. N. Zhang, A. Takaragi, T. Miyamoto, *Cellulose*, **4**, 321 (1997).
11. T. Kondo, *J. Polym. Sci. B: Polym. phys.*, **32**, 1229 (1994).
12. T. Kondo, *J. Polym. Sci. B: Polym. phys.*, **35**, 717 (1997).
13. K. Tashiro, M. Kobayashi, *Polymer*, **32**, 1516 (1991).
14. M. Hirren, C. Chevillard, J. Desbrières, M. A. V. Axelose, M. Rinaoudo, *Polymer*,

39, 6251 (1998).

15. H. Nishimura, N. Donkai, T. Miyamoto, *Macromol. Symp.*, 120, 303 (1997).
16. W. C. McCabe, H. F. Fisher, *Nature*, **207**, 1274 (1965).
17. W. C. McCabe, H. F. Fisher, *J. Phys. Chem.*, **74**, 2990 (1970).
18. K. Buijs, G. R. Choppin, *J. Chem. Phys.*, **39**, 2035 (1963).
19. V. Founés, J. Chaussidon, *J. Chem. Phys.*, **68**, 4667 (1978).
20. H. Itagaki, I. Takahashi, M. Natsume, T. Kondo, *Polym. Bull.*, **32**, 77 (1994).
21. H. Itagaki, M. Tokai, T. Kondo, *Polymer*, **38**, 4201 (1997).

Chapter 4

Characterization of Hydrogen Bonds in *O*-Methylcellulose/Dimethyl Sulfoxide/Water System by FT-NIR Analysis

4.1 Introduction

Dimethyl sulfoxide (Me_2SO)/water mixture, which is known to be a "magic solvent" for reduction of the freezing point, was employed as a solvent system. Commercial *O*-methylcellulose with the DS range of 1.5-1.8, which is soluble in both water and Me_2SO, forms a strong gel in Me_2SO/water mixture. Because Me_2SO interacts strongly with water resulting in the change of supermolecular structure[1] of water, it may affect the gel properties as reported in other polysaccharides such as amylose[2,3], curdlan[4], agarose[5,6], and pectin[7], as well as poly(vinyl alcohol)[8,9,10]. Since the presence of Me_2SO was assumed to change the structures of junction zones in the gel.

In the previous chapter, the gelation mechanism of *O*-methylcellulose aqueous solution was investigated using regioselectively substituted *O*-methylcellulose. The distribution of the methyl substituents may contribute to the formation of hydrogen bonds as well as the hydrophobic interaction engaging cross-linking junction zones for these gels. In this chapter, the author has attempted to elucidate the effect of intermolecular hydrogen bonds and distribution of substituents in the *O*-methylcellulose samples in the Me_2SO/water system by near-infrared spectroscopy (NIR). The author also reports the relationship between the hydrogen bonding formation and the gelation mechanism in this system.

4.2 Experimental

4.2.1 Materials

O-methylcellulose samples were prepared as the partially methylated 2,3- *O*-methylcellulose series (2,3MC-n: n = 0-3) and commercially available *O*-methylcellulose (R-MC) as same samples in Chapter 2. In addition, 2,3MC-0 was

prepared by the single-methylated with the half amounts of the reagent (methyl iodide). Then the above samples were purified as described in Chapter 2.

4.2.2 Characterization of *O*-Methylcellulose Films

HPLC, ^{1}H-NMR, FT-IR data were measured and analyzed according to described methods in Chapter 3.

4.2.3 Measurements of *O*-Methylcellulose Solutions

The dried samples were dissolved in Me_2SO in a vial, and then desired amounts of water were added to the Me_2SO solution. All the solutions were prepared at room temperature. Me_2SO/water composition was 100/0, 90/10, 80/20, 70/30, 50/50, 30/70, and 0/100 (wt/wt%) respectively. The solution was judged to have a gel or sol in the vial when the specimen could flow by itself by tilting from the horizon.

FT-NIR measurements and curve fitting of NIR spectra was same methods in Chapter 3. Peak range for curve fitting was 5400-4700 cm^{-1}.

4.3 Results and Discussion

4.3.1 Gelation of *O*-Methylcellulose Solutions

(1) Sol-gel transition

Table 4-1 indicates the characteristics of 2,3MC-n samples and R-MC and the states of them in three solvent systems: Me_2SO (Me_2SO/water = 100/0), Me_2SO/water mixture (70/30), and water (0/100). All samples in Me_2SO did not form gel, and still remained sol states on heating. This means that Me_2SO is better solvent to the *O*-methylcellulose samples used in this research. 2,3MC-n samples (15 wt%) and R-MC (0.5-2 wt%) in Me_2SO/water mixture (70/30) exhibited high viscosity on increasing water content and finally formed opaque gel at room temperature. This is considered to be due to formation of a strong interaction between Me_2SO and water, which may cause the reduction of the interaction of the samples with either Me_2SO or water. In other words, as the solubility of the samples was reduced, then the solutions were able to form gel. In water, some of the 2,3MC-n samples remained sol at room temperature, and then showed gel formation on heating. However, 2,3MC-0 which was considered to contain more intramolecular hydrogen bonds as listed in Table 4-1, did not exhibit gelation on

heating. Thus, the gelation may be dependent on the flexibility of the cellulose chain, which may be strongly influenced by the intramolecular hydrogen bonds between C(3)-OH and the adjacent ring oxygen. On the other hand, the 2,3MC-n samples having less intramolecular hydrogen bonds in solutions are prone to form a gel as shown in Chapter 3.

(2) Gel-sol transition

In Figure 4-1, the relationship between the concentration of the samples and Me_2SO/water composition is shown as the phase diagrams for R-MC and 2,3MC-0 at room temperature, respectively. These samples did not form gel both in Me_2SO and in water (pure solvent systems) at the room temperature. When either the concentration of the samples or water content in the solutions was increased, both the ability of gel formation and the viscosity of gel were increased. In R-MC/Me_2SO/water system, the concentration where the gel formed was over 0.5 wt% at room temperature, whereas R-MC/water solution was not transformed to gel without heating as shown in Chapter 3. R-MC gel was stable on heating.

Interestingly, the 2,3MC-0 gel, which was formed in Me_2SO/water mixture at room temperature at lower concentration (5 wt%), was turned to sol on heating. This phenomenon indicates that the hydrophobic interaction engaging cross-linking junction zones in 2,3MC-0 gel is weaker than that in other gels, because 2,3MC-0 have more OH groups at C(6) position which are considered to be favorable to formation of the intermolecular hydrogen bonds. Thus the author could assume that the intermolecular hydrogen bonds between 2,3MC-0 and the solvent are maintained in 2,3MC-0 gel.

4.3.3 Characterization of *O*-Methylcellulose Solutions

NIR spectra of the R-MC and 2,3MC-0 in Me_2SO/water mixture were obtained to investigate the hydrogen bonding formation of water in this system. Figure 4-2 shows the OH band of water in NIR region between 4700 and 5400 cm^{-1} which was assigned to be $\nu_s + \nu_{as}$ combination. The ν_s and ν_{as} indicate the OH symmetric and the OH anti-symmetric stretching vibration, respectively. The OH absorption band was resolved into three component bands, where the peak tops were located at 5250, 5160, and 5060 cm^{-1}. These bands were assigned to be the free water molecules (S0), water molecules with one OH engaged in hydrogen bond (S1), and those with two OH engaged in hydrogen

bonds (S2), respectively (shown in Figure 3-7)[11,12].

Table 4-2 indicates the changes of S0, S1, and S2 areas in the OH bands of NIR spectra in relation to the Me_2SO/water composition together with the data for R-MC and 2,3MC-0 samples. When water content was increased from 10 to 50 wt%, the area of S1 was decreased, with increasing in the area of S2. The change in the area of each states of water molecule was more drastic in water content from 10 to 30 wt% than the content from 30 to 50 wt%. The change in the states of water molecules was most prominent, since the area of S0 was the smallest at the water content of about 30 wt%. The phenomenon that the interaction between Me_2SO and water was the strongest at 30 wt% water content was observed for other polysaccharide in Me_2SO/water mixture[2-10]. One possible interpretation is that the appearance of maximum in these systems may correlate to the hydration forms in Me_2SO/water mixture. The two hydration forms in the Me_2SO/water mixture were proposed to be $Me_2SO{\cdot}2H_2O$ from the results based on NMR[13], viscosity[14,15] and ultrasound velocity measurements[16], and to be $Me_2SO{\cdot}3H_2O$ from neutron scattering[1].

When the water content range was from 10 to 20 wt%, the areas of S1 for both R-MC and 2,3MC-0 solutions were larger than that of the solvent alone (Me_2SO/water mixture). When the water content range was from 30 to 50 wt%, the areas of S1 for both solutions were similar to that of the solvent alone (Me_2SO/water mixture). According to Bonner *et al.*[17] and Scherer *et al.*[18], there are some water molecules having one stronger and one weaker hydrogen bonds (S1) and the water molecules having hydrogen bonds of nearly equal strength (S2). Thus in this system, S1 can correspond to be the amount of water molecules interacted with the *O*-methylcellulose or Me_2SO. In the range where Me_2SO interacts poorly with water, *i.e.*, in the range of water content between 10 and 20 wt%, intermolecular hydrogen bonds between the samples and water are suggested to be presented.

The changes of S0, S1, and S2 areas for R-MC and 2,3MC-0 in Me_2SO/water (70/30) as a function of temperature, were listed in Table 4-3. At 90 °C, the area of S1 decreased, whereas the areas of S0 and S2 increased. Because of the breakage of some hydrogen bonds between water and Me_2SO, the resulting water molecules may be altered to be free states (S0) or two hydrogen bonded (S2). The areas of S1 for both R-MC and 2,3MC-0 solutions were larger than that for the solvent alone at 90 °C. This

Table 4-1. Molecular weight and degree of substitution (DS) of methyl and hydroxyl groups in the *O*-methylcellulose samples, and gel formation from the solution of the samples studied.

Samples	M_n[a]	DS in film					Me_2SO/water system (wt/wt%)		
		Total-DS(OMe)[b]	Total-DS(OH)[c]	Free-OH[d]	Intra-OH[d]	Inter-OH[d]	100/0[e] (Me_2SO)	70/30[e]	0/100[e] (water)
R-MC	279,300	1.60	1.40	-	-	-	×	○	●
2,3MC-0	28,700	0.71	2.29	0.009	1.211	1.068	×	○	×
2,3MC-1	18,100	1.05	1.95	0.014	1.121	0.815	×	○	●
2,3MC-2	17,700	1.28	1.72	0.025	0.988	0.707	×	○	●
2,3MC-3	16,200	1.85	1.15	0.008	0.630	0.512	×	○	●

[a] M_n is molecular weight, and determined by HPLC.
[b] Total-DS(OMe) is the degree of substituted methyl groups, and determined by ^{1}H-NMR measurements.
[c] Total-DS(OH) is the degree of unsubstituted hydroxyl groups, and calculate d by subtracting the degree of subsitituents methyl groups of Total-DS(methyl) from 3.
[d] DS of Free-, Intra-, and Inter-OH are calculated by multiplying DS of Total-DS(OH) by the percentage of each area to that of the total area of the OH band.
[e] ○ gelation at room temperature, ● gelation on heating, × no gelation on heating.

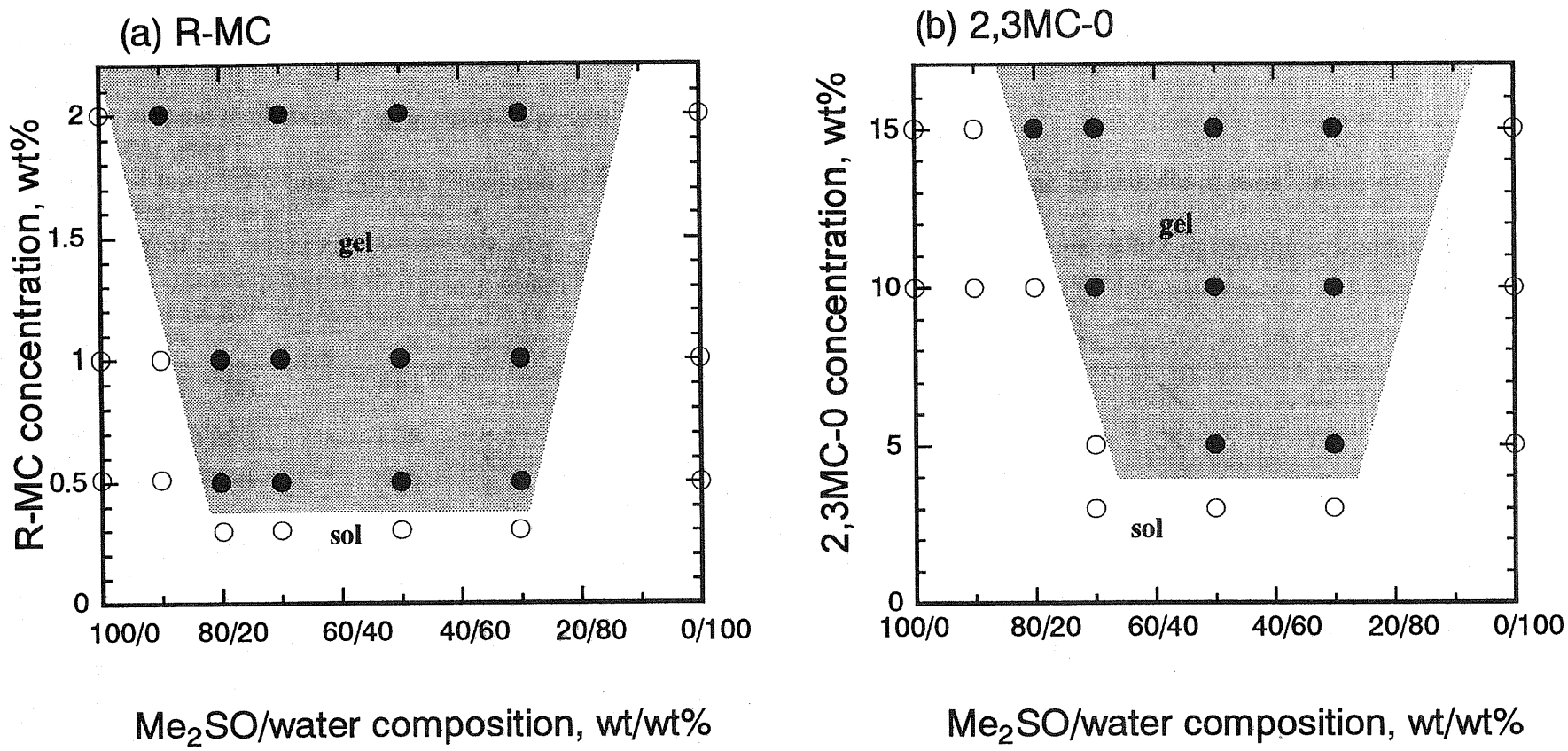

Figure 4-1. The dependence of gelation of (a) R-MC and (b) 2,3MC-0 on the sample concentration and Me_2SO/water composition at room temperature: ● gelation and ○ no gelation.

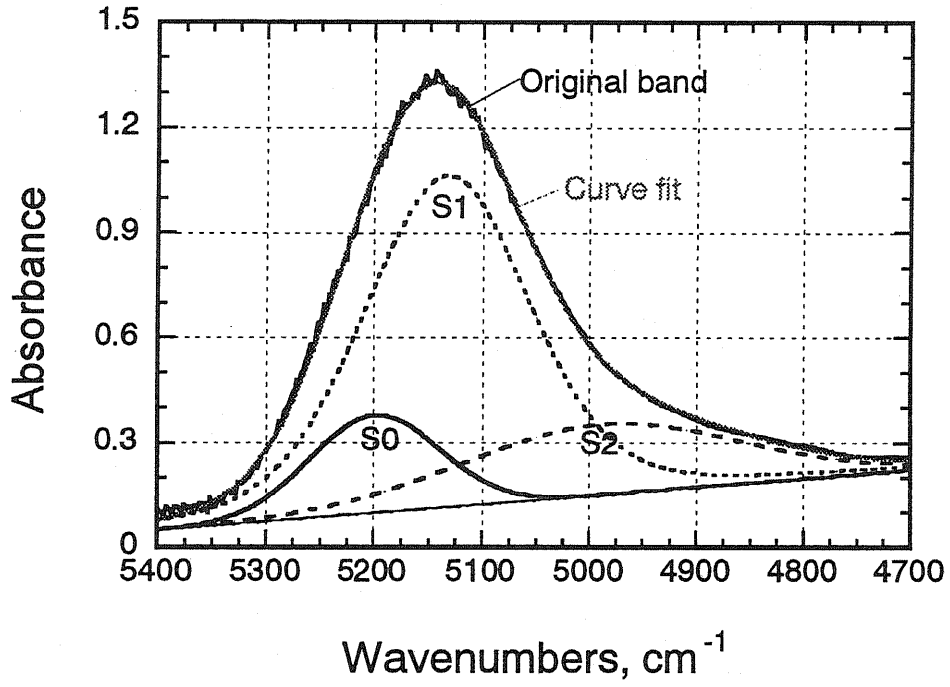

Figure 4-2. Curve fitting and peak assignments for OH band ($\nu_s + \nu_{as}$) of water in NIR spectrum of 2,3MC-0/Me_2SO/water system. The S0, S1, and S2 indicate free OH, one hydrogen bonded OH, and two hydrogen bonded OH, respectively.

Table 4-2. The changes of S0, S1, and S2 areas in the OH bands of water in NIR spectra of the *O*-methylcellulose solutions versus Me_2SO/water composition.

Me_2SO/water (wt/wt%)	Solvent alone (Me_2SO/water)			R-MC solution (1 wt%)			2,3MC-0 solution (10 wt%)		
	S0[a]	S1[a]	S2[a]	S0[a]	S1[a]	S2[a]	S0[a]	S1[a]	S2[a]
90/10	6.0	66.8	26.3	4.3	81.0	14.7	8.8	69.9	21.3
80/20	4.5	53.7	41.8	3.2	60.4	36.4	6.7	54.0	39.3
70/30	2.4	51.9	45.7	1.8	55.5	42.7	3.2	50.5	46.3
50/50	2.9	49.0	47.2	4.2	48.1	41.7	2.2	51.8	46.0

[a]S0, S1, and S2 indicate the water molecules with non hydrogen bond, one hydrogen bond, and two hydrogen bonds, respectively.

Table 4-3. The changes of S0, S1, and S2 areas in the OH bands of water in NIR spectra of the *O*-methylcellulose solutions (Me_2SO/water = 70/30 (wt/wt%)) on heating.

Water species	Solvent alone (Me_2SO/Water)		R-MC solution (1 wt%)		2,3MC-0 solution (10 wt%)	
	30 °C	90 °C	30 °C	90 °C	30 °C	90 °C
S0	2.4	6.3	1.8	7.5	3.2	7.7
S2	45.7	56.1	42.7	43.3	46.3	50.7
S1	51.9	37.6	55.5	49.2	50.5	41.6

indicates the presence of intermolecular hydrogen bonds between the samples and water at the temperature where Me_2SO interacts poorly with water.

4.4 Conclusion

The gel formations of the 2,3MC-n samples and R-MC in Me_2SO/water solvent systems were investigated in this research.

All samples in Me_2SO remained as a sol, and some of them in water showed a gelation upon heating. All samples in Me_2SO/water system (70/30) formed a gel at room temperature. The poor solvent to the samples was in the order of Me_2SO/water mixture > water > Me_2SO. In all samples in Me_2SO/water system, the interaction between Me_2SO and water reduces the solubility of samples, and then enhances the gelation ability of them.

2,3MC-0 gel (5 wt%) in Me_2SO/water mixture was turned to sol upon heating. This indicated that even in the poor solvent (Me_2SO/water mixture), the intermolecular hydrogen bonds between OH groups at C(6) position in 2,3MC-0 gel and the solvent is maintained, because the hydrophobic bonds in 2,3MC-0 gel are weaker than those in other gels.

The OH bands of water in NIR spectra both of R-MC and 2,3MC-0 in Me_2SO/water mixture were decomposed into three water species, S0, S1, and S2 which were indicated as a non-hydrogen bonded species, an asymmetrically hydrogen bonded species, and a symmetrically hydrogen bonded species, respectively. When the water content range was from 10 to 20 wt%, the areas of S1 for both of R-MC and 2,3MC-0 solutions were larger than that for the solvent alone (Me_2SO/water mixture), thus indicating the presence of the intermolecular hydrogen bonding between the samples and water in this system.

References

1. D. H. Rasmussen, A. P. MacKenzie, *Nature*, **220**,1315 (1968).
2. H. Takeyama, M. Kobayashi, H. Yajima, R. Endo, K. Kohyama, K. Nishinari, *Macromol. Chem. Macromol. Symp.*, **76**, 83 (1993).
3. H. Takeyama, M. Kobayashi, H. Yajima, R. Endo, K. Kohyama, K. Nishinari, in "*Food Hydrocolloids -Structures, Properties and Functions-*", K. Nishinari, E. Doi,

eds., Plenum Press, New York, (1994) pp. 183-186.

4. M. Watase, K. Nishinari, in "*Food Hydrocolloids -Structures, Properties and Functions-*", K. Nishinari, E. Doi, eds., Plenum Press, New York (1994) pp. 125-129.
5. M. Watase, H. Arakawa, *Nippon Kagakukaishi*, 7, 1353 (1973) in Japanese.
6. M. Watase, K. Nishinari, *Polym. J.*, **20**, 1125 (1988).
7. M. Watase, K. Nishinari, *Carbohydr. Polym.*, **20**, 175 (1993).
8. M. Watase, K. Nishinari, *Polym. J.*, **21**, 567 (1989).
9. M. Watase, K. Nishinari, *Polym. J.*, **21**, 597 (1989).
10. C. Sawatari, Y. Yamamoto, N. Yanagida, M. Matsuo, *Polymer*, **34**, 956 (1993).
11. V. Founés, J. Chaussidon, *J. Chem. Phys.*, **68**, 4667 (1978).
12. K. Bujis, G. R. Choppin, *J. Chem. Phys.*, **39**, 2035 (1963).
13. J. M. G. Cowie, P. M. Toporowske, *Can. J. Chem.*, **39**, 2240 (1961)
14. R. K. Wolford, *J. Phys. Chem.*, **68**, 3392 (1964).
15. S. A. Schichman, R. L. Amey, *J. Phys. Chem.*, **75**, 98 (1971).
16. D. E. Bowen, M. A. Priesand, M. P. Eastman, *J. Phys. Chem.*, **78**, 2611 (1974).
17. O. D. Bonner, Y. S. Choi, *J. Phys. Chem.*, **78**, 1723 (1974).
18. J. R. Scherer, M. K. Go, S. Kint, *J. Phys. Chem.*, 77, 2108 (1973).

Chapter 5

Durable Water Repellent Cotton Fabrics Prepared by Low-degree Substitution of Long Chain Alkyl Groups

5.1 Introduction

Water-repellent cotton fabrics have the advantage of being breathable, allowing water vapor to transpire through the fabrics but not water droplets. Some typical uses are rain-wear, medical bandages, or cover tapes for adhesive plasters in kitchen and out-door activities. Generally, water and oil repellency is conferred to natural cotton fabrics by spraying synthetic high polymers of suitable compositions, or by resin coating with perfluoro ester aziridines[1,2], zirconium compounds[3], radical crosslinking of methyl or cyanoethyl silicones[4], crosslinking of fluorocarbon resins on the fabrics[5], or covalent condensation of stearamidomethyl-pyridinium chloride on the fabric surface[6], but such water and oil repellency does not persist on repeated launderings or dry cleanings[7]. Water- and oil-repellent cotton fabrics have been produced by covalent modification with perfluoro-chemicals[8,9], but only with additives of chromium complexes, which may cause environmental pollution. One might suppose that water-repellent cotton fabrics may be produced by heavy covalent modification with hydrophobic functional groups such as alkyl or haloalkyl groups, but such fabrics might lose some of important characteristics of natural cotton such as fabric hand, biodegradability, etc. In this chapter, the author reports on water-repellent cotton fabrics prepared by low-degree substitution of long chain alkyl groups. Water repellency of the treated fabrics withstands repeated laundering, and the fabrics also retain biodegradability. Since the use of organic halogen is strictly limited in the preparation, it will not cause any severe environmental hazard in the future.

5.2 Experimental

5.2.1 Material

Cotton fabric (plain weave shirting, 27 × 30 yarns/cm, 36 × 40s) was supplied from Iseikatsu-kenkyukai (Clothing-life Research Assoc.), Tokyo. All fabric was scoured by boiling in 0.5% NaOH for 20 min, rinsed with distilled water several times, and then air

dried before subsequent treatments.

5.2.2 Preparation Methods and Samples

The alkylation was done by two reaction conditions, *i.e.*, alkylation by means of acetylation and by allylation and bromination, as shown in Figure 5-1. The detailed procedures for preparing the samples are reported below.

(1) Sample A: alkylation by acetylation of native cotton

The alkylation procedure was based on the method of Kondo and Gray[10]. Before alkylation, cotton fabrics were acetylated using the following procedure. Scoured cottons were immersed in acetic acid (20 °C, bath ratio 1:30) for 30 min and squeezed to 165 wt%. The squeezed cottons were immersed in acetylation bath at 15 °C for 10 min. The proportion of cotton and chemicals were; 10 cotton: 100 acetic acid: 24 acetic anhydride: 0.7 sulfuric acid. The acetylated cotton was rinsed under running water for 70 h and air dried. The cotton fibers were soaked in a mixture of disperse and direct dye. Microscopic observation of the fiber cross sections revealed that only the surfaces were stained by the disperse dye, indicating that only the surfaces were acetylated. The acetylated cottons were then subjected to the following alkylation procedure. The total amount of octadecyl iodide was 1.3 mol to the glucose unit. Dried acetylated cotton fibers (1 g) were immersed in 60 mL of Me_2SO at 60 °C. Then 5.86 g powdered NaOH and 1 mL water were added to the mixture. Following 1 h stirring under nitrogen atmosphere, two thirds of the total amount of the octadecyl iodide was added step by step to the solution. The remaining octadecyl iodide was added in three equal portions at 2, 3, and 4 h after the first addition. Following the last addition of octadecyl iodide to the solution, the temperature was raised to 70 °C and kept there for 20 h under nitrogen atmosphere. The samples were taken from the mixture and washed with chloroform several times.

(2) Sample B: Alkylation by acetylation of mercerized cotton fabric

Cotton fabrics (1 g) were mercerized in 150 mL of 18% NaOH at 22 °C for 2 h. After the treatment, the fabrics were rinsed with running water for 24 h, with distilled water twice, and then air dried. The mercerized fabrics were treated by the same alkylation method as described for Sample A.

(3) Sample C: Alkylation by allylation and bromination of mercerized cotton

Cotton fabrics were mercerized in the same conditions as for Sample B, then allylated and subsequently brominated following the procedure reported previously[11]. Brominated and dried sample were imersed in the mixture of octadecylamine and 2-propanol at a ratio of 1:1.5 and allowed to stand at 70 °C for 8 h. After the reaction, the fabric was washed thoroughly with the solvent. The unreplaced bromine residue was removed by scouring with 0.5% NaOH solution.

5.2.3 Analysis

The degree of substitution (DS) of replaced octadecyl groups ($C_{18}H_{37}$) in Sample A and Sample B, and 2-bromo-3-octadecylaminoproryl groups ($CH_2CHBrCH_2NHC_{18}H_{37}$) in Sample C were determined by elemental analysis (CHN coda type MT-5, Yanagimoto Co.). The DS of Sample C was also determined by acid-base titration: Sample C and untreated cotton were separately suspended in 0.0025 M H_2SO_4 containing 0.1% sorbitan monolaurate and left to stand for 24 h. Each 3/4 portion of the respective supernatant was titrated with 0.025 M NaOH. From the difference in the end points between Sample C and untreated cotton, the DS of Sample C was calculated to be 0.0063 per glucose unit. Calculated N content of the Sample C was 0.05% was less than the detection limit of elemental analysis.

IR spectra were obtained at 2 cm^{-1} resolution on Perkin-Elmer 1720X FTIR spectrometer using the KBr method at 1.5% sample concentration. The absorbance intensity of the IR band was defined as the peak height from the baseline of the band.

5.2.4 Water Repellency and Its Durability

All the laundry tests were 40 °C throughout. Four of the samples were given repeated launderings according to JIS-L-0844-1973 (A-1). Treated fabrics (7 × 7 cm) were immersed in a test jar containing 100 mL of 0.5% soap (sodium salt of fatty acid, commercial product) solution and stainless-steel globes at 40 °C. The test jar was clamped in a standard launder meter LM-8D (Suga Test Instrument Co.), and run for 30 min. The fabrics were taken from the jar and rinsed in a jar containing 100 mL of fresh water for 1 min with stirring. Rinsing of the washed fabrics was repeated three times,

followed by air drying.

The contact angle of the treated fabrics was evaluated before and after the laundry test. A photographic picture of a water drop (10 μL, 25 °C) on the test fabrics was taken and the contact angle (θ, degrees) was estimated by measuring the height (h) and diameter (d) of the drop as:

$$\tan(\theta/2) = 2h/d$$

Water repellency durability of the test fabrics versus repeated laundry was evaluated by spray test according to the JIS L-1092-1992 (5.2) spray test, defined by the Japanese Industrial Standards Committee. Water (250 mL) was sprayed on fabric fitted on a 20 cm diameter circular frame rotating in a plane 45° to the horizontal. The effect was evaluated as an index between 0 and 100, where 0 is complete wetting out and 100 is total water repellency.

Percent water retained was measured according to the following method. A weighed amount (wt_0) of absolutely dried cellulose sample (Sample A, Sample B, Sample C, or untreated cellulose sample dried at 105 °C) was immersed in water with sinkers, and wetted completely by repeated removal of air-bubbles. The sample was taken out from the water, the excess water was removed by free-hanging in air for 2 min, and the sample was weighed (wt_1). Percent water retained is defined as:

$$\text{Water retained (\%)} = 100\ (wt_1\text{-}wt_0)/wt_0$$

Moisture regain was measured by the method defined by JIS 1096-1990 (6.9). A weighed amount (wt_0) of absolutely dry cellulose sample (Sample A, Sample B, Sample C, or untreated cellulose sample) was left to stand in standard condition (20 ± 1 °C, and 65 ± 2% RH) for 24 h and weighed (wt_2). Percent moisture regain is defined as:

$$\text{Moisture regain (\%)} = 100\ (wt_2\text{-}wt_0)/wt_0$$

Water vapor permeability was determined by the water method defined by JIS L-1099-1993 (A-2).

The dye adsorption of untreated and treated samples was tested with two kinds of dyestuffs (Figure 5-2): Solar orange (acid dye, wavelengths (λ_{max}) = 484 nm) and Direct orange (λ_{max} = 493 nm). The dye concentration in the dyebath was 40 mg/L, and the batl. atio was 500:1. No co-agent was added to the acid dyebath, and 2.5% NaCl was

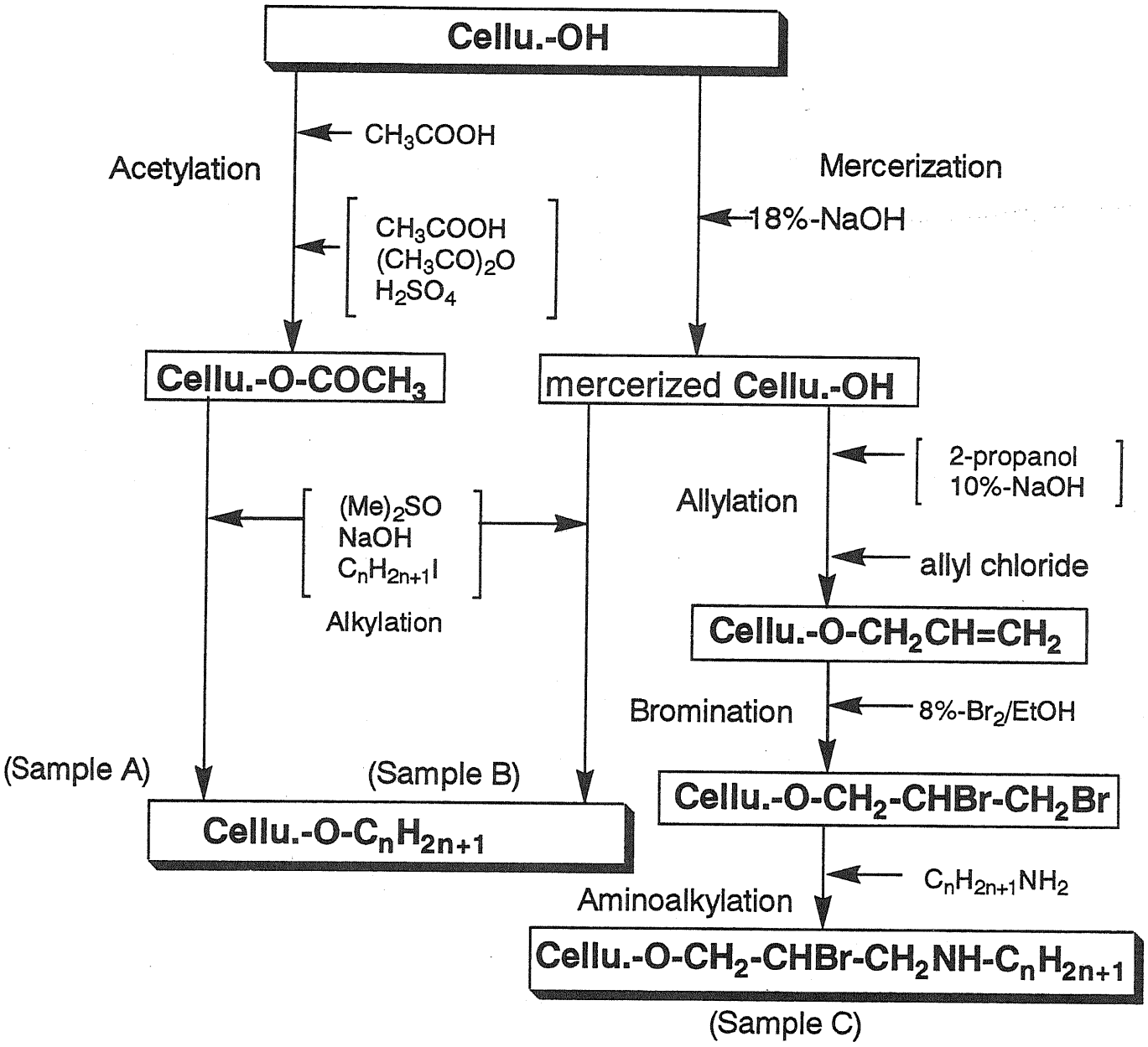

Figure 5-1. Procedure for preparation of water-repellent cotton fabrics.

(a) Direct Orange

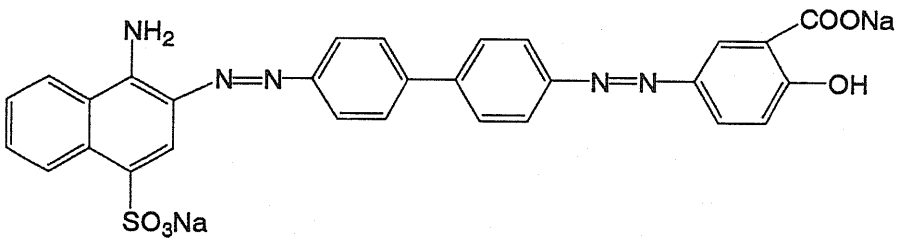

(b) Solar Orange

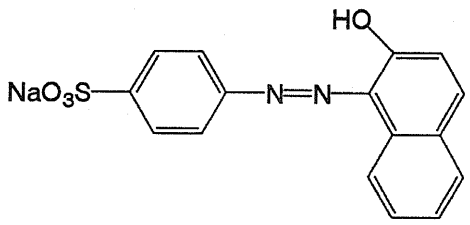

Figure 5-2. The chemical structures of dyestuffs in this study.

added to the direct dyebath. Samples were immersed in the dyebaths at room temperature and heated to 90 °C during 30 min, then dyeing continued for 30 min. After the dyeing, dye concentrations in the baths were determined by the absorbance at each λ_{max} measured with a Shimadzu UV 2000 spectrophotometer.

Biodegradability was measured according to the following method; crude cellulase (0.94 mg/mL) prepared from *Trichoderma viride*[12] dissolved in 20 mmol acetate buffer, pH 5.0, was centrifuged for 20 min at 5,000 rpm to remove turbidity, then used as the cellulase solution. Sample A, Sample B, Sample C, and untreated cellulose, each 5 mg, were suspended in 7.0 mL of the cellulase solution controlled at 37 °C. The suspensions were stirred during the reaction. Enzymatic breakdown of cellulose samples will produce reducing sugar. The reducing sugar in the supernatant was determined by the methods of Somogyi[13] and Nelson[14].

5.3 Results and Discussion

5.3.1 Effect of Alkyl Length on Water Repellency

Table 5-1 shows the contact angle and water repellency of Sample C prepared with alkyl substituents of different lengths. The contact angles of all samples were larger than 90°, but the spray test revealed that the preparation with alkyl substituents shorter than C_6 was rated zero. Sufficient water repellency as evaluated by both contact angle and spray tests was attained with fabrics possessing alkyl substituents longer than C_{12}. The effect of alkyl length is similar to cotton sateen samples treated with 0.5% solutions with different chain length of perfluoro-acid chromium complex[9]. Since the alkyl substituents shorter than C_6 conferred insufficient water repellency on the fabrics, the author used only octadecyl substituent to prepare Sample A, Sample B, and Sample C.

5.3.2 Sample Analyses by Elemental Analysis and IR Spectroscopy

The DS of the substituents per glucose unit was 0.073 for Sample B, 0.075 for Sample C, and 0.12 for Sample A. The IR spectra (Figure 5-3) of treated samples showed the strongest band at 1110 cm^{-1} attributed to C-O-C vibration due to asymmetric in phase breathing of the glucose ring. Since these C-O-C bands were not affected by the treatments, the author used this band as an internal reference for each sample. The strong band at 2920 cm^{-1} attributed to the CH stretching vibration was due to the

octadecyl chains. On the other hand, there were no significant changes in the strong OH stretching band at 3400 cm^{-1} and weak OH out of plane bending band located at 669 cm^{-1}. These results are in accord with the fact that fairly long alkyl chains are introduced with only low DS. Figure 5-4 shows an IR absorbance ratio of νCH(2920 cm^{-1})/νC-O-C(1110 cm^{-1}) and δOH(669 cm^{-1})/νC-O-C(1110 cm^{-1}) of the samples in the correlation for the DS of substituent. Sample A shows the highest νCH intensity ratio whereas the Sample B shows the lowest νCH intensity ratio in the treated samples. The increasing order of DS for octadecyl groups in Sample B, Sample C, and Sample A determined by the IR absorption ratio (νCH/νC-O-C) was in good agreement with that determined by elemental analysis. In Figure 5-3, Sample C shows different peaks at around 1450 cm^{-1}, corresponding to NH bending of the secondary amine. This sample contained 0.5% nitrogen and 1.5% bromine by elemental analysis, which corresponds to 0.04 and 0.06 substituents per glucose unit, respectively.

Nelson and O'Connor attempted to determine the absorbance ratio of 1372 cm^{-1}/ 2900 cm^{-1} for measuring crystallinity in cellulose materials[15], but the ratio was disturbed by the overlapping bands of CH_2 in the octadecyl substituents. Formerly, O'Connor *et al.* had proposed using the absorbance ratio of 1449 cm^{-1}/909 cm^{-1}as crystallinity index, based on their investigation of chemically decrystallized cotton[16]. In this chapter, the author used the absorbance ratio of 1428 cm^{-1}/893 cm^{-1} instead, where the 893 cm^{-1} band is amorphous sensitive, and the 1428 cm^{-1} band is crystallinity sensitive[17]. The intensity ratio of 1428 cm^{-1}/893 cm^{-1} did not change before and after the treatments, indicating that the crystallinity of these samples was not affected by these treatments.

5.3.3 Comparison of Water Repellency of Three Samples

The author evaluated water repellency by contact angles and spray tests for three samples and for cotton fabrics treated with Scotch-Gard®. All samples had sufficient water repellency, as shown in Table 5-2. The spray ratings of the samples were comparable to the data reported for FC-804 or poly(1,1-dihydroperfluorobutyl acrylate)-treated cotton, but surpassed the data reported for cotton print cloth[9]. A photograph of water drops on treated fabrics (Figure 5-5) indicates that all samples exhibited water rep 'lency regardless of DS. The water drops were able to roll about like beads on the sa. ple fabrics. The hand of these samples was different. Sample A was the softest and

had a napped surface similar to peach skin due to the stronger treatment in comparison to the other samples. The yarn density of Sample A was unchanged by the treatment, whereas the yarn density for Sample B and Sample C increased by mercerization from 27 × 30 yarns/cm to 36 × 36 yarns/cm due to the change of softness and other end-use properties, discussed later.

5.3.4 Durability of Water Repellency

Although the substituents are covalently bonded on the fabrics, laundering may damage the fabrics. The author compared durability of water repellency after repeated laundering of treated fabrics, Sample A, Sample B, Sample C, and the Scotch-Gard®, and the results are shown in Table 5-3. Sample C represents the most durable in spray rating even after 100 launderings. In comparison, Scotch-Gard® is a temporary finish, and yields no water repellency after six launderings. For Sample A and Sample B, the spray rating indicated sufficient water repellency up to ten launderings, but it diminished after twenty launderings, apparently because the alkylated surfaces of the fabrics wore out.

5.3.5 Changes in End-Use Properties with Treatments

Figure 5-6 shows the changes in moisture regain, maximum water retained, and water vapor permeability. Mercerization enhances moisture regain, whereas alkyl substituents reduce moisture regain. Sample A was not mercerized during the treatment and had the highest DS, so it showed the lowest moisture regain, 0.47%. Sample B and Sample C were mercerized in the treatment process and had moisture regain (0.77 and 0.70%, respectively), similar to the untreated sample (0.7%), indicating that the hydrophobic property of the substituent was compensated by the effect of mercerization. Water retained at the totally wetted state decreased drastically from 186% to one-half that with the treatments. Therefore, the treated fabrics showed no wicking properties when the fibers were filled with water. This property reduces the chilly feeling caused by wet cotton garments. In this case, water vapor permeability indicates similar values from 135.2 to 166.8 g/m^2h, independent of single factors such as substituents, DS, and yarn density, but these factors canceled each other. Viewing these properties, the treated fabrics had satisfactory water repellency and moisture regain without losing the merit of

Table 5-1. Contact angle and water repellency of sample C prepared by substitution with different alkyl lengths.

Alkyl length	Contact angle θ, degrees	Spray rating
n = 0	0	0
n = 3	118 - 123	0
n = 6	118 - 123	0
n = 12	118 - 130	70
n = 18	120 - 144	80

Table 5-2. Contact angle and water repellency of different samples A, B, and C, using same alkyl length of substituent, as a contrast with Scotch-Gard® treatment.

Sample	Contact angle θ, degrees	Spray rating
Untreated	0	0
Sample A	127 - 144	90
Sample B	127 - 140	90
Sample C	120 - 144	80
Scotch-Gard®	132 - 145	90

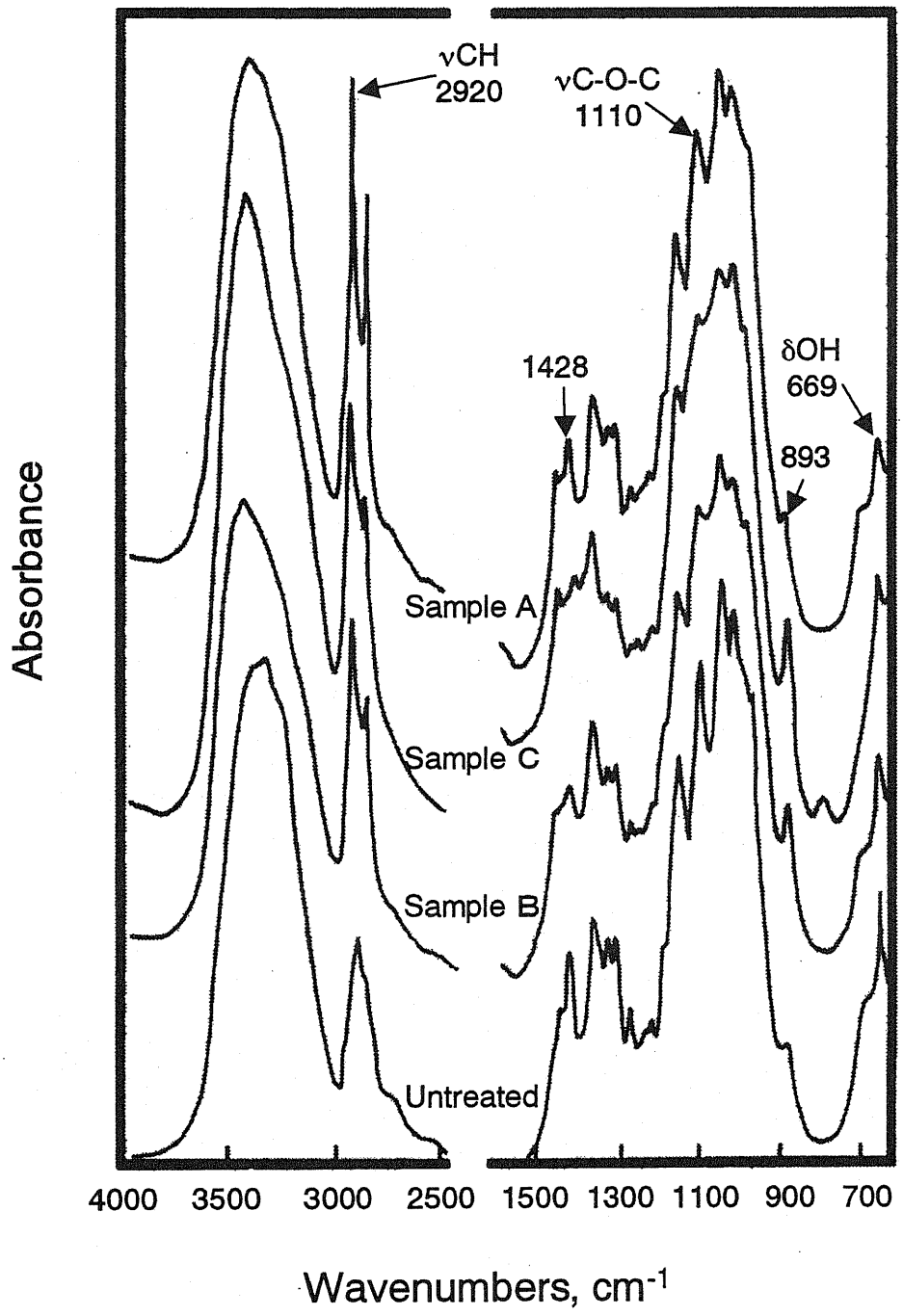

Figure 5-3. IR spectra of untreated and treated cellulose samples.

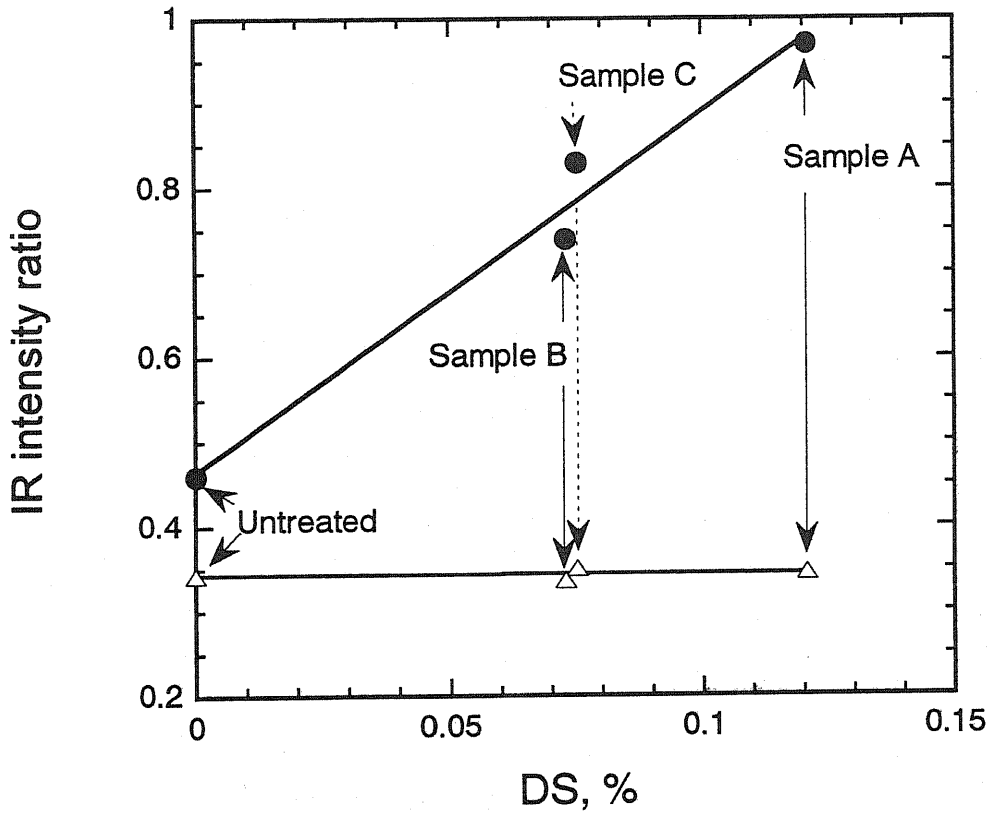

Figure 5-4. Change in IR absorbance ratio in different samples: ● νCH (2920 cm^{-1})/νC-O-C(1110 cm^{-1}), △ δOH(669 cm^{-1})/νC-O-C(1110 cm^{-1}).

(a) Sample A

(b) Sample B

(c) Sample C

(d) Scotch-Gard®

Figure 5-5. Water drops on modified or treated cotton fabrics: (a) Sample A, (b) Sample B, (c) Sample C, (d) Scotch-Gard®.

Table 5-3. Change of contact angle and water repellency of different samples A, B, C, and Scotch-Gard® after laundry cycle.

No. launderings	Sample A		Sample B		Sample C		Scotch-Gard®	
	Contact angle θ, degrees	Spray rating	Contact angle θ, degrees	Spray rating	Contact angle θ, degrees	Spray rating	Contact angle θ, degrees	Spray rating
0	127 - 144	90	127 - 140	90	120 - 144	80	132 - 145	90
3			133 - 137				131 - 145	80
6			134 - 138				0	0
20	127 - 144	30	129 - 139	0	116 - 144	80		
50	124	0			116 - 144	80		
80	123	0			114 - 144	80		
100	122	0			114 - 130	80		

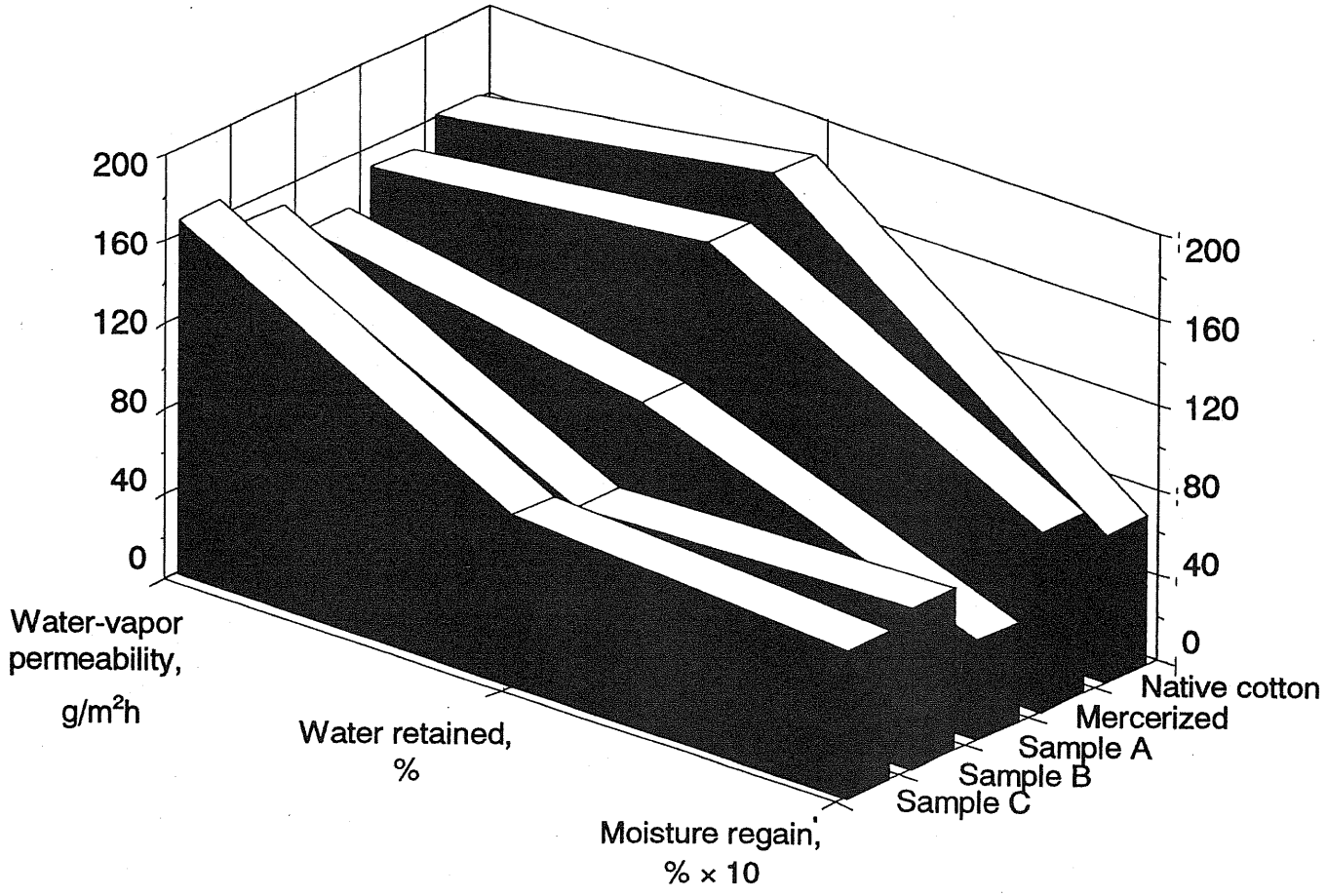

Figure 5-6. End-use properties of cotton fabrics.

Table 5-4. Dye uptake of dyestuffs onto the sample fabrics.

Sample	Direct orange		Solar orange	
	%	mg/g	%	mg/g
Untreated	5.0	1.17	3.1	0.72
Sample A	0.6	0.11	3.1	0.61
Sample C	71.9	14.37	88.9	19.24

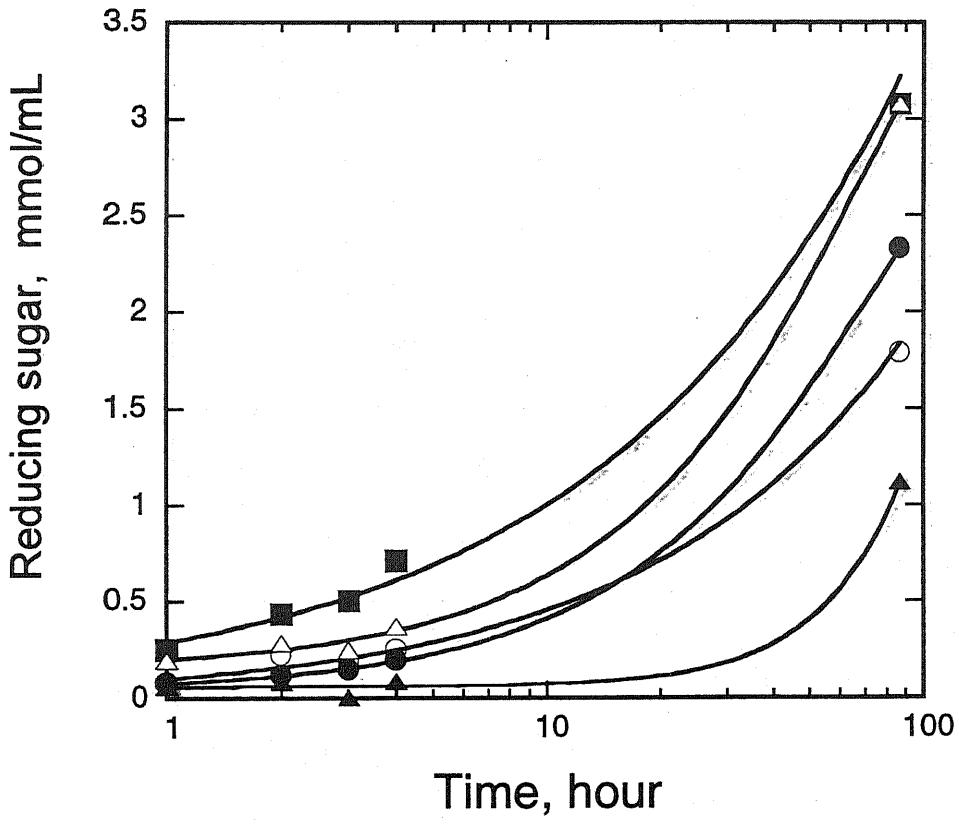

Figure 5-7. Susceptibility of cotton fabrics to the degradation by cellulase: ■ Untreated cotton, ○ Sample A, ● Sample B, ▲ Sample C, △ Scotch-Gard.

cotton.

Table 5-4 shows that dye uptake of Sample C is improved remarkably compared to the untreated sample. Generally, acid dye has no dye ability for cotton, but the Sample C absorbed 88.9% of the acid dye by ionic bonding. The uptake of direct dye also improved in Sample C, from 5.0 % to 71.9%.

5.3.6 Biodegradability of Samples

The long alkyl chain might hinder a microbial attack, because the biodegradability of Sample A, Sample B, and Sample C was diminished. Figure 5-7, compared cellulase susceptibility of Sample A, Sample B, and Sample C with untreated and Scotch-Gard® treated samples. After 87 h of the reaction, Scotch-Gard®-treated sample showed the same susceptibility as the untreated sample, but in the first few hours, there was a lag cellulase penetration into fibers through the coated layer.

Long-term biodegradability for the treated samples was in the order Sample B, Sample A, and Sample C; here, Sample C with a lower DS was more resistant than Sample A, which had more substituents. Basic amino and bulky bromo groups on the substituents of Sample C might have hindered cellulase accessibility.

5.4 Conclusion

Water-repellent cotton fabrics were produced by two alkylation methods with only 0.07 to 0.12 alkylation per glucose unit. Sample A was prepared by alkylation by acetylation without mercerization, Sample B by direct alkylation after mercerization, and Sample C by alkylation after allylation and bromination. The contact angle and spray ratings of as-treated samples were 120-144° and 80-90, respectively, with alkyl lengths of over C_{12}. Water repellency through twenty launderings was attained by alkylation with C_{18}-alkyl groups. Durability of the water-repellency after repeated laundrings depended on the fabric construction. These samples retained fabric hand and water vapor permeability similar to with those of untreated cotton fabric. The biodegradability was diminished slightly in Sample A and Sample B, and appreciably in Sample C. On the other hand, the Sample C's dye ability increased remarkably.

References

1. J. P. Moreau, G. L. Drake Jr., *Am. Dyest Rep.*, **58**(4) 21 (1969).
2. J. P. Moreau, S. E. Ellzey Jr., G. L. Drake Jr., *Am. Dyest Rep.* **56**(4), 117 (1967).
3. W. B. Blumenthal, *Ind. Eng. Chem.*, **42**, 640 (1950).
4. J. B. Bullock, C.M. Welch, *Textile Res. J.*, **35**, 459 (1965).
5. Y. Sato, T. Wakida, S. Tokino, S. Niu, M. Ueda, *Textile Res. J.*, **64**, 316 (1994).
6. H. A. Schuyten, J. W. Weaver, J. G. Frick Jr., J. D. Reid, *Textile Res. J.*, **22** 424 (1952).
7. W. J. Connick Jr., S. E. Ellzey Jr., *Am. Dyest Rep.*, **57**(3) 71 (1968).
8. R. J. Berni, R. R. Benerito, F.J. Philips, *Textile. Res. J.*, **30**, 576 (1960).
9. F. J. Philips, L. Segal, L. Loeb, *Textile. Res. J.*, **27**, 369 (1957).
10. T. Kondo, D. G. Gray, *J. Appl. Polym. Sci.*, **45**, 417 (1992).
11. C. Sawatari, T. Yagi, *Sen-i Gakkaishi*, **47**, 467 (1991).
12. G. Okada, *J. Biochem.*, **77**, 33 (1975).
13. M. Somogyi, *J. Biol. Chem.*, **195**, 19 (1952).
14. N. Nelson, *J. Biol. Chem.*, **153**, 375 (1944).
15. M. L. Nelson, R. T. O'Connor, *J. Appl. Polym. Sci.*, **8**, 1325 (1964).
16. R. T. O'Connor, E. F. DuPré, D. Mitcham, *Textile Res. J.*, **28**, 382 (1958).
17. F. H. Forziati, J. W. Rowen, *J. Res. Natl. Bur. Stds.*, **46**(1) 38 (1951).

Chapter 6

Durable Flame Retardant Cotton Fabric Prepared by Partial Pyrophosphorylation and Metal Complexation

6.1 Introduction

The limited oxygen index (LOI) value of cotton fabric is only 16, which means that the fabric catches fire easily in an air atmosphere that contains 21% oxygen. An increase of the LOI to a value higher than 21 will improve the safety of cotton fabric, and extend its use in every aspect of life.

Among various techniques available for making cotton flame retardant, resin finishing with organophosphorus compounds[1-7] seems to be the most prevailing and reliable, but such treatment causes the drop in tensile strength, deterioration of fabric hand, and sometimes makes skin irritation due to the liberation of formaldehyde. Conferring flame retardancy by covalent modification usually results in the loss of the superior properties of cotton such as fabric hand and biodegradability. One formula for cellulose fiber flame retardancy is to orthophosphorylate the fabric by heating it in an aqueous mixture of urea and phosphoric acid, but the drop in tensile strength can not be avoided[8,9]. Poly(vinyl alcohol), another polyhydroxyl material, was successfully made durably flame retardant by orthophosphorylation followed by metal complexation[10,11].

In this chapter, a new durably flame retardant cotton fabric is prepared by treating mercerized cotton with pyrophosphoric acid followed by metal complexation. The author demonstrates the superiority of pyrophosphorylation (esterification with pyrophosphoric acid) over ordinary phosphorylation, and compares the effect of various metal ions to endow fabric flame retardancy.

6.2 Experimental

6.2.1 Materials

Cotton fabric (plain weave shirting, 27 × 30 yarns/cm, 36 × 40s) was supplied by Iseikatsu-kenkyukai (Clothing-life Research Assoc.), Tokyo. The fabric was scoured and mercerized in the same condition as described in Chapter 5.

Orthophosphoric acid was prepared by mixing 100 g commercial 85% phosphoric acid with 39.4 g phosphorus (V) oxide. Pyrophosphoric acid was prepared by mixing 50 g of 85% phosphoric acid and 38.8 g phosphoryl chloride, and the mixture was heated until no more HCl gas was evolved. *N*-cyanoguanidine was dissolved in hot water and recrystallized. *N,N*-dimethylformamide (DMF) was dried with a 5A molecular sieve before use.

6.2.2 Preparation Methods

The mercerized fabrics were phosphorylated by two methods, as shown in Figure 6-1. The detailed procedures for preparing the samples are reported below.

(1) Orthophosphorylation

The cottons were orthophosphorylated by a method similar to that reported by Kurose and Shirai[10,11] to orthophosphorylate poly(vinyl alcohol). A 15 g portion of urea was mixed with 10 g *N*-cyanoguanidine in 50 mL DMF with stirring at room temperature. After complete dissolution, 10 mL of 100% orthophosphoric acid and 50 mL DMF were added to the solution, and the temperature was raised to 140 °C. Then stirring stopped and the mercerized cotton fabric (6 g) was immersed in the hot mixture, which was kept at 140 °C. At definite time intervals the fabric was removed from the mixture and rinsed in running tap water for 24 h, rinsed in distilled water twice, and then air-dried.

(2) Pyrophosphorylation

Mercerized cotton fabric (6 g) was pyrophosphorylated in the same conditions as for orthophosphorylation, except that the reaction temperature was kept at 110 °C. The pyrophosphorylated fabric was immersed in 10% $NaHCO_3$ solution to neutralize the remaining pyrophosphoric acid and then rinsed as described before.

(3) Metal complexation

Phosphorylated cotton fabric (1 g) was immersed in 20 mL aqueous 0.02 mol/L metal salt solution ($CaCl_2$, $MgCl_2$, $ZnSO_4$, $NiSO_4$) at room temperature for 30 min, rinsed with distilled water three times, and air-dried.

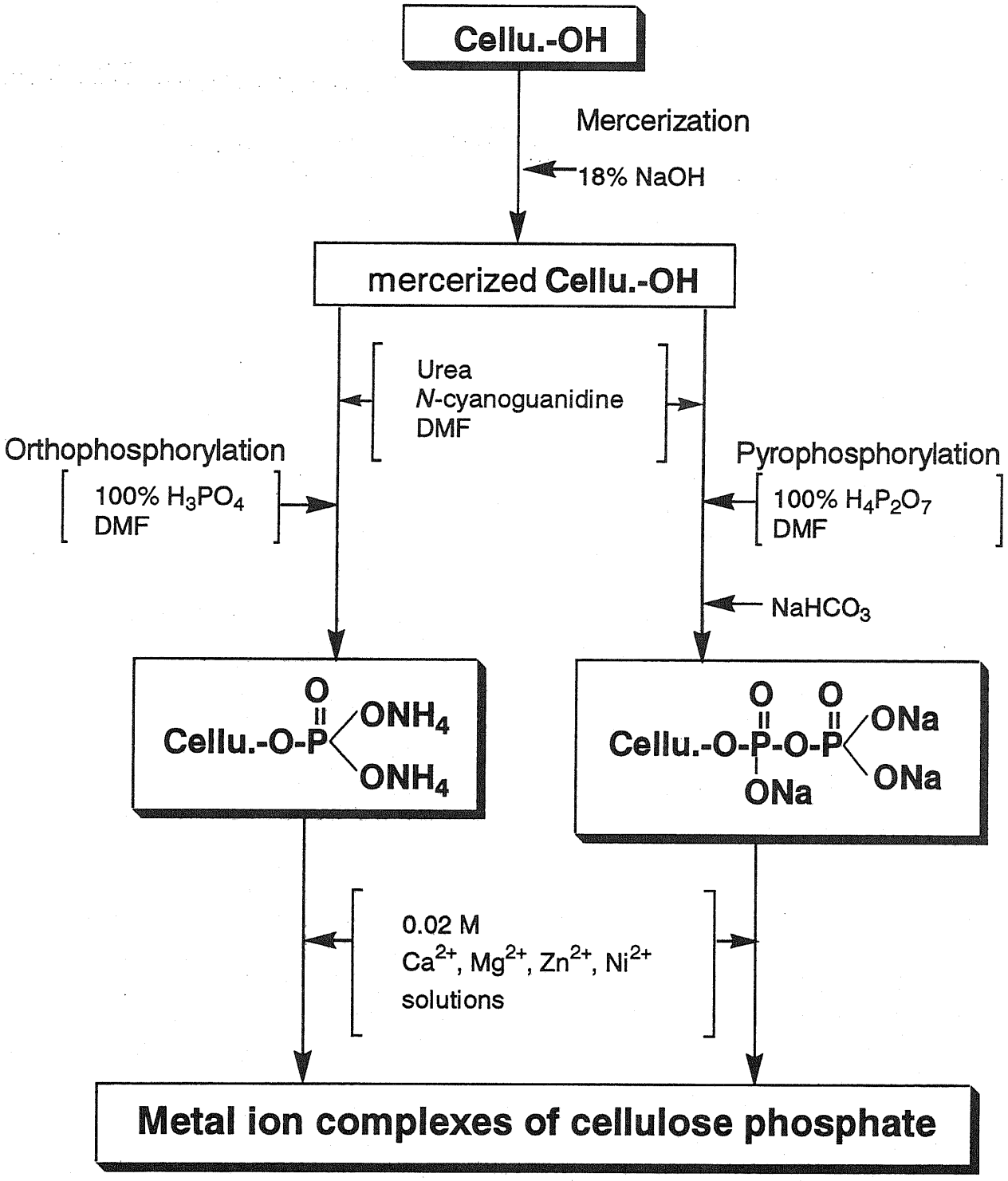

Figure 6-1. Procedure for preparation of flame retardant cotton fabrics.

6.2.3 Analysis

IR spectra were obtained at 2 cm^{-1} resolution with a Perkin-Elmer FTIR spectrometer Spectrum 1000 using the KBr method at 1% sample concentration.

Total phosphorus content of the fabric was measured according to the method of Fiske and Subbarow[12]. The sample fabric (1 mg) was suspended in 1 mL of 2.5 mol/L H_2SO_4, and the mixture was evaporated over a free flame. The contents of the tube became brown. After cooling, one drop of 2 mol/L HNO_3 was added and the mixture was heated again until a white fume appeared. HNO_3 was added and heating was repeated until the contents became clear. The mixture was cooled, added to 1 mL H_2O and the tube was placed in a boiling water bath for 5 min. After cooling, 2.5% ammonium molybdate was added. Phosphorus content was determined by absorbance at maximum wavelengths (λ_{max}: λ_{max} = 660 nm) measured with a Shimadzu spectrometer UV240. The phosphorus content in pyrophosphoric ester form was measured as follows: the sample fabric (1 mg) was suspended in 1 mol/L HCl, heated at 100 °C for 7 min, and cooled, and the phosphorus content of the solution was measured. Since this released only one of two phosphorus atoms contained in the pyrophosphoric esters, the amount of phosphorus in pyrophosphoric ester forms was twice that obtained. The phosphorus content of the residual cotton fabric was determined by the method of Fiske and Subbarow as described for the total phosphorus content.

Bound metal content was measured as follows; the sample fabric (1 mg) was digested with concentred HCl at 100 °C for 18 h. The brown color that developed was decolorized with HNO_3 as described above. The mixture was cooled, added to 3 mL HCl-$LaCl_3$ mixture, which is required for metal content measurements in the presence of phosphoric acid[13], was prepared by mixing 200 mL of 0.3 M HCl and 10 mL of 10% $LaCl_3$. Metal content was measured with a Jarell Ash atomic absorption spectrometer AA-1 MK-2.

6.2.4 Flame Retardancy

The flame retardancy of the sample fabric was estimated by thermal analysis and LOI measurement. For the thermal analysis pulverized cotton fabric (5 mg) sample was measured with a Mac Science TG-DTA 2000S. The heating scans were carried out in the temperature range of 20-480 °C in air at a heating rate of 10 °C/min. Al_2O_3 was used

as a reference.

LOI was determined with a combustor ON-1 (Toyo Rika Industrial Co.) by the method defined by JIS K-7201-1976 (A-2). The test fabric (2 × 15 cm) was mounted in a cylinder through which mixture of oxygen and nitrogen of known composition was passed. The sample was then ignited at the top and flow of gases regulated (ratio of oxygen to nitrogen adjusted) so as just to maintain combustion. The volume percent oxygen needed at that point is LOI.

Laundry tests were made according to JIS L-0844-1986 (A-3) as described in Chapter 5, except that the temperature was 60 °C throughout.

The tensile strength of the fabric was measured with a Toyo Seiki Strograph-R3. Tensile strength and elongation of the test fabric, 4 cm long and 2 cm wide, were tested before and after laundering at a strain rate was 15 mm/min.

Biodegradability was tested by the Somogyi-Nelson method[14,15] as described in Chapter 5.

6.3 Results and Discussion

6.3.1 Effect of Additives on Phosphorylation

The author tested the effect of additives on the extent of phosphorylation, shown in Table 6-1. The degree of phosphorylation was highest with the amount of additives described for Sample 4. In the following experiments, the amounts of cyanoguanidine and urea were fixed at 15 and 10 g, respectively, for 6 g cotton fabrics.

6.3.2 Conditions of Phosphorylation

Figure 6-2 shows the content of the covalently bound orthophosphoric and pyrophosphoric esters of the treated fabrics as a function of the time of treatment. Considering that the prolonged treatment of the fabric by acid at higher temperatures might degrade the cellulose, the author fixed the treatment time at 120 min at 140 °C for orthophosphorylation, or at 180 min at 110 °C for pyrophosphorylation, respectively. The phosphorus content of the fabric treated with orthophosphoric acid increased rapidly in 80-120 min at 140 °C, and less rapidly thereafter. The phosphorus content of the 120 min treated sample was 2.5%. The phosphorus content of the fabric treated with pyrophosphoric acid increased rapidly at 110 °C, and there was sufficient phosphorus

content at a pyrophosphorylation time of 180 min.

Table 6-2 shows the phosphorus content in orthophosphoric and pyrophosphoric esters of the treated fabrics. Some pyrophosphoric ester formed by treatment with orthophosphoric acid may have been produced by condensation of orthophosphoric acid at higher temperatures. The treatment with pyrophosphoric acid produced more pyrophosphoric esters.

6.3.3 FTIR Spectroscopy

The IR spectra (Figure 6-3) of the treated and untreated samples showed the covalent bond formation by phosphorylations. The band at 820 cm^{-1} in the treated samples was attributed to the asymmetric C-O-P stretching vibration, and that at 1710 cm^{-1} to the PO stretching vibration, and a weak band at 3450 cm^{-1} (not shown in this figure) attributed to the NH stretching vibration. The band at 1420 cm^{-1} attributed to the OH bending vibration found in the untreated sample weakened in the phosphorylated samples. These results suggest that the treated cotton fabric was converted to ammonium cellulose phosphate[16].

6.3.4 Metal Ion

Table 6-3 shows the contents of bound metal ions in the phosphorylated cotton fabrics. The metal content in the pyrophosphorylated fabric with a phosphorus content of 1.067 mmol/g was higher than that in the orthophosphorylated fabric.

6.3.5 Comparison of Flame Retardancy and Durability

The TGA curves of untreated and treated samples are shown in Figure 6-4. The untreated cotton started rapid degradation at 320 °C, and lost 96% of its weight at 480 °C, leaving little ashes. The phosphorylated samples started degradation at 280 °C but the weight loss was less than 60% at 480 °C. The author believes that the covalently bound orthophosphoric and pyrophosphoric esters caused dehydrating carbonization of cellulose at lower temperatures, which prevented oxidative degradation at higher temperatures as discussed by Bhatnagar[17-19]. The higher the phosphorus content of fabric, the more residue left after thermal degradation, and the more flame retardant. Th presence of metal ions did not have significant effects on TGA curves (figures not

shown).

The results of the LOI measurements are summarized in Table 6-4. The LOI value of cotton fabric rated only 16, that of orthophosphorylated fabrics rated 18, and that of pyrophosphorylated fabrics rated 26, in accordance with increasing phosphorus contents. Significantly higher LOI values observed for pyrophosphorylated fabrics over phosphorylated ones may be due to the higher affinity of pyrophosphoric esters for bivalent metal ions over phosphoric esters. The maximum LOI value of 28 was recorded for the pyrophosphorylated fabric treated with Ni^{2+}, but it was colored pale green. This is in accord with foregoing reports[10,11,18,19] that the Ni^{2+}-complexes of orthophosphorylated substrates were flame retardant. Pyrophosphorylated cotton fabrics treated with Ca^{2+} and Mg^{2+}, as well as those merely rinsed in running tap water, had significant amount of Ca^{2+} and Mg^{2+} ions. Despite the reported adverse effect of Ca^{2+} on fire retardancy[5], these samples had LOI values of over 26. The presence of pyrophosphoric ester in these samples probably compensated the reported effect of Ca^{2+} on LOI values. Because Ni^{2+} or Zn^{2+}-containing wastes might cause environmental pollution, Ca^{2+} or Mg^{2+} treatment may be preferred.

6.3.6 Tensile Strength

Table 6-5 shows the tensile strength and elongation of untreated and treated samples before and after laundering. Tensile properties were highest for the mercerized fabric, and those of the orthophosphorylated, pyrophosphorylated, and untreated fabrics were similar after laundering. These results may be explained by the combination of two opposing effects: mercerization improves tensile properties by causing higher packing of threads (35 × 35 yarns/cm), and phosphorylation lowers the tensile properties due to degradation during acid treatment at higher temperatures. In addition to improving effect of mercerization on the tensile properties, this treatment raises the reactivity of hydroxyl groups of cellulose. The orthophosphorylated and pyrophosphorylated samples retained a hand similar to that of untreated fabrics.

6.3.7 Biodegradability

A comparison of the cellulase susceptibility of untreated and treated fabrics is shown in Figure 6-5. The untreated cotton was nearly completely digested after 45 h

Table 6-1. Effect of additives on phosphorus content treated with pyrophosphoric acid.

Sample No.	Additive			Phosphorus content, mmol/g
	Urea, g/6 g Cellu.	*N*-cyanoguanidine, g/6 g Cellu.	DCC[a], g/6 g Cellu.	
1	-	-	-	0.323
2	10	-	-	0.822
3	-	15	-	0.725
4	10	15	-	1.067
5	20	30	-	0.770
6	-	-	41.3	0.765

[a]Dicyclohexylcarbodiimide

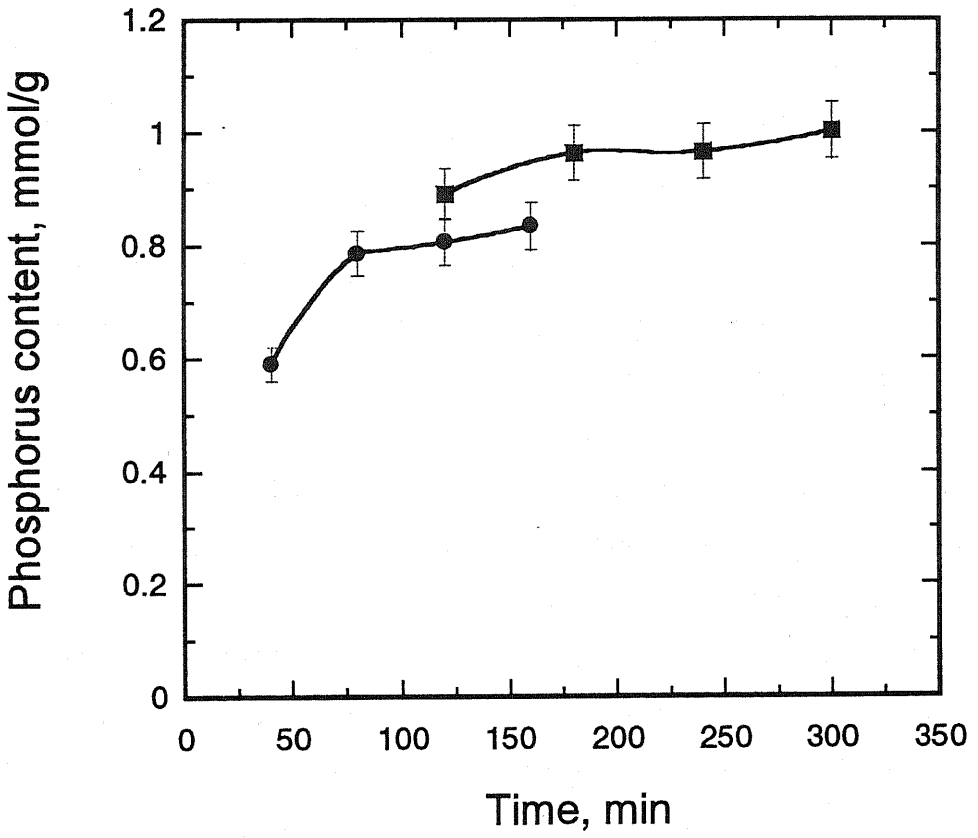

Figure 6-2. Phosphorus content as a function of reaction time. ● ortho-phosphorylation at 140 °C and ■ pyrophosphorylation at 110 °C.

Table 6-2. The phosphorus content in orthophosphoric and pyrophosphoric esters of cellulose with different treatment.

Treatment with	Total phosphorus		Phosphorus in pyrophosphoric ester form		Phosphorus in orthophosphoric ester form	
	mmol/g	DS	mmol/g	DS	mmol/g	DS
Orthophosphoric acid	0.782	0.115	0.210	0.018	0.557	0.097
Pyrophosphoric acid	1.067	0.136	0.644	0.058	0.431	0.078

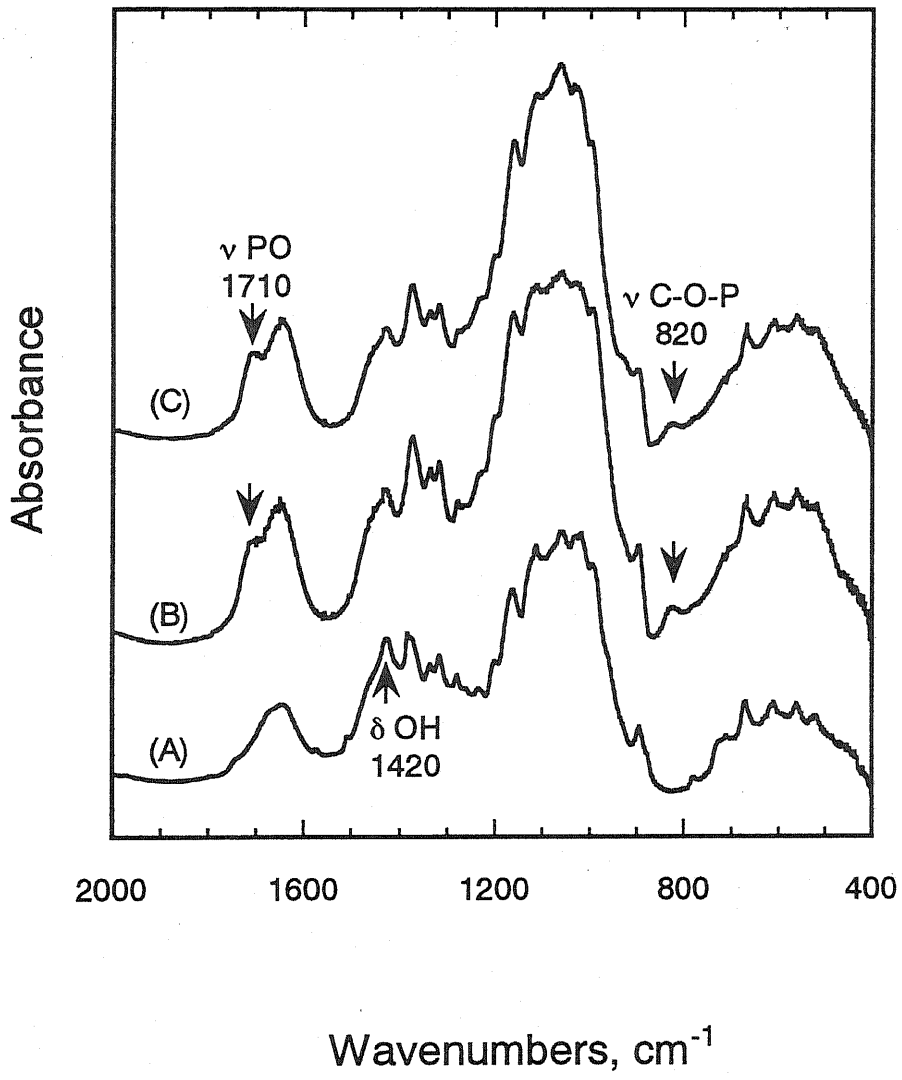

Figure 6-3. IR spectra of (A) untreated cotton fabric, (B) treated with orthophosphoric acid, and (C) treated with pyrophosphoric acid.

Table 6-3. The contents of metal ions of treated cotton fabrics.

Treatment with (P content, mmol/g)	Tap water[a]		Metal solutions[b]			
	Ca^{2+}, mmol/g	Mg^{2+}, mmol/g	Ca^{2+}, mmol/g	Mg^{2+}, mmol/g	Zn^{2+}, mmol/g	Ni^{2+}, mmol/g
Orthophosphoric acid (0.782)	0.385	0.257	0.428	0.283	0.129	0.003
Pyrophosphoric acid (1.067)	0.432	0.273	0.535	0.311	0.165	0.004

[a]Both Ca^{2+} and Mg^{2+} contents were measured for the cotton fabric rinsed in running tap water.

[b]Only Ca^{2+} content was measured for $CaCl_2$ treated fabric, Mg^{2+} content for $MgCl_2$ fabric, etc.

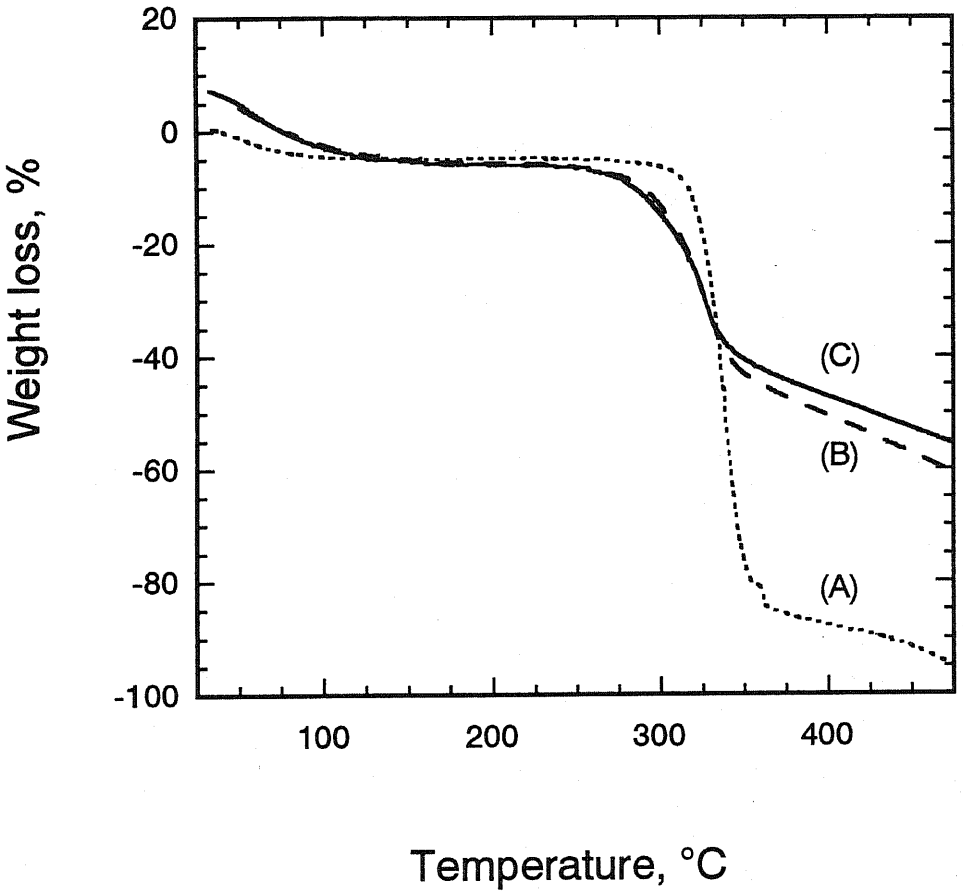

Figure 6-4. TGA curves of (A) untreated cotton fabric, (B) treated with orthophosphoric acid, and (C) treated with pyrophosphoric acid.

Table 6-4. LOI values of metal complexes of treated cotton fabrics before and after laundry.

Sample	Tap water, %	Ca^{2+}, %	Mg^{2+}, %	Zn^{2+}, %	Ni^{2+}, %
Untreated	16.1	-	-	-	-
Mercerized	16.9	-	-	-	-
Treated with orthophosphoric acid					
before laundry	18.0	21.4	20.9	20.2	22.1
after laundry	20.7	22.1	22.1	21.7	23.7
Treated with pyrophosphoric acid					
before laundry	26.2	26.8	26.5	26.2	28.3
after laundry	26.8	26.2	26.2	26.2	27.7

Table 6-5. Tensile strength and elongation of treated cotton fabrics before and after laundry.

Sample	Tensile strength, kg/cm^2	Elongation, %
Untreated	15.4	23.6
Mercerized	19.9	40.2
Treated with orthophosphoric acid		
before laundry	17.8	30.5
after laundry	15.9	34.8
Treated with pyrophosphoric acid		
before laundry	17.2	25.6
after laundry	15.4	29.8

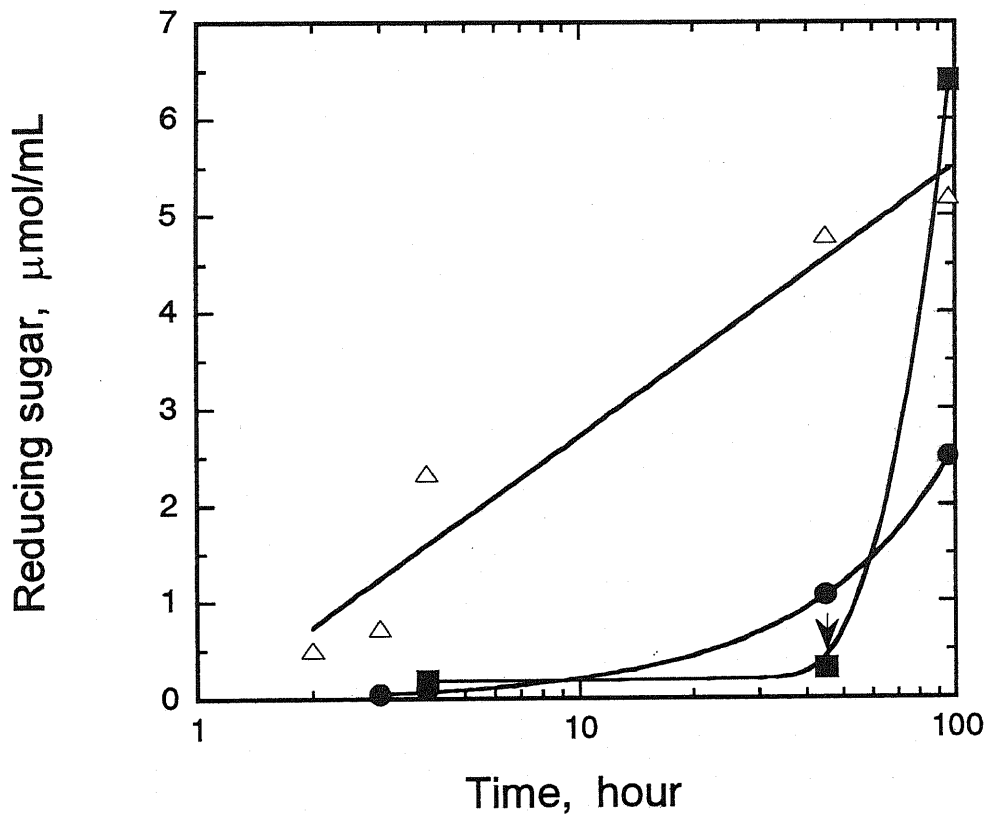

Figure 6-5. Susceptibility of cotton fabrics to the degradation by cellulase: △ Untreated cotton fabric, ● treated with orthophosphoric acid, and ■ treated with pyrophosphoric acid. Pancreatin was added at the arrow.

incubation with cellulase. The treated fabrics were digested more slowly, probably due to the inhibitory effect of pyrophosphoric groups which might hinder cellulase accessibility. Adding pancreatin (lyophilized pancreatic juice which contains various digestive enzymes including phosphatases, at a concentration of 1 mg/mL) to the reaction mixtures at 45 h started rapid degradation of the fabric pyrophosphorylated fabric. Probably pancreatin hydrolyzed pyrophosphoric esters to supply the cellulase substrate.

6.4 Conclusion

Flame retardant cotton fabric is prepared by pyrophosphorylation followed by metal complexation. The pyrophosphorylation proceeds rapidly at a comparatively low temperature (110 °C), which may protect the fabric from deterioration due to a strong acid at higher temperatures. Metal content, residue after thermal degradation, and flame retardancy are higher in pyrophosphorylated fabric than in orthophosphorylated fabric. The covalently bound phosphoric esters cause dehydrating carbonization of cellulose at lower temperatures, which prevents oxidative degradation at higher temperatures. The flame retardancy depends on the species of metal ions. Pyrophosphorylated cotton fabric treated with Ni^{2+} has an LOI value of 28, which is similar to that obtained by the resin finishes of cotton fabric with an organophosphorus compound. Pyrophosphorylated cotton fabrics have LOI values of over 26. The Ca^{2+} and Mg^{2+} complexes are colorless and nonpolluting, and may be preferable in practical uses. The tensile strength and elongation of the treated fabrics do not decrease after laundering, in contrast to the behavior of resin-finished fabrics. The pyrophosphorylated samples retain a hand and biodegradability similar to those of untreated fabrics.

References

1. B. M. Baum, *Chemtech*, 311 (1973).
2. J. D. Reid, J. G. Frick Jr., R. L. Arceneaux, *Textile Res. J.*, **26**, 137 (1956).
3. C. Hamalaonen, W. A. Reeves, J. D. Guthrie, *Textile Res. J.*, **26**, 145 (1956).
4. W. A. Reeves, G. L. Drake Jr., L. H. Chance, J. D. Guthrie, *Textile Res. J.*, **27**, 260 (1957).
5. R. B. LeBlanc, *Textile Res. J.*, **59**, 307 (1989).

6. S. Nakanishi, C. Aoki, *J. Home Econ. Jpn.*, **42**, 67 (1991) in Japanese.
7. S. Nakanishi, F. Ohkouchi, *J. Home Econ. Jpn.*, **43**, 121 (1992) in Japanese.
8. R. Kitawaki, T. Ozawa, *Nippon Kagaku Kaishi*, 606 (1974) in Japanese.
9. T. Ozawa, R., Kitawaki, *Nippon Kagaku Kaishi*, 2040 (1975) in Japanese.
10. A. Kurose, H. Shirai, F. Simizu, N. Hojo, *Textile Res. J.*, **54**, 277 (1984).
11. A. Kurose, H. Shirai, *Textile Res. J.*, **66**, 184 (1995).
12. L. F. Leloir, C. E. Cardini, eds., in "*Methods in Enzymology*" vol. 3, Academic Press, New York (1957) pp. 840-850.
13. D. R. Osborne, P. Voogt, in "*The Analysis of Nutrients in Foods*" Academic Press, London and New York (1978) p. 168.
14. N. Nelson, A Photometric, *J. Biol. Chem.*, **153**, 375 (1944).
15. M. Somogyi, *J. Biol. Chem.*, **195**, 19 (1952).
16. K. Katsuura, H. Mizuno, *Sen-i Gakkaishi*, **22**, 510 (1966).
17. R. K. Jain, K. Lal, H. L. Bhatnagar, *J. Appl. Polym. Sci.*, **30**, 897 (1985).
18. B. Kaur, I. S. Gur, H. L. Bhatnagar, *Fire Safety J.*, **14**,151 (1989)
19. B. Kaur, R. K. Jain, I. S. Gur, H. L. Bhatnagar, *J. Anal. Appl. Pyrolysis*, **11**,465 (1987).

Chapter 7

General Conclusion

Throughout this thesis, the formation of hydrogen bonds and physicochemical properties of regioselectively substituted celluloses and randomly substituted celluloses were clarified as following.

In first part (Chapter 2), a new convenient method to determine the distribution of methyl groups in regioselectively substituted *O*-methylcellulose on anhydroglucose unit was developed using solution ^{1}H-NMR analysis. The determination was deduced from the assignment of the signals of each proton, which directly attached to the glucopyranose ring carbon for 2,3-di-*O*-methylcellulose (2,3MC-n: n = 1-3) samples observed in D_2O. These data for the distribution of the methyl groups corresponded to those based on the gas-chromatographic analysis. This method using the ^{1}H-NMR spectroscopy also make possible facile the measurements of the distribution of methyl groups for randomly substituted and commercially available *O*-methylcellulose (R-MC).

This method to determine the distribution of methyl groups will be widely applicable in the characterization of cellulose derivatives having methyl groups. This will have the applications in characterizing other cellulose derivatives as well as other polysaccharides.

Second part (Chapter 3,4) is the elucidation of the effects of the hydrogen bonding formation on the gelation of regioselectively substituted *O*-methylcellulose in two-components solvent systems.

At first, the effect of the formation of hydrogen bonding and the distribution of methyl groups on the gelation in aqueous solution was studied by comparing two types of *O*-methylcelluloses; *i.e.* one type in the 2,3MC-n series having regioselectively substituted methyl groups only at C(2) and C(3) positions and the other, R-MC having randomly substituted methyl groups through the cellulose chain. 2,3MC-n and R-MC showed the differences of the concentration to form a gel and the DSC thermograms on

heating scan. The formation of hydrogen bonds of each water molecule in the sample solution was revealed by the curve fitting of OH stretching region of water in the NIR spectra, which were composed of water species S0, S1, and S2. The presence of intermolecular hydrogen bonds between samples and water was observed. The gelation of *O*-methylcellulose was attributed to the hydrophobic interactions and also to hydrogen bonds which depended on amount of hydroxyl groups at C(6) position.

Next, the effect of dimethyl sulfoxide (Me_2SO)/water composition on gelation behavior of 2,3MC-n and R-MC was investigated by using NIR. With all the 2,3MC-n series and R-MC, it was observed that the gelation occurred at room temperature in Me_2SO/water (70/30 (wt/wt%)) system, while all the samples remained as a sol in Me_2SO. On the other hand, some of them showed a gelation upon heating in water. Based on the above gelation behaviors in combination with the monitoring the change of the areas of S0, S1 and S2 of OH bands in sample solutions, the following conclusions were made. When Me_2SO/water composition was between 90/10 and 80/20, Me_2SO interacts poorly with Me_2SO or water, which suggests the presence of intermolecular hydrogen bonds between the samples and water. The strong interaction between Me_2SO and water causes the reduction of the interaction of the sample with either Me_2SO or water when Me_2SO/water composition was between 70/30 and 50/50.

The knowledge about the relationships between the distribution of substituents and solution behavior will be applied to produce the cellulose derivatives of desired properties. The method to evaluate the formation of hydrogen bonding in *O*-methylcellulose by using NIR analysis will be applied to other cellulose derivatives and polysaccharides.

In third part (Chapter 5,6), the preparation of two kinds of improved cotton fabrics is presented as examples of randomly and low degree substitution of cellulose molecule, as summarized below.

At first, three kinds of water-repellent cotton fabrics, A, B, and C, were produced by low degree substitution of long chain alkyl groups. Sample A was prepared by alkylation by means of acetylation without mercerization, Sample B, by direct alkylation after mercerization, and Sample C, by alkylation by means of allylation and br[illegible]ination. Water repellency of the treated samples with alkyl length of over C_{12} were

similar to that of cotton fabric treated with Scotch-Gard®, however water repellency of C_{18}-alkylated samples did not fade out through twenty launderings in contrast to the cotton fabric treated with Scotch-Gard®. Durability of water-repellency after repeated launderings depended on the fabric construction. These samples retained a fabric hand, water-vapor permeability, and biodegradability similar to those of untreated cellulose fabric. At the same time, the dyeability of Sample C improved remarkably.

Next, durable flame retardant cotton was prepared by partial orthophosphorylation and pyrophosphorylation, followed by metal-complexation. The pyrophosphorylation proceeded rapidly at a comparatively low temperature (110 °C), which may protect the fabric from deterioration due to strong acid at higher temperatures. Metal content, the residue after thermal degradation, and flame retardancy depended on total phosphorus content. Pyrophosphorylated cotton fabric treated with Ni^{2+} had an LOI (limited oxygen index) value of 28, which was similar to that obtained by the resin finishes of cotton fabric with an organophosphorus compound. Flame retardancy, tensile strength and elongation of the treated fabrics did not decrease after laundering. The pyrophosphorylated sample had a tensile strength, elongation, and fabric hand similar to those of untreated fabrics, and was susceptible to enzymatic hydrolysis to release reducing sugars.

Water repellent and flame retardant cotton fabrics proposed in this thesis have satisfied durability. Commercial application of these products will be beneficial to the human society, since the covalently modified cellulose derivatives will not be hazardous to human body.

Finally, the author expects that the conclusions in this thesis could be applied further in cellulose science and industry.

List of Publications

Chapter 2.

A Facile Method of Determination for Distribution of the Substituent in *O*-Methylcelluloses Using ^{1}H-NMR Spectroscopy.

Y. Sekiguchi, C. Sawatari and T. Kondo

Polym. Bull., accepted.

Chapter 3.

A Gelation Mechanism Depending on Hydrogen Bonding Formation in Regioselectively Substituted *O*-Methylcelluloses.

Y. Sekiguchi, C. Sawatari and T. Kondo

Carbohydr. Polym., Submitted.

Chapter 4.

Characterization of Hydrogen Bonds in *O*-Methylcellulose / Dimethyl Sulfoxide / Water System by FT-NIR Analysis.

Y. Sekiguchi, C. Sawatari and T. Kondo

Report of the Graduate School of Electronic Science and Technology Shizuoka University, **22,** 19-24 (2001).

Chapter 5.

Durable Water-Repellent Cotton Fabrics Prepared by Low-Degree Substitution of Long Chain Alkyl Groups.

C. Sawatari, Y. Sekiguchi and T. Yagi

Textile Res. J., **68**(7), 508-514 (1998).

Chapter 6.

Durable Flame Retardant Cotton Fabric Prepared by Partial Pyrophosphorylation and Metal Complexation.

Y. Sekiguchi, C. Sawatari and T. Yagi

Textile Res. J., **70**(1), 71-76 (2000).

Acknowledgements

The author acknowledges with great pleasure the expert guidance and encouragement of her supervisor Professor Chie Sawatari, The Graduate School of Electronic Science and Technology, Shizuoka University, in the preparation of this Thesis.

The author wishes to express her thanks to Professor Toshihiko Nagamura, The Graduate School of Electronic Science and Technology, Shizuoka University, for his valuable suggestions and comments relating to the completion of this thesis.

The author also gratefully acknowledges in valuable discussions and comments on many points in this thesis with Professor Shinkichi Yamada and Professor Hideyuki Itagaki of Shizuoka University.

The author is also gratefully indebted to Emeritus Professor Tatsuhiko Yagi, Shizuoka University, and Dr Tetsuo Kondo, Forestry and Forest Products Research Institute, for their valuable discussions, comments, and suggestions.

Thanks also due to many colleagues, co-operation in carrying out the experiments described, as follows: Ms Mayumi Kuwahara for ^{1}H-NMR measuments. Dr Masayuki Suzuki for HPLC operation. Dr Hideto Shibata for elementary analysis, and Ms Yayoi Ogi for Laundaring tests.

The author would like to express special thanks to the members of "Sawatari" Laboratory, Faculty of Education, Shizuoka University, for their assistance and discussion.

The author would like to most sincerely express thanks to all her family members.